U.PORTO

FEUP FACULDADE DE ENGENHARIA UNIVERSIDADE DO PORTO

NON-DESTRUCTIVE AND MECHANICAL ASSESSMENT OF ENVIRONMENTAL DECAY IN MASONRY: A LABORATORY EXPERIENCE

ANA CUNHA LOUREIRO SILVA

Dissertation Submitted to partial fulfilment of the requirements for

MASTER IN CIVIL ENGINEERING - BUILDING CONSTRUCTION

Supervisor: Prof. Doc. Maria Helena Póvoas Corvacho

Co-Supervisor: Doc. Camilla Colla

Co-Supervisor: Doc. Elena Gabrielli

JULY, 2014

MASTERS IN CIVIL ENGINEERING 2013/2014

DEPARTMENT OF CIVIL ENGINEERING

Tel. +351-22-508 1901

Fax +351-22-508 1446

✉ miec@fe.up.pt

Edited by

FACULTY OF ENGINEERING OF UNIVERSITY OF PORTO

Rua Dr. Roberto Frias

4200-465 PORTO

Portugal

Tel. +351-22-508 1400

Fax +351-22-508 1440

✉ feup@fe.up.pt

http://www.fe.up.pt

Partial reproductions of this document are allowed on the condition that the Author is mentioned and that reference is made to Masters in Civil Engineering - *2013/2014 - Department of Civil Engineering, Faculty o Engineering of University of Porto, Porto, Portugal, 2014*.

The opinions and information included in this document represent solely the point of view of the respective Author, while the Editor cannot accept any legal responsibility or other with respect to errors or omissions that may exist.

This document was produced from an electronic version supplied by the respective Author.

LISG - Laboratory of Structural and Geotechnical Engineering

http://www.dicam.unibo.it/Centro-laboratori/lisg/laboratorio-di-ingegneria-strutturale-e-geotecnica-lisg

http://www.dicam.unibo.it/Centro-laboratori/lisg/Ricerca_LISG_RM.htm

DICAM Department

(Department of Civil, Chemical, Environmental and Materials Engineering)

School of Engineering and Architecture

Alma Mater Studiorum-Università di Bologna.

I dedicate this thesis to my parents,
friends and Gonçalo for all the support.

"A teoria também se converte em graça material
uma vez que se apossa dos homens."
Karl Marx

ACKNOWLEDGEMENTS

This thesis is a result of the Erasmus exchange programme between Oporto University of Engineering and University of Bologna, where all the research was carried out.

To the university of Bologna, a special thanks. For the conditions that provided me over these five months, and for all the help and close accompaniment.

I want to thank Professor Giovanni Pascale, and a special acknowledgement to Professor Camilla Colla and Elena Gabrielli, for the close support, patience, knowledge and every day encouragement, the chance to have been accepted so well and to take active part in this group of researchers.

An additional thanks to the members of the Laboratory of University of Bologna, LISG.

I would also like to thank Professor Maria Helena Corvacho, that supported me from Portugal, and helped me every time I needed, even being far from me.

To all my friends in Portugal, who have given me all the support to go through this experience.

Finally, to my family, for the kindness and hard work to give me the possibility to achieve an old dream, to do the Erasmus programme that made me grow up as a person and as a future civil engineer.

To all, a big thank you.

ABSTRACT

The main focus of this thesis is to analyse the applicability of different non-destructive tests such as ultrasonic tests, sonic tests, infrared thermography, and ground penetration radar, to different constituent materials of masonry specimens, bricks, stones, mortars and a large scale walls when exposed to weathering agents and rising damp with different types of salt. It was also made an assessment of the mechanical damaging effects in the specimens.

A brief theoretical introduction of the concept of salt weathering and the working principles, description of the equipments and methods of application of the non-destructive tests used are presented in order to show a background of the experimental work. This preliminary part is very important, as it is the base of the study and is essential for the interpretation of the results obtained.

The investigation of rising damp and degradation due to different salts present in ground water, in masonry structures, and the monitoring over time, when subjected to this type of phenomenon is an issue that was never completely investigated.

The conditions of salt and moisture transference in porous materials, such as those that constitute masonry, vary with the season and the meteoric agents, so, it is important to study different inspection techniques, that can be useful for the continuous monitoring of the behaviour of this type of materials.

All the work was carried out in the LISG (Laboratory of Structural and Geotechnical Engineering) and constitute a continuation of a work that has been carried out for four years, in order to understand the damage causes by different salts present in ground water due to capillary rise in porous material. All the objects studied, suffered four cycles of natural aging, thus, this is the fifth analysis that was done in order to understand the beginning and the evolution of the damage over all this time.

Moreover, some mechanical test were performed, also in the laboratory, so the mechanical characterization and mechanical behaviour of decayed materials can be identified.

KEYWORDS: Damage Causes, Rising Damp, Diagnoses, Masonry, Non-Destructive Tests

RESUMO

O principal objetivo da tese apresentada é analisar a aplicabilidade de diferentes testes não destrutivos como o teste de ultrassons, o teste sónico, termografia e o radar de penetração no solo, a diferentes materiais constituintes de uma estrutura de alvenaria quando expostos ao agentes atmosféricos e ao fenómeno de humidade ascensional com diferentes tipos de soluções.

Uma primeira introdução teórica ao conceito de degradação devido ao sal, uma descrição dos princípios, e dos equipamentos e ainda os métodos de aplicação dos ensaios não destrutivos, são apresentados para mostrar a base de trabalho subjacente ao trabalho experimental realizado. Esta parte preliminar é muito importante pois é a base de todo o estudo e é essencial para a interpretação dos resultados obtidos

A investigação da humidade ascensional e da degradação dos materiais devido a presença de sais em águas subterrâneas, em estruturas de alvenaria, e a sua monitorização ao longo do tempo, quando sujeitas a este tipo de fenómenos, é um assunto que ainda não foi completamente investigado.

As condições em que ocorre a transferência de sais e humidade em materiais porosos, como os que constituem as estruturas de alvenaria, variam com a época e os agentes meteorológicos. Assim, é importante o estudo de diferentes técnicas de inspeção e de ensaios, úteis para a monitorização do comportamento dos diferentes tipos de materiais e na estrutura no seu conjunto.

Todo o trabalho de pesquisa foi feito em laboratório e constitui a continuação de um trabalho que tem vindo a ser realizado há quatro anos, com o objetivo de perceber as causas de degradação devido a diferentes tipos de sais presentes na água subterrânea e que afetam as estruturas por ascensão capilar. Todas as amostras foram sujeitas a quatro ciclos de envelhecimento natural, assim, esta á a quinta analise feita, para perceber e comparar o inicio e a evolução da degradação ao longo do tempo

Para além disto, foram realizados testes mecânicos ao material em estudo para que possa ser feita a caracterização mecânica do material e ainda o estudo do seu comportamento mecânico ao longo do tempo.

PALAVRAS-CHAVE: Causas de Degradação, Humidade Ascensional, Diagnostico, Alvenaria, Ensaios Não Destrutivos.

MAIN INDEX

FIGURE INDEX

TABLES INDEX

NOMENCLATURE

$\boldsymbol{\gamma}$- Surface tension

θ - Contact angle,

r - Capillary radius

ρ - Liquid density

g - Gravity

z - Impedance

ρ - Density

Vp - P-wave velocity

E_s - Static modulus of elasticity

E_d - Dynamic modulus of elasticity

$\boldsymbol{\upsilon}$ - Poisson ratio

λ - Wavelength

f - Frequency

σ* - Electrical conductivity

μ - Magnetic permeability

ε* - Permittivity

σ - Strain

ε - Deformation

ABBREVIATIONS AND ACRONYMS

LISG - Laboratory of Structural and Geotechnical Engineering

ASTM - American Society for Testing and Materials

DT - Destructive tests

MDT - Minor destructive tests

NDT - Non-destructive tests

NIST - The National Institute of Standards and Technology

NBS - National Bureau of Standards

US - Ultrasound

GPR - Ground Penetration Radar

IRT - Infrared Thermography

WT- Weight

S - Na_2SO_4 samples

C - NaCl samples

H - Water samples

LP - Longitudinal Path

TP - Transversal Path

ST - Superficial Transmission

DT - Direct Transmission

1

INTRODUCTION

1.1. BACKGROUND OF THE THESIS

Rehabilitation of heritage buildings has become an important issue in our society, mainly in developed countries around the world. It is the result of the need to improve them due to the different conditions of use and also to recognition of the importance of preservation of the architectural heritage.

Mostly in developed places, grows a necessity of maintaining the existing architectural heritage, as a counterpoint to the changes caused by all the scientific development and the fast technological progress. There is a feeling that keeping the historical buildings is very important so it can be passed to future generations.

The ancient structures are liable to a long period of aggressive agents, which conduct to degradation over time. Furthermore, with the lack of maintenance during the years, they stop fulfilling the purpose they were built for. However, conservation of old buildings is not a simple task because a structural intervention can conflict with the cultural value of the building. The methodologies used in new structures are dominated by a large group of professionals and are very different from those used in rehabilitation of heritage buildings.

Some different types of interventions can be applied depending on the cultural value of the building, from a maintenance where the intent is to keep the historical value of the building to rehabilitate with a deep intervention where the purpose is to improve the performance of the building (Modena et al., 2010).

A considerable part of the built heritage consists on masonry buildings, mostly in historical centres of the cities but, unfortunately, most of these buildings are degraded, don't present any type of maintenance and also have structural problems. In recent years, a concern is growing about the revitalization of urban centres and historic monuments, which leads to a bigger interest in restoration and rehabilitation.

In order to deepen the knowledge about various types of historic structures and their state of conservation as well as on evolution of materials decay due to environmental factors, the role of non-destructive techniques for assessment purposes becomes fundamental in these cases however their use is still not sufficiently widespread or the techniques' limits and possibilities are completely explored.

Taking into account the stagnation period that Portuguese new construction industry is going through, it is necessary to invest on the heritage already built. This requirement concerns not only the structural preservation of the buildings, but also the use of the buildings itself.

1.2. IMPORTANCE OF THE WORK

The first scientific studies of the experiences and techniques of restoration and rehabilitation of old masonry buildings began mainly due to the consequences of World War II. However, only recently they start to be a priority in terms of type of intervention. (Binda et al., 2000). In the last 50 years many experiences of restoration and rehabilitation of damaged masonry have been carried out in Europe. Several unsuccessful results have emphasized the need for adequate assessment before any restoration or rehabilitation. In fact, when neither the real state of damage or the effectiveness of repairs are known, the results of any project is also unknown. Prevention and rehabilitation can only be successfully realized if the diagnosis of the state of the building is well known.

Non destructive evaluation can be helpful when a overall knowledge is needed, in finding hidden characteristics like internal void, defects and flaws, characteristics of a wall section, and the state of preservation of the structure. Sampling the masonry is a costly operation which can also lead to misunderstanding when the operation in not carried out in the appropriate manner (Binda et al., 2000).

In case of non-destructive tests, a correlation between the measured parameters and the mechanical ones is usually difficult, but they can give an overall qualitative response of the masonry.
Currently, the most diffused non-destructive techniques are the sonic, ultrasonic, radar and thermophaphy tests. Sonic and radar tests seem to be very promising used in inhomogeneous materials. Most of non-destructive procedures can give only qualitative results, however the designer can interpret the results and compare the results of different parts of the same masonry structure by using different non-destructive techniques (Binda et al., 2000)**.**

The historical heritage identity and value should be preserved when an intervention has to be done. Thus, interventions in older buildings should be inspired by specifically developed and defined regulations. The Venice Charter, Athens Charter and Krakow Charter clarify the main principles that should be behind the concept of rehabilitation. These letters must be considered even in the buildings that individually are not considered a historical monument but in its context have some heritage relevance.

The conservation of architectural heritage is a very difficult task due to the complex geometry of buildings and large variability of construction materials. Such task requires substantial research work as well as construction techniques and materials, which are different from those used in new constructions.

In the last decades, the strategic importance of historic buildings due to cultural and economical reasons caused a large increase in studies dealing with historic structures and materials. These studies focus mainly on mechanical properties and behaviour of the composite material, seismic vulnerability, physical and chemical deterioration and pollution.

Phenomena such as weathering, water infiltration, in some cases combined with the action of chemicals and exposure to the freeze-thaw cycles, for example, result in degradation of the materials. In the most severe cases, it can cause structural damage (Sadri, 2003). Frequently the correlations between effects and causes can't be done without a previous experimental work. Several investigation procedures have been implemented in recent years, the attempt is to use non-destructive tests as much as possible. Despite this, there is still very little possibility at the current time to correlate non-destructive evaluation tests with masonry performance.

One of the main causes of deterioration of masonry surfaces in aggressive environment is the salt decay, phenomenon emphasized by the presence of the mortar joint, faster vehicle of the salts. (Tedeschi et al., 2011)

Salt weathering is one of the most common deterioration mechanisms in porous materials and may lead to severe damage in buildings and artworks. In the last decades, a lot of research has been devoted to explaining the mechanisms of crystal growth and crystallisation pressure inside pores and their relation with crack propagation in materials such as natural stone, brick, mortar and concrete. However, the effect of salts on the structural behaviour of masonry has not been completely clarified. (Gentilini et al., 2012)

With the currently growing demand to ensure structural safety, maintenance and repair of the old masonry buildings, raise new issues that need to be resolved. (Binda et al., 2000). Only with technique knowledge and culture sensibility working together a successful intervention can be done.

1.3. OBJECTIVES OF THE WORK

The present thesis is part of a enlarged research work developed within the PhD thesis of Elena Gabrielli, in university of Bologna, since 2010. This work complements the studies that have been done since 2010, in order to evaluate the evolution of the damaging effects of masonry specimens due to rising damp with different types of salts and natural weathering.

Its objective is the assessment of masonry objects subjected to a natural weathering and in contact in the base with water with different types of salt. So it can be possible to study the phenomenon on capillary rise, using different types of non-destructive tests. Two types of tests were used, acoustic techniques and electromagnetic. The aim of the work is also the evaluation of the mechanic behaviour of the material.

The experimental work was carried out in order to determine the damaging effects of soluble salts in several different specimens, the environmental decay and the applicability of several non-destructive tests to the analysis of these phenomena. The performance of mortars, bricks and stones was evaluated based on ultrasonic tests, and the outdoors large scale wall were evaluated using sonic tests, infrared thermography and gpr.

1.4. OUTLINE OF THE THESIS CHAPTERS

Chapter 1 presents a brief introduction of the work developed, as well as a background, the importance and the objectives that motivated the presented work and also the organization of the thesis.

In chapter 2 is presented the state of the art and the main concepts of the work are explained. First, is presented a background of masonry construction and its evolution over time. It is also explained some fundamental concepts as salt weathering, rising damp and the influence of the salts on the material decay. The chapter finishes with the description of the inspections procedures when rehabilitation is carried out and the availability of the application of non-destructive tests.

Chapter 3 presents the literature review of two types of non destructive tests, acoustic tests as sonic tests, ultrasonic tests, sonic tomography and impact-eco and electromagnetic tests such as thermography and gpr and also the working principles, description of the equipment and methods of application.

Chapter 4, focus on the experimental work, the description of the specimens used in the laboratory as well as the aging procedures.

Chapter 5 explains the ultrasonic test carried out and the results obtained.

Chapter 6 describes the experimental work about the sonic tests, thermophy and gpr in the large-scale walls as well as the results.

Chapter 7 presents the mechanical assessment of mortar prims and bricks.

Finally, chapter 9 summarizes the conclusions and future developments of the present work.

2

STATE OF ART

2.1. MASONRY CONSTRUCTIONS

2.1.1. HISTORY

The use of masonry is recorded from the remote antiquity. It is common to consider ancient buildings those that were constructed with traditional technologies, until the massive use of concrete, in the middle of XX century. The ancient traditional masonry construction was, generally, resistant masonry and besides that, it had other functional requirements. In these construction regional materials were used but also with a strong presence of stone, bricks and timber.

It was in the Mesopotamia where the oldest traces of masonry buildings were found. These structures were mainly made by natural rocks connected by mortar and bricks reinforced with straw or sand, subsequently baked. The brick, invented over 100.000 years ago, is the oldest construction product produced by man. Its strength and durability led to its extensive use and gave it a dominant place in the history of construction in parallel with stone. In classical antiquity with Greeks and Romans the construction will present a great development that characterized the construction to the present days. On the one hand with the Greeks, about 500 A.C., the art of construction reached a high degree of perfection. On the other hand, Etruscans transmitted to Romans knowledge in the art of building, such as technical dome. Thus, through the Romans, masonry application become varied and experienced great progress.

In Europe, masonry has not made significant progress during the period from IV to X century. Was the development of Catholicism that motivated the initial progress, adopting the model of the Roman basilica for public first temples. One of which most emblematic is the St. Peter basilica in Rome, Fig 2.1.

Fig 2.1 - Dome. San Peter Basilica, Rome (Sousa, 2003).

With the industrial revolution, around 1800, the discovery of the steam engine led to the industrialization of the production process of ceramic bricks with molding equipment pressing so masonry, was not able to compete with the new solutions based on iron, steel and reinforced concrete. The invention of portland cement and the improvement in steel production, in first half of the nineteenth century, made masonry construction disappear. Masonry structures scaled by intuitive rules with very thick walls, couldn't compete with solutions based on metal structures and concrete, with economic and functional advantages as loss of space, cost and time of implementation (Sousa, 2003).

In addition, no engineering schools existed, neither dissemination of innovations and new constructions techniques. The "calculus" was based on experience in practice to build and observe the structure behaviour over time, so the development followed by empirical rules and intuitive knowledge (Gouveia et al., 2007).

Masonry construction has a large number of advantages. The first one is the fact that a single element can fulfill several functions including structure, fire protection, thermal and sound insulation, weather protection and sub-division of space. Masonry materials are available with properties capable of meeting these functions. The second major advantage relates to the durability of the materials which, with appropriate selection, maybe expected to remain serviceable for many decades or centuries, with relatively little maintenance.

From the architectural point of view, masonry offers advantages in terms of great flexibility of plan form, spatial composition and appearance of external walls for which materials are available in a wide variety of colours and textures (Hendry, 2001).

Throughout the first half of the twentieth century only a few architects have preserved masonry with structural function. In this period, it was considered that masonry and plain concrete were unsophisticated solutions not resisting to traction. Otherwise, concrete could solve this problem by associating with steel, technology that developed rapidly (Sousa, 2003).

2.1.2. MASONRY EVOLUTION

History shows evidence for the evolution of masonry with caves, sidewalks, construction of buildings, palaces, cathedrals, bridges and overpasses. Most of them have visible and structural satisfactory performance.

Between 1700 and 1900, the concepts of reinforced masonry and high rise buildings in masonry were developed. With the construction of Pantheon in Paris, Gauthey lays the bases for the concept of reinforced masonry. Some constructions in reinforced masonry appear, like bridges and tunnels

This was followed by nearly 60 years of stagnation in the development of new construction methods. In this period, the development of reinforced concrete technology and steel production, allowed to carry out works with reticulated structures, more slender and high-rise structures. With the development of techniques for mechanized and controlled and rational production method, it was the beginning of the concrete production elements with different characteristics, shape, dimensions, lightness and mechanical resistance. Thus, the traditional techniques of masonry construction was used to closing and compartmentalization of framed structures performed with most modern materials, even in small buildings. Their application as structural function and the importance that was given to them, in times above was completely forgotten. As result, research and development of masonry structures stagnated (Gouveia et al., 2007).

However, in 1951, Paul Haller performed experimental works studies leading to the construction of a unreinforced masonry building in Basel, with 13 floors and 41,4 m heigh. This building is considerate as a landmark of unreinforced structural masonry. This period marked the return of research and interest in this construction technique, resulting in 1967, in the first congress of masonry structures in Austin, Texas. So, this construction technique became accepted as a technique with a similar validity, interest and application as the technique of reinforced concrete or metal structures. This reality extends to some European countries by the end of the twentieth century with the process of European standardization and regulation which leads to the encourage the development in this technology research and industry.

There are, currently, dimensioning documents for masonry structures based on similar requirements defined for structures of other materials, as well as procedures tests defining the experimental characterization of materials and structures systems. Eurocode 6, dedicated to masonry walls, defines a generic basis for the design of buildings and construction works in masonry and Eurocode 8 structures in seismic zones, have a part regarding masonry structures. There are some European norms as the EN 772-Methods of test for masonry units defining procedures for characterization of masonry.

In Portugal, although this solution has been dominant in the past, at present its use is also very limited, watching a great use to of concrete made "in situ" without parallel in other country. With the international expansion of this constructive and structural solution and motivated by the advantages of implementation, evaluation and economics benefits, in Portugal, several research works have been developed in recent years, showing interest in this area.

Nonetheless, there is some inertia in institutions which are considered essential for the collaboration in implementation of this technology in the market. Engineering schools, remain teaching a strong component of reinforced concrete technology, not always clearly approaching the advantages and disadvantages of the other constructive solutions. The technical community in general, traditionally puts into practice knowledge acquired in their training and searches simplified forms of solutions that the market knows better in order not to spend resources in learning new methodologies or application of new material. The industry construction companies in general, do not have motivation to evaluate and support the development of knowledge of different processes (Gouveia et al., 2007).

2.2. DAMAGE CAUSES

2.2.1. INTRODUCTION

Decay of the building materials can be defined as the degradation over time of the materials' properties (physical, chemical, mechanical, etc.) and characteristics (mineralogical, texture, etc.), leading to their failure as building components. Decay phenomena develop at the interface of materials with the environment or at the interface of materials with other materials and are a function of intrinsic and extrinsic factors. The analysis of these factors is essential to the study of the decay pathology of the structure, but also in helping to elucidate the information obtained by the non-destructive tests. Intrinsic factors include the type of building materials and their properties, their mass distribution, their origin and the processing technology, their 'history' (prior conservation interventions) and their compatibility with other materials.

Extrinsic factors include the climate characteristics (distribution, orientation, and environmental factors), the prevailing microclimate, the type of the atmosphere (urban, marine, etc.), the action of water (aerosol, rain, rising damp, condensation, and salt crystallization) and the static and dynamic loading patterns (Moropoulou et al., 2013).

The norm ISO 15686, classify the agents of decay of building components according to their nature. There are four types of agents (mechanical agents, electromagnetic agents, thermal agents, chemical agents, biological agents), table 1.

Table 1 - Agent categories in terms of nature and class (ISO15686-1, 2011)

Nature	Class
Mechanical agents	Gravity; Forces and imposed or restrained deformations; Kinetic energy (impacts); Vibrations and noises
Electromagnetic agents	Radiation (solar or ultraviolet radiation); Electricity; Magnetism
Thermal agents	Extreme levels or fast alterations of temperature
Chemical agents	Water and solvents (Air Humidity, ground water); Oxidizing agents; Reducing agents(Sulphides); Acids (Carbonic acid, bird droppings); Alkalis, bases (lime, hydroxides); Salts (Nitrates, phosphates, chlorides); Chemically neutral (Limestone, fat, oil)
Biological agents	Vegetable and microbial; Animal

The decay of materials under the environmental loads is not generalised. Each case should be dealt in the direction of revealing the specific active decay mechanism. This is performed at two scales, the macroscale, which focuses on determining the type of decay (morphology), and the microscale, which focuses on determining the decay rate and its susceptibility to decay. Non-destructive tests, unlike many analytical techniques, are advantageous as they can be used at both levels (Moropoulou et al., 2013).

2.2.2. MOISTURE

2.2.2.1. Introduction

Architectural heritage undergoes several decay processes due to the exposure to aggressive environmental conditions that threaten its durability and preservation. Moisture, whose presence may be due

to rain, condensation, construction humidity or capillary rise, plays a key role in the degradation of porous materials, being directly or indirectly responsible for several decay processes, such as freeze-thaw cycles, soluble salts crystallisation cycles, biological growth, chemical attack by acid rain and wind erosion (Gentilini et al., 2012).

There are three fundamental mechanisms for setting moisture: hygroscopicity, condensation, and capillary action. The mechanisms that determine the transport of moisture in building elements are complex. The diffusion and convective motions affect the transport in vapour phase whereas the capillarity, gravity and the effect of the pressure gradient control the transfer of moisture in the liquid phase. The transportation of moisture in liquid phase and vapour phase occurs simultaneously and depends on the conditions of temperature, precipitation, relative humidity, solar radiation, wind pressure and characteristics of the material (Freitas et al., 2008).

2.2.2.2. Rising Damp

Rising damp is a well known phenomenon and occurs when groundwater rises into the base of a construction and rise through the porous structure. There are two sources: the groundwater and surface water. The height reached by the capillary rise in a wall depends on factors like the amount of water in contact with the element, the conditions of evaporation at the surface, thickness, orientation, and the presence of salts (Freitas et al., 2008).

Ground water contains soluble salts, the most significant of which are chlorides, nitrates and sulphates. When rising damp occurs, this pass with the water up the wall, salts are left behind when the water evaporates. Both chlorides and nitrates are usually hygroscopic, (i.e. they can absorb moisture from the surrounding environment) and, in general, the greater the amount of salts, is higher the absorption of moisture, especially under humid conditions.

Water is an essential part of the process of brick and mortar manufacturing. In brick production, the wet clay is moulded and then fired to produce a structure with a network of pores. The pores are the residual volume that the evaporating water has left behind. Likewise in cement mortar, a large volume of unreacted water evaporates in the mortar curing process and leaves a network of pores behind. Similar pore networks are found in many types of natural stone. Pores and voids are inherently present in these building materials. It is these networks that subsequently become the pathways through which groundwater can rise as shown in fig 2.2 (Rirsch and Zhang, 2010)**.**

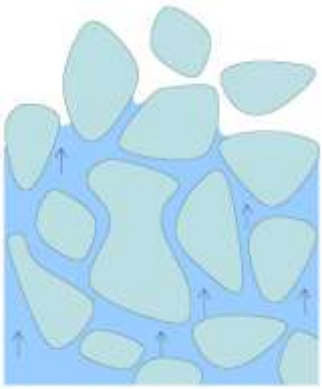

Fig 2.2 - Illustration of water flow through capillaries (Rirsch and Zhang, 2010)

Water has a strong affinity with the capillaries present in materials such a brick, mortar and stone. This affinity brings about the rise of water into the structure through the force of capillarity. The suction is greatest for small capillaries and inversely proportional to the pore radius as Jurin's law describes (1.1). The height of rise of water in a capillary (h) depends on the following equation where: γ = surface tension, θ = contact angle, r = capillary radius, ρ = liquid density and g = gravity.

$$h = \frac{2\gamma \cos \theta}{r\rho g} \tag{1.1}$$

Evaporation is an important factor in rising damp. The surface of an affected wall contains moisture that has risen from the ground and this moisture is then subject to evaporation. The factors controlling evaporation include: (i) temperature, (ii) humidity, (iii) air movement and (iv) surface condition.

The flow processes through the capillary structure form an equilibrium with evaporation. With evaporation introduced, the height of rise is governed by the factors relating to capillary pores, wall thickness and evaporation rate. Evaporation equilibrium is an n-shaped profile of water distribution. The equilibrium between capillarity and surface evaporation is schematically shown in fig. 2.3 (Rirsch and Zhang, 2010).

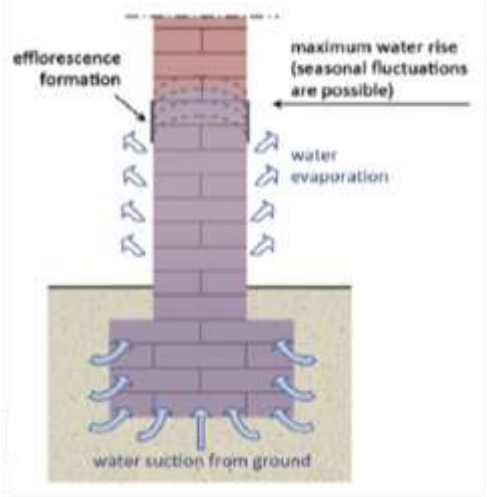

Fig 2.3 - Schematic diagram of a brick wall showing the equilibrium between capillary rise and evaporation (Franzoni, 2014)

The slow process of absorption of water into the structure with subsequent evaporation leads to the gradual deposit of salts in the wall. Moreover, the rising water can dissolve and redistribute the salts in the masonry, allowing high concentrations of salt to build up.

The consequences of the salt build-up are:

- The salts can block the pores and capillaries through which the water evaporates and push the rising damp front even higher;
- Moisture content is increased in the mortar from the hygroscopic nature of the salts with the possibility of attracting further moisture into the wall. This contribution would be relatively small in comparison with capillary moisture;
- Damage to the structure from constant dissolution and recrystallisation of certain salts is due to humidity and temperature changes. Sodium sulphate salts deposited from groundwater can be particularly destructive to the structures (Rirsch and Zhang, 2010).

Crystallization occurs in particular areas of buildings often corresponding to rising damp. This phenomenon carries different cations and anions including sulphates, nitrate, nitrite, sodium, potassium and calcium from the ground, the consequent crystallization of sulphates and nitrates leads to accelerated ageing associated with potentially major damage (Rirsch and Zhang, 2010). Moisture in building structures presents severely threatens both conservation and performance of ancient masonries, as it is responsible for:

- Degradation of building materials;
- Inappropriate indoor thermal–hygrometric conditions. Wet walls lead to high values of indoor air relative humidity and mould growth on cold surfaces, so causing uncomfortable indoor conditions;
- Poor thermal insulation efficiency of walls. The presence of water within building material pores affects their thermal insulation performance. Such unsuitable thermal transmittance implies a large energy consumption for heating historical buildings and a large environmental impact;
- Decrease in mechanical performance of the masonry. The presence of water within building material pores negatively affects also their compressive and shear strength (Franzoni, 2014)

2.2.3. SALT WEATHERING

Salt weathering is one of the most common deterioration mechanisms in porous materials and may lead to severe damage in buildings. In last decades, a lot of research has been devoted to explain the mechanisms of crystal growth and crystallisation pressure inside pores and their relation with crack propagation in materials such as natural stone, brick, mortar and concrete. The phenomenon of salt decay is emphasized by the presence of the mortar joint, faster vehicle of the salts However, the effect of salts on the structural behaviour of masonry has not been fully elucidated (Tedeschi et al., 2011).

The presence of salts is a major mechanism of degradation, it is based on the pressure of the formation of salts in the porous structure with an increase in volume and is dependent on the type of salts involved and the size and arrangement of the pores. The most characteristic salts are: carbonates, chlorides which absorb large quantities of water; nitrates of organic origin, being the most common calcium nitrate and sulphates that are hygroscopic, soluble and crystallize with increasing volume.

The major damage caused by the presence of salts are: surface changes (efflorescences and stains or moisture), cracking, crusting, separation of masonry materials in layers, loss of cohesion, mortar arenization, formation of voids (Freitas et al., 2008).

Micro and macroscale experiments which document the dynamics of salt damage to porous stone have produced data showing some weaknesses in earlier interpretations. Previously unexplained differences are found in crystal morphology, crystallization patterns, kinetics and substrate damage when comparing the growth of mirabilite (Na_2SO_4 $10H_2O$) and thenardite (Na_2SO_4) versus halite (NaCl).

No convincing and experimentally verified answer yet exists to the following question: Why are some salts more damaging than others? Moreover, there is little agreement on the importance of the various parameters contributing to salt weathering. For instance, some consider as more determinant the material's properties, others, the environmental conditions, while still others focus on the salt composition.

It has been observed that the presence of salt affects the structural behaviour of masonry depending on the type of salt and on the duration of the weathering cycles. Some research effort has been dedicated to investigate the damage mechanisms due to salt in materials such as natural stone, concrete and ma-

sonry. Several aspects have been considered, such as the generation of stress due to salt crystal growth and the consequent mechanical disintegration of pores, the pressure due to the confined crystallisation within stones, the crystallisation phenomenon in porous materials subjected to accelerated aging and the migration and crystallisation of salts within porous and cracked materials (Rodriguez and Doehne, 1999).

Efflorescence are salts crystals (fig2.4), usually white, that lay on the surface of bricks, mortars, roof tiles, ceramic tiles, concrete floors and masonry rock walls. The efflorescence formation involves processes of dissolution-crystallisation of salts and it essentially depends on three main aspects: presence of soluble salts, water and hydrostatic pressure.

Fig 2.4 - Salt crystallization in a brick wall (Tedeschi et al., 2011)

While the effects of moisture and salts on material degradation processes have been widely investigated, the effects of moisture and salts on the masonry structural performance still deserve further investigation (Gentilini et al., 2012).

In addition, little attention has been paid to the fact that a salt solution in a porous rock can reduce the mechanical strength of the material. Dunning and Huf (1983) demonstrated experimentally that the presence of a liquid in the pores of a rock submitted to stress, greatly increased the rate of crack propagation. They explained this phenomenon as a reduction in the interfacial tension between rock minerals, due to wetting by the liquid.

Considering the importance of this decay mechanism from a geomorphologic point of view, but also from a cultural and economic viewpoint, it is essential to reveal the fundamental mechanisms leading to salt damage, identify the main parameters controlling this process, and determine how a better understanding of salt weathering can lead to new methods of mitigating this problem in the fields of engineering and heritage conservation (Rodriguez and Doehne, 1999).

2.2.3.1. Sodium chloride and sodium sulphate

Not only these salt influence the process of salt weathering however only these two salt will be analysed with the experimental procedure described in this thesis. So, a brief theoretical information is presented.

Chloride salts deposited from the atmosphere are freely mobile and can rapidly accumulate in the masonry. The crystallization of chlorides may cause a build up of pressure in pores, this phenomenon is particularly damaging at the maximum evaporation level, and may also lead to an overall weakening of structural properties (Tedeschi et al., 1998). It is well known that in porous stones, NaCl precipitation on and beneath a surface depends on the solution supply and the evaporation rate according to the microclimate and the effective pore structure (Theoulakis and Moropoulou, 1999). Some salts are more soluble than others and therefore have a greater potential for penetration of fabric. Sodium chloride for example exhibits consistently high solubility values across a wide range of temperatures in contrast to calcium sulphate, which, in its pure form, has poor solubility characteristics (Warke, 2013).

Sodium Sulphate, which crystallize as the dacahydrate mirabilite (Na_2SO_4 $10H_2O$), or the anhydrous thenardite (Na_2SO_4), is known to cause greater deterioration and at much faster rate than a non-hydrating salt such as sodium chloride.

This damage potential has led to the widespread use of this salt for testing the durability of building materials. However, according to many authors the exact mechanism of sodium sulphate-induced decay is still not well understood. Cooke (1981) concluded that sodium sulphate is so damaging because: (i) sodium sulphate undergoes a high degree of volume change when hydrated; (ii) sodium sulphate suffers a decrease of solubility at temperatures above (slow decrease) and below (rapid decrease) 32,4ºC; (iii) is very soluble, thus a substantial quantity of solid salt is available for crystals to grow when evaporation takes place; (iv) the needle-shaped nature of sodium sulphate crystals might tend to increase their destructive force due to the crystallization pressure being concentrated over a smaller surface area (Rodriguez and Doehne, 1999).

2.2.3.2. Crystallization

Salt crystallization tests have been used since 1828 to evaluate the durability of construction material. However, recent debate as to the suitability of the standard sodium sulphate test for aggregate durability has also brought into focus our imperfect knowledge of this process

Salt crystallisation cycles deserved particular attention, since they cause pressure inside porous materials (sub-florescence) and may induce the rupture of the pores walls, leading to disruptive effects, such as pulverisation, crumbling, blistering and flaking. Bricks as well as natural stones react to salt weathering in a similar way.

In the first phase, salt crystals grow favourably in the larger pores, connecting with the empty evaporation channels, and being supplied by solution from the next smaller pores. In a second phase, the crystals already exceed the pore size and overlap other smaller pores. As the rate of evaporation exceeds the solution supply, the solution retires and the substrate dries out, the area where the crystal contacts the solution is reduced, and consequently, crystals grow. The pressure exerted by crystallization against the pore walls, when the crystals fill entirely the coarse pores and continue growing, leads to disruption (Theoulakis and Moropoulou, 1999).

The pressure inside the porous varies not only with the type of salt but also with different hydrates of the same salt. Because the inverse relation between crystal growth pressure and molar volume, hydrates of a salt exert lower crystallization pressures that the anhydrous salt. Thus, for example, the anhydrous form of sodium sulphate, thenardite (Na_2SO_4), creates higher crystal growth pressures than decahydrate, mirabilite (Na_2SO_4 $10H_2O$). Thus, the morphology and growth rate of the formed salt crystals appear to be important keys to understanding this particular decay phenomenon.

Another important issue to be dealt with when approaching salt decay problems is the difference between the process of salt crystallization on the surface of a porous material (efflorescence) and the crystallization within the porous (subefflorescence). Efflorescence, while appearing impressive, typically results in little damage to the material, whereas, on the other hand,, the latter typically creates extensive damage. Certain salts are prone to effloresce, while others crystallize more often inside a pore, and it is important to understand why. Environmental changes, mostly relative humidity, can promote changes in the location and/or in the way salt crystallization and growth take place, either promoting the formation of efflorescence or generating sub efflorescence (Rodriguez and Doehne, 1999).

Salt crystallization is a complex mechanism, with its effectiveness determined by factors such as fluctuating temperature and humidity conditions and the solubility and crystallographic properties of different salts. Strong evaporation and high temperatures favour effective crystallization, although some salts such as sodium sulphate exhibit a significant decrease in solubility when temperatures decrease.

The crystallographic characteristics of salts are also important in determining their efficacy. For example, salts with an acicular (needle-like) crystal nature (e.g., calcium sulphate, sodium sulphate) and a preferred crystal orientation appear to be the most effective in producing breakdown primarily because of the focused crystal growth pressures exerted on confining pore walls and within micro fractures.

2.2.3.3. Hydration/dehydration

Some salts exhibit significant volumetric change associated with phase change as they alter from dehydrated to hydrated forms and vice-versa. The volumetric increase or decrease associated with such phase changes can be considerable.

Not all salts exhibit phase change, sodium chloride, for example has no stable hydrated format temperatures above 0ºC and is therefore ineffective with regard to rock breakdown through the formation of hydration pressures alone, however it is a deliquescent salt, which means that it is strongly hygroscopic, readily absorbing moisture from the atmosphere. Deliquescence differs from phase change in that the former results in salt absorbing sufficient moisture to go into solution (Warke, 2013).

2.2.3.4. Thermal expansion / contraction

A wide theoretical knowledge exists regarding the potential role of volumetric expansion and contraction of salt crystals associated with heating and cooling but not knowledge based on actual data from field and real laboratory studies. It's almost impossible not to connect the disruptive weathering effects directly attributable to salt crystallization in the first instance from those resulting from subsequent thermal expansion and contraction. As Smith et al.(2005) suggest, the actual disruptive effect of repeated expansion and contraction of salt in pore spaces within surface and near-surface layers of material may be minor in comparison with the effects of the other salt weathering mechanisms and may operate over long time periods but it should not be discounted because of this (Warke, 2013).

2.2.3.5. Chemical dissolution effects

The chemically disruptive effect of salt is commonly ignored in a general review of salt weathering, However, the combination of salt and moisture creates alkaline conditions that have the potential to

destabilize normally stable and durable elements with release of material through disintegration creating openings for subsequent moisture ingress (Warke, 2013).

2.3. INSPECTION PROCEDURES

Knowledge of historic masonry building is a fundamental prerequisite both for the purpose of a reliable assessment of the building safety and for the choice of an effective intervention., the problems are the same as in the other type of buildings, although in the case of heritage buildings, even more, it's important to know the original features of the building, the changes suffered over time due to the phenomena of damage resulting from human activity, aging of materials, catastrophic and accidental events, etc.

However, sometimes, the execution of a complete campaign survey may be too invasive. So, there is a need to refine techniques of analysis and interpretation of historical buildings through the different stages of degree of reliability, even in relation to their impact (culturali, 2010).

Knowledge can, be achieved, with different levels of detail, depending on the accuracy of the survey operations, historical research and experimental investigations. These operations will be function of the final objective and will be interesting for all or just one part of the building, depending on the type of intervention.

Thus, it is proposed a methodological path, with an increasing knowledge of the structure that is used to assessing the current state and the future interventions:

- The identification of the building, its location in relation to particular areas at risk, and the relationship with the context of the urban environment;

- Functional characterization of the building and its spaces. The functional evaluation is aimed at recognizing what uses have succeed in time and in such environments. It is important to understand some of the reasons for the structural and geometrical changes over the time;

- The eventual action of significant environmental conditions, such as, climatic effects, sudden temperature changes, fire, or any accidental loads (impacts, etc.) (Modena et al., 2010);

- Geometric survey of the building in its present state, as descriptions including all the damages found (deformation, cracking, etc.). Identification of the plan-altimentric characteristics of the constituent elements. Therefore, will be detect the geometry of each masonry element, the location of possible niches, cavities, openings closed, chimneys, and types of foundations. The difficulties are linked to the accessibility of some spaces, such attics, false ceilings, roofs or the excessive height of the elements. However there are tools like endoscopy (direct investigation) and IR Thermograpy, GPR radar (indirect investigation) available that give a quick survey and a accurate return, even in the case of complex elements;

- Identification of the components of the resistant structure, including materials and components with a particular focus to the constructions techniques, construction details and the connections between the elements. The resistant structure of the building and the quality and condition of materials and constituent elements should be identified. This recognition requires the acquisition of information often hidden, so thanks to some non-destructive techniques like IR Thermography, GPR Radar, Sonic Tests or Endoscopies, it can be performed (culturali, 2010);

- In the preliminary inspection it will als important to verify which agents are degrading the building in a particular way. In fact, those effects are often aggravated if adequate measures have not been taken during construction (adequate drainage, for example), or, if there has not been efficient conservation of the building;

- Mechanical characterization of materials is one of the most important points of the project. Visual inspections and some investigations can allow to reach a good knowledge and assessment of the quality materials and their degradation. To make a quantitative analysis of the structure, some mechanical parameters could be necessary, like deformability and resistance of materials, mainly in masonry. Non destructive techniques, can be used to assess the homogeneity of the mechanical parameters in different parts of the building but do not provide direct quantitative values. The direct measurement of the mechanical parameters of the masonry, just can be performed by semi-destructive or destructive tests even in small portions. Both type of test can be complementary used to reduce the invasiveness of the investigation. The characterization of the constituent elements like mortar, bricks or stone can be performed on-site or in small samples collected and analysed in laboratory;

- Knowledge of the subsoil, foundations structures and changes that occurred over time. It will still be important to obtain information about the geotechnical conditions of the soil supporting the foundations of the building. If there are degradations in the lower part of the building, it will be convenient to get samples of the soil, in order to verify if there is contamination by aggressive substances, like sulphates, etc (Modena et al., 2010);

- Finally, monitoring the building is the main tool for a good preservation of the structure because it allows the implementation of a maintenance programme and actuate it when it is necessary**.** The monitoring of the building consists in the measurement of parameters, such as deformations, movements of cracks, temperature variations, etc., in strategic points of the building, at certain moments, during a certain period of time (culturali, 2010).

This description of procedures illustrates the difficulty faced by the designer who must select the most technically and economically correct method to define the state of preservation or damage of the structure.

When the design of the survey is previously available, then conclusions from the experimental and numerical investigation will bring to the diagnosis the real state of the structure. Since every investigation described in the previous sections has its cost, it is evident that every single operation must be designed to obtain the results desired by the designer.

A survey can never be considered as a stream of required steps, but must be designed every time according to the knowledge requirements for the building under consideration (Binda et al., 2000).

Information can be available from in situ and laboratory surveys shows how they can define the procedure and the input data for the structural analysis, fig 2.2.

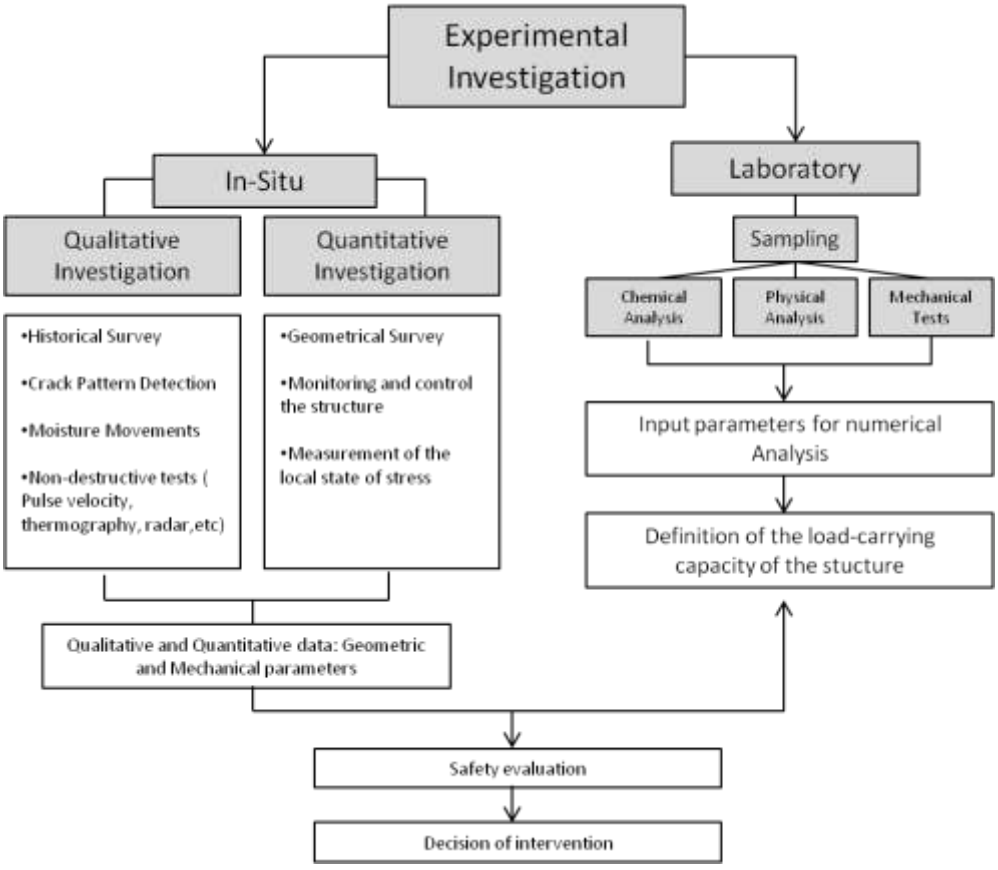

Fig 2.5 - Input data for the structural analysis adapted from (Binda et al., 2000)

The diagnostic is a very delicate task, because the available data refers to the symptoms while the causes that are their origin, are what needs to be identified. So, intuition and experience are essential components of the diagnosis.

2.4. APPLICATION OF NON DESTRUCTIVE TESTS

The structural performance of masonry structures can be understood through the history of their construction, their geometry, the characteristics of their masonry texture, and the characteristics of the masonry as a composite material. In order to obtain all these data, on-site testing program, which can involve the application of different test methodologies as a combination of destructive tests (DT), minor destructive tests (MDT) and non-destructive tests (NDT), should to be performed (Bosiljkov et al., 2010). Methods of non-destructive test and moderately destructive test are research tools that can be applied with or without small interventions in the examined object, considering that the damage caused by the MDT tests are irrelevant, so when referring tests belonging to the two groups, is used only the acronym NDT.

NDT can be grouped into two main groups: those that allow to obtain qualitative analysis and those that allow quantitative analysis of the materials tested. There are a number of ND techniques capable of being used for characterizing masonry but there are not a technique that itself provides entirely reliable results, instead, various techniques of NDT must be used to reach an outcome closer to reality.

Depending on the particular problem and methodology, ND techniques are useful for an initial assessment of large areas of a structure prior to the execution of the intervention projects. These tech-

niques can also be applied in long-term observations (monitoring) or used as quality control after repair operations. Generally, the applications of NDT techniques are a part of the overall investigation of the building. They do not replace other investigative techniques however in case of historical monuments, NDT testing should be chosen instead of traditional tests (Maierhofer and Köpp, 2006). These aims may be achieved by the application on site of some categories of NDT, if the application procedures, the level and extension of the application, the testing aims and possible use of the results are well clear to the user or to the subject responsible of the investigations, the information gained by this experimental evaluation may also be used as input calibration information into analytical models properly applied for structural safety, and in discriminating the choice of intervention techniques (Pascale et al., 2005).

However it is very often difficult to apply the results of an investigation, even a very good one, when the designer is not sufficiently skilled. In that case a great amount of data remains unused or can be used incorrectly. It must be clear that even if there is a need of consulting experts in the field, it is the designer, or a member of the design team, who must be responsible of the diagnosis. Thus, information is needed for architects and engineers on the availability and reliability of the investigation technique (Binda and Saisi, 2001).

The first applications of NDT techniques to cultural heritage on site dates back to about 20 years ago, but it was in the last decade that their use has become more extended and consolidated, thanks to a better comprehension of testing procedures and capabilities. Recently, several investigation procedures have been implemented, whose aim is to use as much as possible, NDT techniques but most of the procedures can give only qualitative results (Binda and Saisi, 2001).

Dynamic and estensimetric monitoring, infrared thermography, radar investigation, ultrasonic and sonic pulse velocity are the most sophisticated non destructive methods applied to in-situ investigation and can be applied for various purposes:

- Detection of hidden structural elements such as slabs, pillars and arches;
- qualification of masonry and masonry materials, mapping of nonhomogeneity of the materials used;
- Evaluation of the extent of mechanical damage in cracked structures;
- Detection of the presence of voids and flaws;
- Evaluation of moisture content and capillarity rise;
- Detection of surface decay;
- Evaluation of mortar and brick or stone mechanical and physical properties;

The correlations between the data of non-destructive evaluations and mechanical and physical properties of masonry are quite complex, especially stone masonry, mainly because of their heterogeneity (Binda et al., 2000).

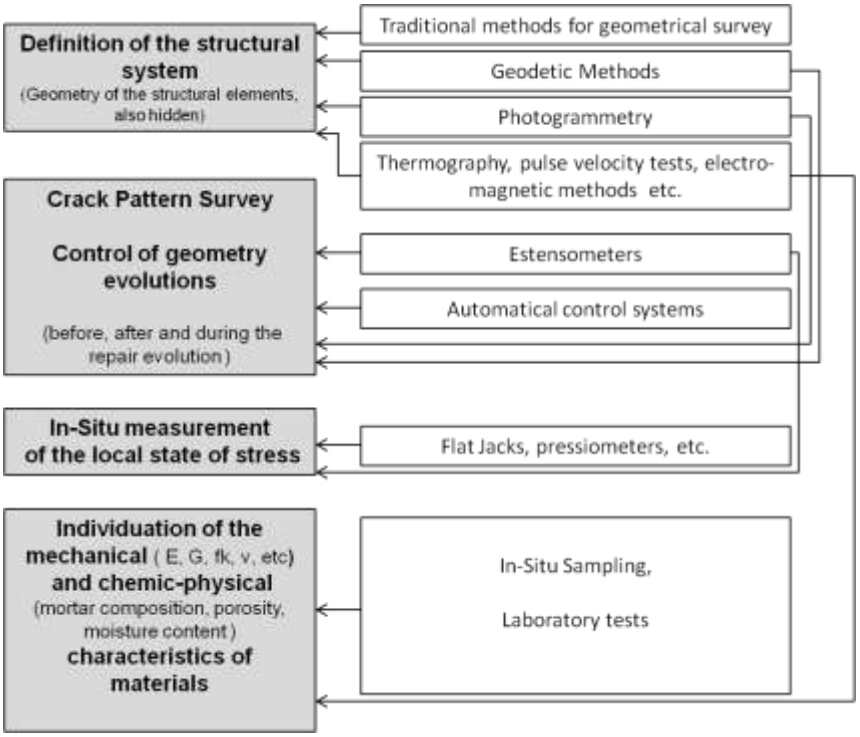

Fig 2.6 - Information required and the correspondent investigation techniques, adapted from (Binda et al., 2000)

The application to masonry of NDTs, although advanced, can be sometimes frustrating due to several factors, like the differences in masonry typologies and materials, inonhomogeneity of the materials, the interpretation of the results of each single technique but also the harmonisation of the results. Furthermore, most of the NDTs come from other research fields and applications to more homogeneous materials as steel and concrete and need a specific calibration.

Non destructive techniques have to be applied according to the needs of the buildings so it is important before choosing the appropriate NDT technique to know which type of problem has to be solved. The solution of some difficult problems cannot be reached with a single investigation technique, but with the complementary use of different techniques. To this purpose it is important the production of guidelines for the correct application of investigation techniques to diagnosis problems of different classes of masonries. The procedures for in situ research began to be applied before testing its effectiveness and application problems particularly masonry. Extensive research in the interpretation of results of non-destructive testing and the correlations of these with the characteristics of the masonry is still required. Knowing that no test can provide the necessary information individually, there is also a need to investigate the complementary relationships between different tests for a correct definition of the physical and mechanical properties of masonry (Binda and Saisi, 2001).

3

NON-DESTRUCTIVE TESTS

3.1. ACOUSTIC TECHNIQUES - PRINCIPLES

When a solid is excited by a continuous or impulsive vibration applied at a point of its surface, mechanical waves are propagated. A wave can be defined as a disturbance that propagates without transportation of material. The waves propagation in solid medium are quite similar to the acoustic waves that propagate in the air. For this reason, we generally speak of acoustic or sound waves and make reference at the physical laws of acoustics. When a wave propagates in a solid there is no movement of the subject but propagation of energy happens from the point of emission (Pascale, 2008).

Methods based on elastic wave propagation provide an overall qualitative response of the masonry, detect and relate the physical properties of the wall and its materials with the integrity, load carrying capacity, geometry and characteristics of the section. In addition, in the appropriate conditions they may deliver detailed information related to the masonry texture, depth of discontinuities, the location and size of defects and inner features.

Conventional ultrasonic and sonic techniques operate in transmission or single reflection of the signal, with the receiving transducer positioned in different configurations with relation to the input point. Contrary to these, another acoustic method, the impact-echo method, operates by multiple reflection of the signal and the data analysis is carried out in the frequency domain instead of the time domain. Together these methods have achieved a number of goals in the investigation of concrete and masonry, also thanks to recent developments and applications (Pascale et al., 2005).

Tests can be conducted according to three ways of data acquisition, fig 3.1:

- Direct transmission or through-wall: In this type of tests the hammer and accelerometers are placed in line on opposite sides of the masonry element. The stress wave goes through the thickness of the wall. The points of emission and reception of stress wave are aligned on opposite sides of the element. The speed of the sonic pulse detected is then affected by the quality and consistency of the section of the masonry.

- Semi-direct transmission tests: In which the hammer and accelerometers are placed at a certain angle to each other;

- In indirect transmission tests the hammer and accelerometer are both located on the same face of the wall in a vertical or horizontal line. The stress waves recorded using this transmission

method are those which generally pass through the wall face. Thus, the quality and consistency of the wall face will affect the detected values of the speed of the sonic pulse. For a complete evaluation it is necessary to check the transmission of acoustic waves in both horizontal and vertical directions (Binda et al., 2000).

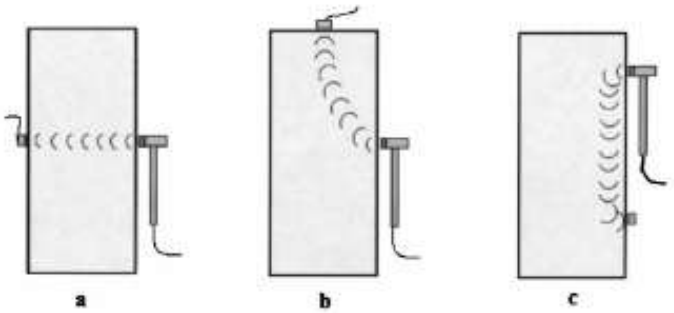

a) Direct transmission b) Semi-direct transmission c) Indirect transmission

Fig 3.1 - Schematic representation of the method for acoustic testing (sonic tests) (McCann and Forde, 2001)

When a disturbance is applied suddenly at a point on the surface of a solid, such as by impact, the disturbance propagates through the solid as three different types of stress: P-wave, S-wave and R-wave, Fig 3.2. Longitudinal waves or compression waves (P-waves) have the direction of vibration of particles, parallel to that of the wave propagation. Each particle moves in the same direction of the wave moving forward to backwards from its potion of balance. Thus, there are areas of rarefaction (low pressure or cold zones) and zones of compression (high pressure or hot zone). Longitudinal waves are also known as P waves: their symbol comes from the Latin "undae primae" because, having the greater speed of propagation than the other waves, arrive first in the area of observation. In the presence of transverse or shear waves (S waves), the particles vibrate perpendicularly to the direction of wave propagation. The propagation of these waves occurs only in the solid mediums. The shear waves are also known as S-waves, the symbol takes origin from the Latin "undae secundae" because their speed is lower than that of the waves P. Surface waves or Rayleigh (R-waves) are originated from the incidence of P waves can spread on the surface layer of the medium. Rayleigh waves have a speed of propagation in solids equal to 92% of the waves S. The surface waves are similar to those that occur on the surface of the water and are characterized by longitudinal and transverse displacements of the particles in the plane of propagation of the wave itself (Menditto and Menditto, 2008).

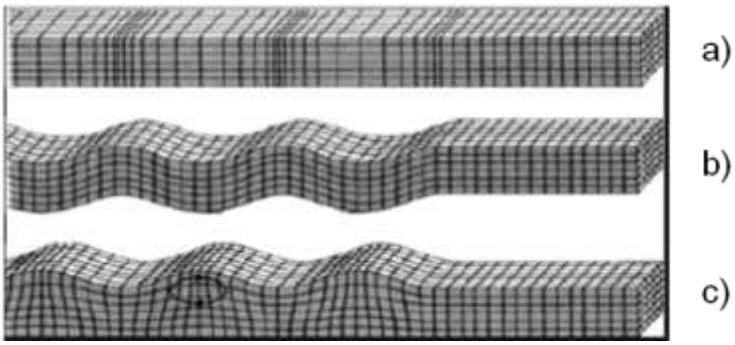

Fig 3.2 - a) P-waves; b) S-waves; c) R-Waves (Carino, 2001)

The longitudinal waves present maximum amplitude in the direction of impact and their energy dominates that of shear waves. For this reason, propagation and reflection of these waves, faster than shear one, is generally preferred in wave techniques.

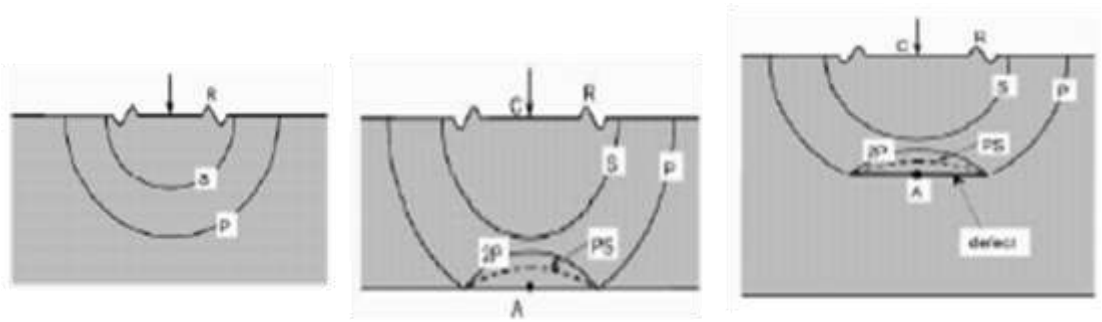

Fig 3.3 - a) Propagation of S,P and R waves (left) ; b)- Reflection due to the an opposite surface (middle); c) Reflection due to an internal defect (right) (Pascale et al., 2005)

The data collected by the acoustic tests can be analyzed in both the time domain and the frequency, the latter using the Fourier transform. In the time domain, analyzes the velocities of compression waves and surface, while in the frequency domain analyzes the phase speeds (speeds characteristic of a certain period) and the coefficients of attenuation.

Wave reflection happens at layer interface with sufficient acoustic impedance and dimensions in relation to signal wavelength, such as at external surfaces and/or internal targets, Fig. 3.3 b) and 3.3 c): where *z* is the impedance, ρ, the material density and Vp , the wave velocity.

$$z = \rho . Vp \tag{1.2}$$

Analysing a monodimensional solid, homogeneous and isotropic, the wave propagation velocity is a function of the material density and of its mechanical properties, where E is the elasticity modulus of the material:

$$Vp = \sqrt{E/\rho} \tag{1.3}$$

Otherwise, applying to a tridimensional solid, the equation to determinate the velocity of the P-waves is that present below, where the $\boldsymbol{\upsilon}$ is the Poisson ratio:

$$Vp = \sqrt{\frac{E}{\rho}\frac{(1-\upsilon)}{(1+\upsilon)(1-2\upsilon)}} \tag{1.4}$$

Besides that, the minimal signal wavelength, λ, is inversely proportional to the maximum frequency of the generated wave.

$$Vp = f . \lambda \tag{1.5}$$

Therefore, with increasing frequency, the wavelength decreases, thus improving data resolution. It follows that the resolution of the smallest recognisable feature is directly related to the dominant wavelength of the employed wave, besides the size and geometry of the tested element.

Nevertheless, the wave frequency content also determines the propagation distance of the wave in the material. In fact, if high frequency components, those with small wavelengths, are suitable for locating small or superficial features, they are characterised by less energy and greater attenuation due to absorption and scattering in the masonry .The rate of attenuation is directly proportional to the frequency increase, limiting the thickness of wall section that can be tested. However, if the wave contains sufficiently small wavelengths, a defect or other anomaly can be located depending on its lateral dimensions and depth (Pascale et al., 2005). Consequently, the measurement of the velocity and attenuation of mechanical waves can be used to assess changes in material properties, detailed information related to the texture of the masonry, the depth of discontinuities and the location and size of defects or inside features (Cascante et al., 2008).

Wave attenuation and resolution are two important limiting parameters of the wave techniques. From those it depends the choice of signal frequency to be used on site, according to the testing aims and conditions (Pascale et al., 2005).

3.1.2. SONIC TESTS

3.1.2.1. Introduction

The first applications of sonic tests to the evaluation of masonry materials and structures have been carried out a long time ago in the 1960s. The difficulty of interpretation of the results in the case of inhomogeneous materials like masonry was always known and the first results were clearly interpreted as qualifying rather than quantifying values.

The analysis of materials and structures by sonic pulses has been used for various purposes from assessing the dynamic properties of a structure to the detection of flaws in masonry. The method has been used also to relate pulse velocity to the mechanical compressive strength of the masonry. Besides that, the use of sonic tests for the evaluation of masonry structures has the following objectives: (a) to qualify masonry through the morphology of the wall section; (b) to detect the presence of voids, flaws and to find crack and damage patterns; (c) to control the effectiveness of repair by injection technique; (c) to detect changes in the physical characteristics of materials.

However, there are some limits to sonic tests in masonry such as the cost of the operations due to the high number of measurements which has to be carried out; difficult elaboration of the results due to the difficulties created by the inhomogeneity of the material and the need for the calibration of the values to the different types of masonry (Binda et al., 2000).

3.1.2.2. Working principles and equipment

Pulse velocity tests are based on the generation of sonic impulses in the form of an elastic wave at a point on the structural element surface. This wave is obtained by a percussion device, generally a medium size instrumented hammer. The hammer tips are usually interchangeable to fit the different site conditions and to adapt to the material surface stiffness and roughness.

A smaller or stiffer tip would produce a higher frequency wave. Adopted input frequencies in the case of sonic tests are around 5 kHz or lower. These low frequencies are ideal for crossing considerable masonry and concrete thickness, although their large wavelengths are to the detriment of resolution. (Pascale et al., 2005)

The equipment to perform sonic tests consists of impulse hammer to initiate the stress waves and piezoelectric accelerometer to measure the vibrations of the wall, resulting from the propagation of the waves. Hammer and accelerometer are connected to an amplifier and an analogical-to-digital converter, coupled to a laptop computer, in order to view in real time and store both the generated impulse waves and the propagating pulse waves do (Porto et al., 2003).

Once the signal has crossed the material, it is picked up by a receiver which can be a displacement transducer or an accelerometer. The instrumentation allows reading the time of arrival of the signal between in and out points from which the signal propagation velocity in the material may be calculated by knowing the relative distance of the in and out positions (Pascale et al., 2005).

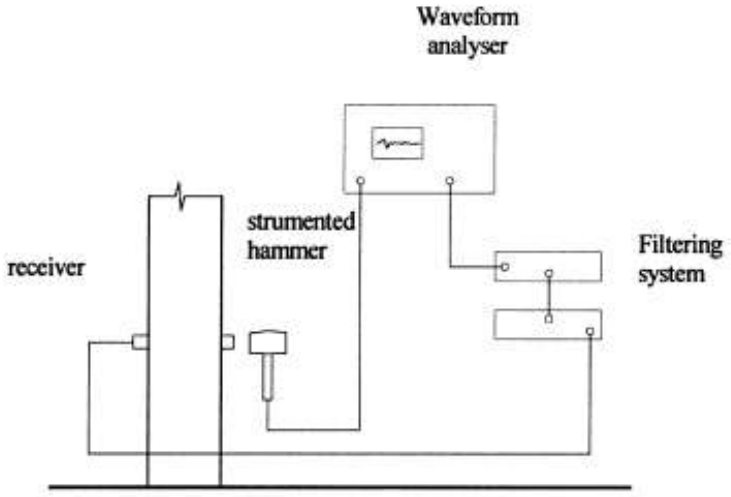

Fig 3.4 - The sonic test equipment (Binda et al., 2000)

3.1.3. SONIC THOMOGRAPHY

3.1.3.1. Introduction

Tomography, from Greek "tomos" (slice), reproduces the internal structure of an object from measurements collected on its external surface. Tomographic imagining is a computational technique which utilizes an iterative method for processing a large quantity of data.

Among the ND applications applying wave propagation, the tomographic technique is very attractive for the high resolution that can be obtained. Tomography, developed in medicine and in several other fields, seems to be a valuable tool to give two or and three dimensional representation of the physical characteristics of a solid (Binda et al., 2000).

3.1.3.2. Working principles and equipment

Sonic tomography represents an improvement in the sonic test method not only because it combines direct and indirect methods but also because tests are performed in the direct mode also along paths which are not perpendicular to the wall surfaces.

The testing technique gives a map of the velocity and/or attenuation distribution on a plane section of the structure under investigation. The method consists in obtaining the travel time taken by a wave along in several directions, which uniformly cover the section under investigation by a dense net of

raypath. The computation of velocity is made by using the inversion process which, starting from the time of signal propagation, reconstructs the velocity field and create a three dimensional reconstruction of the velocity distribution across the structure. So that local variations in velocity can be identified and correlated with zones of weakness or flaws in the internal fabric of the structure

3.1.4. ULTRASONIC TESTS

3.1.4.1. Introduction

Ultrasonic testing is a non-destructive method that detects surface and sub-surface flaws or discontinuities in materials. It is commonly used in construction sectors, mainly to identify flaws (cracks, inclusions, etc.) in materials, also can provide, non-destructively, the elastic properties of historic building materials, in particular, the elastic constants parameters (dynamic modulus of elasticity (E_d) and Poisson ratio ($\boldsymbol{\upsilon}$)).

As the ultrasonic wave propagation velocity can be correlated with some of the materials microstructure parameters and since decay directly affects the microstructure of materials, ultrasonic testing is often used to assess their decay state. Furthermore, ultrasonic tests can determine the depth of the decayed layer within a material which is evaluated using the indirect ultrasonic (Moropoulou et al., 2013).

Ultrasonic technique successfully used for the detection of flaws in metal castings and is the first non-destructive technique that was developed for the testing of concrete. However, it is much less practical masonry, which have much higher attenuation characteristics and lower frequency signals are required to obtain a reasonable penetration. In addition, the numerous material boundaries in these materials result in scattering of both incident and reflected waves. Despite this fact, it has been successfully used for identifying and locating specific flaws in concrete and is also applicable to the investigation of small defects within masonry walls due to a number of technical difficulties. In the case of ultrasonic signals the main factors to overcome are the need for good coupling of the transducer to the surface, which is often rough, and the scattering of the wave due to material heterogeneity. This makes the process of moving the points of measurement quite slow and it is often difficult to achieve adequate coupling on some irregular surfaces.

Scattering of the signal limits the propagation through the material and also leads to a complicated series of return signals. This makes it difficult to identify defects amongst the noise. In addition, surface waves, which travel more slowly than the compression waves, may arrive at the receiver within the same time interval and confuse interpretation. Further developments of the ultrasonic technique, for example improvements in signal generation, detection and data processing are underway and may lead to a practical tool if the problems mentioned above are overcome (McCann and Forde, 2001).

3.1.4.2. Working principles and equipment

The ultrasonic being mechanic waves, they have a strong interaction with matter, especially in the solid state and are therefore suited to provide a lot of information on the properties of the medium with which they interact. High-frequency sound waves are introduced into the examined surface which travel through the material with some loss of energy (attenuation) and are reflected at any interfaces encountered. The reflected beam is then detected on the surface and analysed to determine the presence and location of flaws or discontinuities. The generation of a train of ultrasonic impulses is carried out by an ultrasonic transmitter generally operating at frequencies around 50 kHz (Menditto and Menditto, 2008).

A transducer when is placed on the surface of a solid will transmit several kinds of waves. The transducer will transmit plate waves (P and S waves) in an axial direction as well as edge waves, including P and S waves, in a radial direction. When a transmitter and a receiver are positioned in a surface of the material to the tested, the waveform is generated like is shown in fig 3.5.

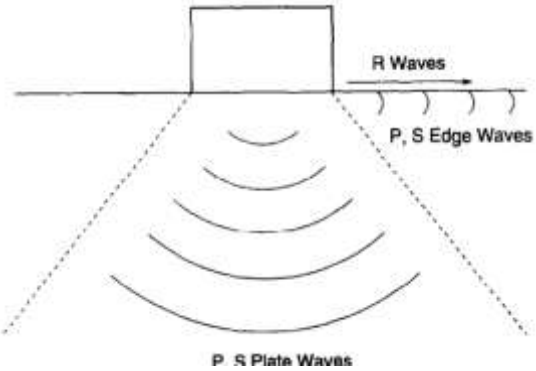

Fig 3.5 - Types of waves generated by a transducer (Qixian and Bungey, 1996)

The front of the waveform should be due to P waves because these have the greatest velocity, however the amplitude of the P waves is very low. The leading edge of P waves is indicated as "1" in figure 3.6. The increase in amplitude of the following waveform should be due to the arrival of R waves because although the velocity of R waves is lower than that of P waves, they are much stronger. The arrival of R waves is indicated as "2" and the first peak of the arrival is indicated as "3".

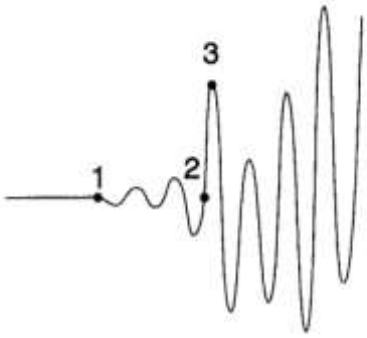

Fig 3.6 - The waveform received and its characteristic points (Qixian and Bungey, 1996)

The velocities of P and R waves which propagate along the surface of the solid can be calculated after measuring the time from the start of transmission to point 1 and point 2 for any distance between transmitter and receiver (Qixian and Bungey, 1996). The ultrasonic signal, after crossing the material, is picked up by the receiving unit, which is usually positioned on the opposite side of the wall, either exactly opposite the input position or at some angled distance (Pascale et al., 2005).

A tool for ultrasonic control, comprises at least one transmitting section, which has the task of generate the ultrasonic vibration to be introduced in the element under consideration and a receiving section which has instead to collect, amplify and analyzer ultrasound that, after having crossed the element, bring the information relating to the possible presence of defects.

The ultrasound are mechanical vibrations, while the greater part of the available instruments employs electronic systems both for the receiving section, and for the transmitting, thus it is necessary one or

more transducers capable of transform the mechanical vibration into electrical signals and / or vice versa (Pascale, 2008).

In the fig 3.7, a schematic process of ultrasound test is presented:

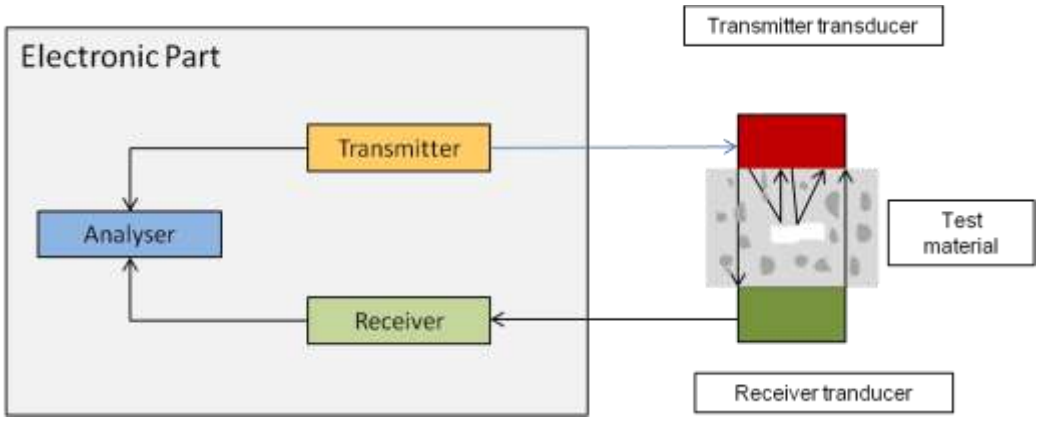

Fig 3.7 - Schematic process of ultrasound test. Adapted from (Pascale, 2008)

Two parameters can be evaluated from the measurements of ultrasonic transmission: the first is the change of the time of flight and the second is the attenuation as the reduction of the pulse amplitude from the received signal. Different researches have shown that the latter is more suitable because of its higher sensibility with respect to the alteration of material properties (Kroggel et al., 2006). Attenuation of the intensity of an acoustic vibration during its propagation in the medium is due to the divergence of the pattern (attenuation geometric), waves moving away from the origin, the energy input is distributed on surfaces of increasing extension and attenuation related to the constitution of the material traversed (structural attenuation) (Pascale, 2008).

The number of collected measurements depends on the aims of the tests. If a punctual estimate of the signal velocity in the material is to be achieved, the average of some readings may be sufficient, but if the testing aim is, for example, an estimate of the inner configuration of the wall or the damage detection, a much higher number of readings may be necessary. The limitations in signal attenuation of ultrasonic waves make the sonic tests more appealing for masonry (Pascale et al., 2005).

3.1.5. IMPACT-ECHO

3.1.5.1. Introduction

The National Institute of Standards and Technology (NIST), formerly known as the National Bureau of Standards (NBS), has historically provided the basis for measurements in the area of public health and safety. Research conducted in the 1940s to the 1960s provided the technical basis for standards on classical NDT methods employed routinely by industry, such as X-ray radiography, ultrasonic methods, and magnetic methods.

In 1983, the focus of NBS research on NDT of concrete shifted toward the detection of internal defects. Based on a review of available methods, it was decided to develop a test method based on stress waves, since stress wave propagation in a solid is affected directly by mechanical properties. In 1987, research shifted to Cornell University, under the direction of Professor Mary Sansalone. The Cornell research expanded the applicability of the method and resulted in the development of the first patented field instrument. In addition, Sansalone and Streett [1997] produced a book that provides a compre-

hensive summary of the results of analytical, laboratory, and field studies dealing with different applications of the method. The book also provides practical guidelines for field-testing.

In the late 1990s, NIST and Cornell cooperated on the development of a draft standard test method on the application of the impact-echo method. ASTM adopted the standard in 1998 (Carino, 2001).

Impact-echo can be used to determine the localization and extent of flaws such as cracks, delaminations, voids, honeycombing and debonding. The method can be also used to determine thickness or to locate cracks, voids, and other defects in masonry structures. When properly used the impact-echo method has achieved unparalleled success in locating flaws and defects in highway pavements, bridges, buildings, tunnels and other types of structures (Sensalone and Streett, 1997).

3.1.5.2. Working principles and equipment

The impact-echo method is an acoustic technique which makes use of the multiple reflection of low frequency waves (typically up to 50 kHz) in the section of material. These are excited by mechanical impact of a small steel hammer on the surfer of the structure that generate elastic waves. The receiving transducer can be a displacement transducer or an accelerometer and is located adjacent to the impact point and it measures the wave reflections after the impact. The train of wave echoes produces transient resonances in the section of the structural element, whose frequencies depend on the element geometry and material characteristics (Pascale et al., 2005).

The impact-echo method focuses on multiple P-waves reflections between the impact surface and the opposite surface or intermediate interfaces with sufficient impedance variation and dimension in comparison with the wavelength employed. Relevant signal reflections in the structure are highlighted by the frequency position of peaks with dominant amplitudes. The depth (d) of each reflector could be calculated by dividing the wave velocity (v) by twice the measured frequency (f) of the peak on the frequency spectrum as shown in fig 3 (Colla and Lausch, 2003).

This signal is recorded as a waveform in a time window of a few milliseconds. Through a Fast Fourier Transform, the time domain signal is transformed in a frequency spectrum, which highlights the frequency components and amplitudes, fig, 3.8.

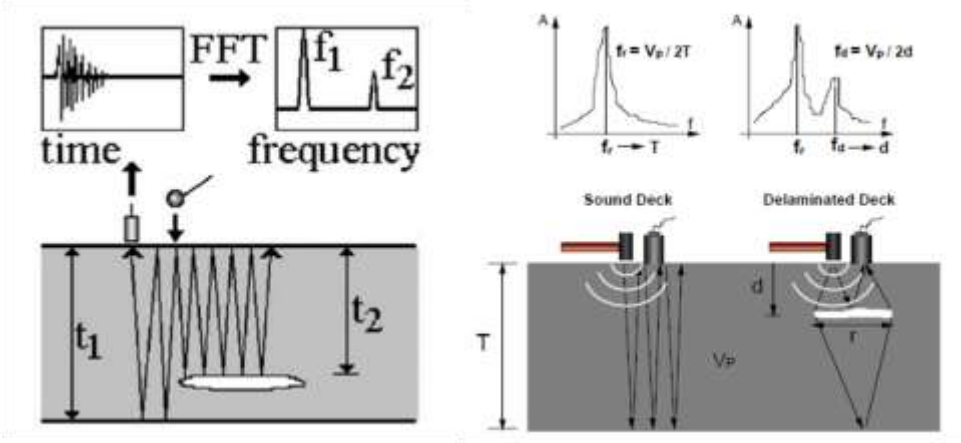

Fig 3.8 - Principle of the IE technique (Colla and Lausch, 2003) (left); Evaluation using IE (Shookouhi et al., 2006) (right)

Analysis of the registered waveforms takes, then, place in the frequency domain, where the predominant signal frequencies appear as peaks. The measured transient resonance frequencies serve to calcu-

late the section thickness and the depth of any internal feature. The peaks' position, amplitude and shape are useful parameters to evaluate the structural integrity of the tested element. An important discriminating criterion between the peaks on the spectrum is their amplitude. This parameter can be largely influenced by the frequency content of the wave, consequently it is necessary to carefully select the impact source (Pascale et al., 2005).

One disadvantage of the technique is that essentially all stress wave energy is reflected at air boundaries, and no information can be obtained on materials beyond an initial void or delamination. The method also provides limited localized information, requiring a series of point-by-point measurements to map larger regions (Schuller, 2003).

The wave resolution may be a critical point in impact-echo testing. The relative small lateral dimensions or the superficial position of some of the targets (flaws, layer thickness, void inclusions) searched in civil engineering structures force to select the wave characteristics. Especially in masonry structures, it is often necessary to obtain great penetration depths and still maintain high wave resolution (Colla, 2003).

The instrumentation of impact-echo testing relies on three basic components:
• A mechanical impactor, capable of producing short-duration impacts;
• A high-fidelity receiver to measure the surface response;
• A data acquisition-signal analysis system to capture, process, and store the waveforms of surface motion (Carino, 2001).

3.2. ELECROMAGNETIC TECHNIQUES

3.2.1. GPR RADAR

3.2.1.1. Introduction

The use of electromagnetic waves for remote probing started in the beginning of the 20th century, by experiments that evidenced the possibility of transmitting electromagnetic waves through space as a beam of energy and receive the reflected signal from the object.

During the Second World War, this technique was used for the detection of submarines from airplanes and for the precise planning of massive air bombings. During this period, this technology experienced an intense development. Although the use of electromagnetic methods started as a military application, the potential of its use within the civil and scientific communities was foreseen rapidly. The first experiments with electromagnetic waves were carried out by Hulsmeyer, in 1904, and published by Leinback and Lowy in 1910. They attempt to remotely detect the presence of metallic objects buried in the soil by employing a continuous wave transmission.

Civil engineering applications of GPR started to appear in the mid of 1970-80's. This led to an expansion of the range of applications, including building and structural non-destructive testing, archaeology excavations, road and tunnel quality assessment, location of voids, capillarity rise, mine, pipe and cable detection (Fernandes, 2006). Especially for historic buildings, the inner structure of masonry is usually very inhomogeneous, this still remains a problem for the interpretation of radar data. Despite these problems, this method is being used increasingly for the assessment of the structural safety and durability of historic masonry including the determination of the structural thickness of masonry; determination of kind, location and size of voids and unfilled joints in masonry, determination of moisture, salt content and its distribution.

Thus, radar is a very important tool for the non-destructive characterisation of ancient monuments but there is a necessity to increase the accuracy of measurement and data interpretation techniques

(Maierhofer and Leipold, 2001). Continuous research on processing algorithms with the final objective of producing more reliable data that generates accurate results and which can be easily readable for any operator not involved in NDT investigation (like designers, architects, etc.) has been carried out during the last decade. Among the investigation techniques and procedures which have been used in these last years, GPR Radar seems from one hand to be most promising, from the other to need a great deal more of study and research (Fernandes, 2006).

3.2.1.2. Working principles and equipment

Ground Penetrating Radar consists on the propagation of high frequency electromagnetic radiation to detect subsurface and underground features. The radar application is based on the fact that the velocity of propagation of the electromagnetic energy and its reflection in the interfaces between different materials are affected by the electric and magnetic properties of these materials (Fernandes, 2006).

The GPR system consists of pulse generator connected to a transmitter antenna that emits electromagnetic pulses and the receiving antenna that records the reflected signals from the target of interest. Two types of antennas are commonly used: monostatic and bistatic. In bistatic antenna, the source and the receiver antennas are physically separated while in monostatic antenna, both transmitter and receiver are together . The resolution of the data is dependent on the antenna frequency, which also controls the depth of penetration. In general, there is trade-off between the resolution and depth of penetration. Higher frequencies antenna gives better resolution but has lower depth of penetration due to high signal attenuation (Halabe and Pyakurel, 2007).

The velocity of propagation and attenuation of the radar signal are the parameters that describe its transmission through the materials encountered and are the function of their electrical properties. These parameters are, therefore, directly related to dielectric constant and electric conductivity of the material. The dielectric properties of materials constitute a dimensionless measure that defines the capacity of a material to store an electrical charge when placed in an electric field. Dielectric properties include the complex electrical conductivity (σ^*), the magnetic permeability (μ) and the complex permittivity (ε^*) of materials. These properties constitute fundamental parameters and can influence the way radio waves propagate, reflect and attenuate through different earth and construction materials (Fernandes, 2006).

A typical modern radar system is generally constituted by the following components (i) control unit; (ii) radar antennas(s); (iii)visualisation unit and data storage device, as is illustrated in fig 3.9.

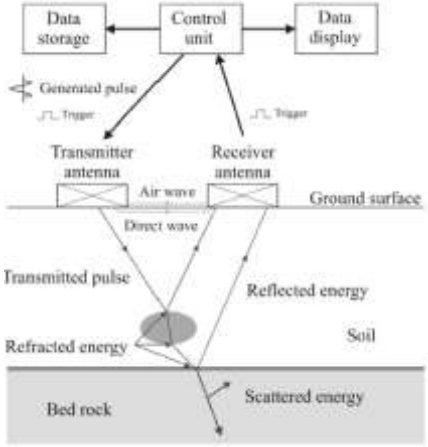

Fig 3.9 - Description of the components and operative mode of a GPR system (Fernandes, 2006)

The control unit generates an electromagnetic pulse and sends it to the transmitter antenna that irradiates a broad beam of electromagnetic energy. Typical antennas are constituted by transducers, that convert electrical current on the metallic antenna elements into electromagnetic energy that is radiated towards the medium in the form of electromagnetic pulses and are characterised by their central frequency, *f*. In the last years, GPR suppliers have been marketing new antennas with frequencies higher than 2GHz (Binda et al., 2008).

The electromagnetic wave is reflected by each interface between adjacent dielectric materials encountered during its propagation in the investigation medium and the reflected echoes are collected by the receiver antenna

The control unit generates several thousand of pulses per unit time, which results in a repetition rate of several kHz that are sent to the transmitter antenna. The system records the time taken by the radio wave to travel from the transmitter to the radar reflectors, and then back to the receiver, commonly designated by "two-way travel-time", usually expressed in nanoseconds (ns). In each position, the system samples an entire trace (or waveform), which is a set of several samples collected during a certain time interval (in terms of nanoseconds). The traces are placed successively one after another and displayed in a monitor in the form of a continuous radargram, which represents a two-dimensional image of the variation of the dielectric properties of the materials located under the alignment of the profile, fig 3.10. Digital recording systems display the amplitudes of the signal according to a grey scale or colour menu, with the strongest reflections being shown by the brightest colours.

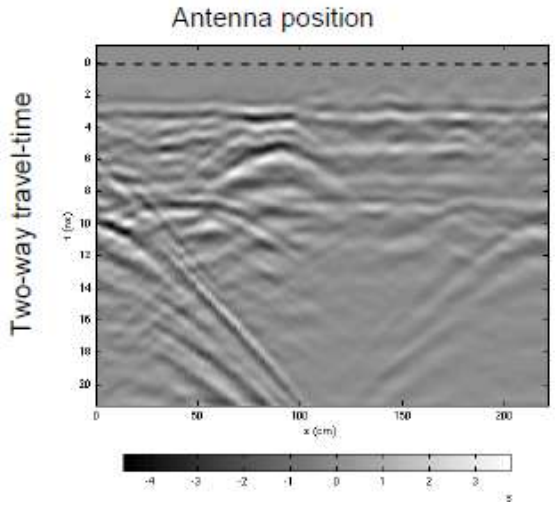

Fig 3.10 - Radargram

Another way of presenting results of radar data is a three-dimensional display, which consists of placing 2D profiles in a three-dimensional block view. Three-dimensional acquisitions are more expensive but they produce effective reconstructions that facilitate the transmission of the results to the end-users and extend the application of the GPR to specific problems that absolutely need a 3D approach to get an answer (Fernandes, 2006).

3.2.3. THERMOGRAPHY

3.2.3.1 Introduction

The origin of Infrared Thermography comes back to 1800s when William Herschel discovered thermal radiation, the invisible light called infrared, but only in the mid-sixties the Infrared Thermography became a technique of temperature mapping. During the past several years this technique has been evolved into a powerful investigative tool of non-destructive control since it is capable of providing useful information for the characterisation of materials and structures in a wide range of applications needed (Clark et al., 2003).

IR Termography has been successfully used for the damage assessment of historic structures and also for the assessment of conservation materials and techniques such as restoration of masonry by repair mortar and stone consolidation. Moreover, Infrared Thermography has been applied to detect and disclose artificial and in-depth defects, hidden structures like niches and buried openings, and substrate features. In addition, one major advantage of Thermography applications is the detection of moisture and rising damp in buildings and masonry structures. Infrared Thermography is a potent tool for damage characterization such as, crack mapping, insulation deficiencies and can combine well with ultrasound for assessment of the depth of defects (Kordatos et al., 2013). Table2, presents some advantages and disadvantages of the IRT technique.

Table 2 - Advantages and disadvantages of IR Thermography, adapted from (Maldague, 2002).

Advantages	Disadvantages
Fast inspection and in real time;	Difficulty in obtaining a quick, uniform and highly energetic thermal stimulation over a large surface (active termography);
Security of personnel, there is no harmful radiation Involved;	Emissivity problems;
Wide span of applications;	Effects of thermal losses (convective, radiative) which induce spurious contrasts affecting the reliability;
No direct contact is required between the camera and the object under investigation;	Cost of the equipment;
Portability. Thermal imaging equipment is lightweight and can be easily transported;	Ability to inspect a limited thickness of material under the surface;
Data manipulation. The recorded data can be monitored and processed on a standard PC running dedicated imaging software.	Requirement of qualified technicians to interpret the results;
	Presence of obstacles

3.2.3.2. Working principles and equipment

Infrared radiation is the region of the electromagnetic spectrum between visible light and microwaves, this infrared region is often further subdivided into sub-regions as shown in fig 3.11 (Clark et al., 2003).

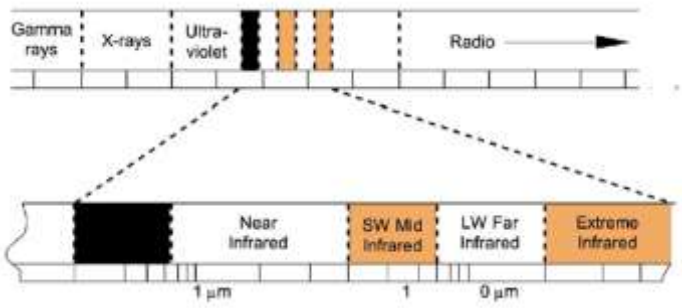

Fig 3.11 - Partial electromagnetic spectrum (Clark et al., 2003)

All objects radiate energy that is transported in the form of electromagnetic waves, which travel at speed of light. The quantity of energy leaving a surface as radiant heat is proportional to its emissivity and the fourth power of its absolute temperature.

Any object with a temperature other than absolute zero (-273.15ºC or 0 K) radiates within a range of wavelengths from 0 to ∞. For the temperatures commonly found in building, the major part of the emissive power ranges within the IR part of the electromagnetic spectrum. For these conditions, the higher the temperature of an object the more IR radiation it emits (Balaras and Argiriou, 2002).

Infrared Thermography transforms the thermal energy, radiated from objects in the infrared band of the electromagnetic spectrum, into a visible image, each energy level is represented by a colour, or grey level. Any object emits energy proportional to its surface temperature. However, the energy really detected (by the infrared detector) depends on the emissivity and on some physical conditions and material properties such as relative humidity, atmospheric temperature, reflected apparent temperature (Clark et al., 2003).

This technique is based on the monitoring of object's surface temperature variation. IR cameras detect infrared radiation emitted by materials and create a thermal image depicting the surface temperature distribution. The thermal energy propagates under the surface by conduction while the infrared camera monitors surface temperature variations. Obviously, the temperature distribution is uniform in case of uniform heating and homogeneous material, the presence of a defect at a certain layer interferes with the propagation of the thermal energy and causes a localised temperature difference.

IR Thermography can be divided into two different approaches, the passive and the active approach. The passive approach tests materials and structures which are naturally at different (often higher) temperature than ambient. Active thermography is based on the thermal excitation of the specimen inspected in order to obtain significant temperature differences evidencing the presence of subsurface defects (Maldague, 2002). In buildings, usually, passive thermography have predominance, the difficulties in the external thermal excitation by the dimensions of the target and the great amount of energy required lead to the choice of this method. In building heritage interventions, is also better the use of passive thermography to prevent addition heat load accelerate pathological processes.

The basic equipment includes a camera, equipped with a series of changeable lenses, and a computer. The core of the camera is the infrared detector, which absorbs the infrared energy emitted by the object and converts it into electrical voltage or current (Clark et al., 2003).

As an example of application of thermography test is presented. Two images of a thermographic test carried out in an ancient building, in Bologna, fig 3.12. It is possible to detect some hidden features in the wall analysed by the termogram. It's easy to observe an old arc above the window that was later covered. The termocamera used was a FLIR P620, fig 3.13.

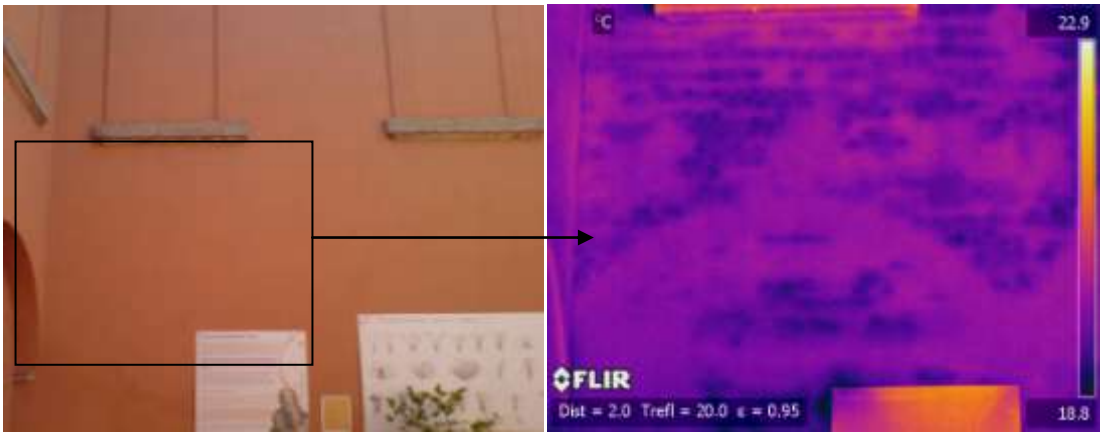

Fig 3.12 - Wall, Casa Non Grande, Bologna (left) ; Termogram (IR_20894) (right)

Fig 3.13 - Termocamera - FLIR P620("FLIR")

Diagram presented below in fig 3.14 is a synthesis of the non-destructive techniques described in chapter 3.

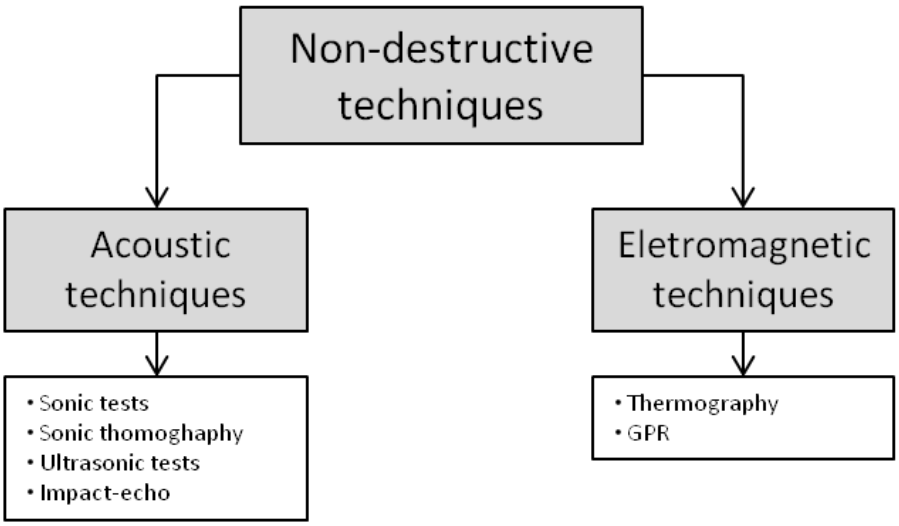

Fig 3.14 - Synthesis of non-destructive techniques presented in chapter 3

4

DESCRIPTION OF THE SPECIMENS

4.1. MATERIAL PROPERTIES OF MORTARS, BRICKS AND STONES

With the aim of analyze the behaviour of masonry, samples of materials consist of bricks, mortars and stones, constituent materials of masonry specimens. So, samples of natural hydraulic lime mortar were cast in laboratory, full fired clay bricks from local production were used and four types of stones from different locations in the world, such as: sandstone from Varignana, Bologna, sandstone from Stuttgart, limestone from Lecce, South Italy, and limestone from Palestine. All these specimens are part of a research developed within the PhD thesis of Elena Gabrielli and were made available for the development of this thesis.

The sets of specimen tested by ultrasonic test, consisted in mortar prisms (4*5*16cm), bricks (12*5.5*25cm) and stones with different shapes, tables 3,4 and 5.

Table 3 - Bricks - Quantity, type of solution and number of cycles

Bricks			
Number of specimens	**Solution**	**Concentration**	**Number of cycles**
10	Tap water	-	4 seasons of aging
10	NaCl	0.05%	4 seasons of aging
10	Na_2SO_4	0.05%	4 seasons of aging

Table 4 - Mortar Prisms - Quantity, type of solution and number of cycles

Mortar Prisms			
Number of samples	**Solution**	**Concentration**	**Number of cycles**
5	Dry	-	4 seasons of aging
16	Tap water	-	4 seasons of aging
16	NaCl	0.05%	4 seasons of aging
16	Na_2SO_4	0.05%	4 seasons of aging

Table 5 - Stones - Code, type of solution and number of cycles

Stones					
Types	**Tested Specimens**	**Dimensions (mm)**	**Solution**	**Concentration**	**Number of cycles**
Sandstone from Varignana, Italy	B1	(213.98*57.12*140.7)	NaCl	0.05%	4 seasons of aging
	B2	(195.95*56.61*140.7)			
Sandstone from Stuttgart, Germany	S1	(249,50*120.14*119.51)	Tap water	-	4 seasons of aging
	S2;S3	S3(249.27*120.67*119.42)	NaCl	0.05%	4 seasons of aging
		S4(249.21*119.98*119.93)			
	S4	(250.53*120.64*119.29)	NaCl	0.1%	4 seasons of aging
	S5	(250.47*120.45*119.85)	Na_2SO_4	0.05%	4 seasons of aging
	S6	(249.75*119.61*120.43)	Na_2SO_4	0.1%	4 seasons of aging
Limestone from Lecce, Italy	L1	(251.06*55.83*103.69)	NaCl	0.05%	4 seasons of aging
	L2	(251.91*54.14*113.24)	NaCl	0.1%	4 seasons of aging
	L3;L4	L3(239.94*40.21*91.12)	Na_2SO_4	0.05%	4 seasons of aging
		L4(239.52*40.26*91.36)			
	L5	(239.93*40.19*90.54)	NaCl	0.1%	4 seasons of aging
Limestone from Palestine	RWQ	(192.49*62.68*114.3)	NaCl	0.05%	4 seasons of aging

4.2. LARGE SCALE WALLS

Like the material units, different large-scale walls (PNDA, PNDB, PNDC, PNDD, PNDE and PNDF) were exposed to the natural weathering conditions during four summer seasons. They were also subjected to capillarity rise from the base using water, NaCl and Na_2SO_4 at low concentration (0,05% and 0.1% by weight). Six different walls were built at the beginning of the research in 2010, with full fired clay bricks and natural hydraulic lime mortar joints, materials used in ancient masonry structures. Each wall had different geometrical and structural characteristics in order to analyze their different behaviour. The walls PNDE and PNDD have a thickness of 38 cm, and the others 25 cm. Structural characteristics are also different, presenting internal voids, plaster in the surface or inclusions of the stones, table 6.

Table 6 - Walls -Type of solution, characteristics and number of cycles

Large Scale Walls				
Wall	**Solution**	**Concentration**	**Characteristics**	**Number of cycles**
PNDA	NaCl	0.1 wt-%	Plaster at the back; stone inclusions	4 seasons of aging
PNDB	NaCl	0.05 wt-%	Stone inclusions	4 seasons of aging
PNDC	Rain Water	-	Stone inclusions	4 seasons of aging
PNDD	Na_2So_4	0.1 wt-%	Voids	4 seasons of aging
PNDE	Na_2So_4	0.05 wt-%	Voids	4 seasons of aging
PNDF	Tap water	-	Voids	4 seasons of aging

Wall PNDE will be analysed applying tree non-destructive tests, sonic tests, gpr and thermography, while the wall PNDA, PNDC, PNDD will be analysed with infrared thermography technique. Structure of the wall PNDE, has inside, different internal holes with various dimensions, as can be seen in the Fig 4.2. From the middle section, 4 sets of cores were extracted in order to analyse the moister content at different heights (courses 6,9,12 and 15) and compare it with the results of gpr test. As happened with the specimens of mortar, bricks and stones, all these walls are part of a research developed within the PhD thesis of Elena Gabrielli.

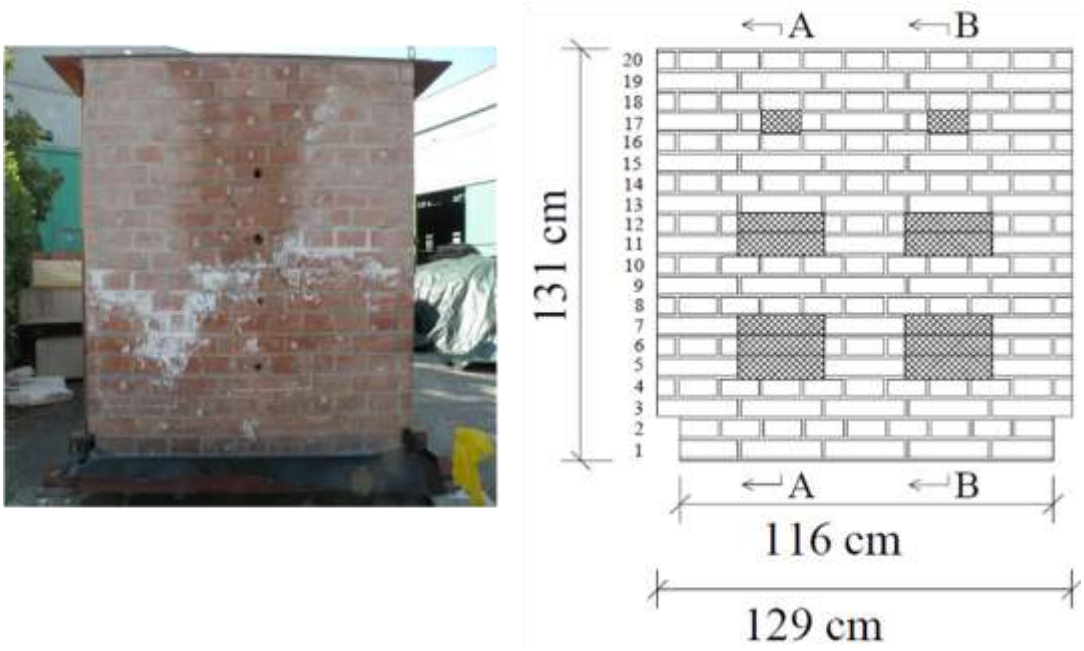

Fig 4.1 - Frontal view of wall PNDE (left) ; Scheme of the frontal view of the wall PNDE (right) (Colla and Gabrielli, 2010)

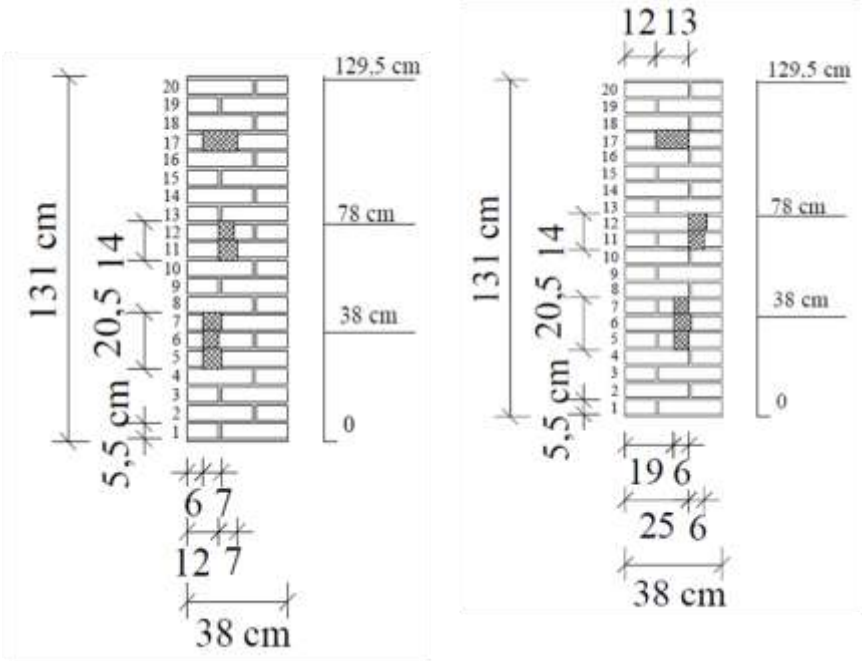

Fig 4.2 - Section A-A, wall PNDE (left). (Colla and Gabrielli, 2010) ; Section B-B, wall PNDE (right) (Colla and Gabrielli, 2010)

4.3. AGING PROCEDURES

The experimental work was carried out in order to determine the mechanical damaging effects of soluble salts in several different specimens (samples and large-scale walls) when expose to the weathering agents and the applicability of several non-destructive tests to the analysis of this phenomenon.

Specimens were subject to four summer seasons of natural aging (3 months), each one in a different consecutive year, since 2010. This method avoids the damage effects due to other phenomena such as by freeze-thaw cycles, which occur during the winter because this is not the scope of this research study. Thus, the experimental work consists in the fifth analysis of the same material after another season of aging (2013).

Non-destructive testing of material was carried, consisting in four sets of mortars prisms (Fig 4.4), tree sets of bricks, fig 4.5 and four sets of different stones fig 4.6, these specimens were partially immersed in different solutions to induce capillary rise. Effect of salt damaging were analysed, with solutions of sodium chloride and sodium sulphate. Moreover, it was performed the tests with dry samples and with samples in contact only with tap water. These type of salts were chosen because they are one of the most common damaging salts for existing masonry structures and the low-concentration of the solution is similar to cases of low-salinity groundwater. Every season cycle the samples were turned, changing the side in contact with the solution, thus can be achieved a constant impregnation of the material.

The procedure with the walls was similar, six different large-scale walls were positioned outside during four summer seasons, fig 4.3. These walls were partially immersed is different types of solutions, tap water, NaCl, Na_2SO_4 and just with the action of the rain water.

Fig 4.3 - Walls exposed to the natural weathering and immersed in different types of solutions on the base.

Fig 4.4 - Four sets of mortar prims (Dry, NaCl, Na_2SO_4 and Water)

Fig 4.5 - Tree sets of bricks (NaCl, Na_2SO_4 and Water)

Fig 4.6 - Stone Samples

5
EXPERIMENTAL WORK IN THE LABORATORY

5.1. VISUAL INSPECTION OF UNITS OF MORTAR, BRICKS AND STONES

In order to determinate the state of damage of the material, the first analysis done should be a visual assessment of the state of the specimens that will be analyzed. In this case, an ultrasonic test was carried out in samples of mortars, bricks and stones. Through a visual inspection, it is observed that the samples of mortar are already quite damaged, having a configuration with rounded edges and lost some of their mass. The material seems quite porous, rough, and little homogeneous, Fig 5.1. Samples in contact with Na_2SO_4 show salt efflorescence in the base in contact with the solution in the last season.

Fig 5.1 - Mortar Prism - NaCl (left) ; Mortar Prism - Na_2SO_4 (right)

Samples of brick on the other hand have a fairly homogeneous surface with no apparent loss of mass however the brick samples present soft edges and changes in the surface colour. The samples in contact with Na_2SO_4 present a large amount of efflorescence, fig 5.2.

Limestone samples from Lecce, present quite deterioration as well as a large amount of mass loss, fig 5.2. Trough the visual inspections, the others types of stones seem to have a more regular surface.

Fig 5.2 - Na_2SO_4 brick sample (left) ; Limestone from Lecce (right)

5.2. ULTRASONIC TESTS

The use of ultrasonic test for the characterization of materials is here described. This chapter will analyze in detail the direct ultrasonic tests conducted in laboratory. All the tests were carried out in LISG (Laboratory of Structural and Geotechnical Engineering), in University of Bologna.

Three different materials are considered. The choice has been made to include mortar, bricks, and stones used in masonry construction of the large walls outside the lab. Direct ultrasonic test is performed in order to determine the velocity of P-waves that propagate through the thickness of the element. The study of this wave speed through the material is quite useful because the propagation of stress waves is directly related to the mechanical properties of the material.

In order to accomplish the ultrasonic test, samples were previously marked with a grid to help performing the tests with the greatest possible accuracy. These acoustic tests were performed in two different paths, a longitudinal path, and a transversal path. Direct measurements were taken at different locations in each sample, on the lateral surface, designed 1-1', 2-2' and 3-3' and one on top of the specimen, designed A-B, fig. 5.3 and fig 5.4. Path 3-3' for mortars and bricks and C-C' for stones are the bottom part in contact with the water in the last season. Before performing the tests, samples were let 5 days in a dry controlled environment, with a temperature of 22ºC, so that all the samples would be in the same moisture conditions and in particular with a low moisture content.

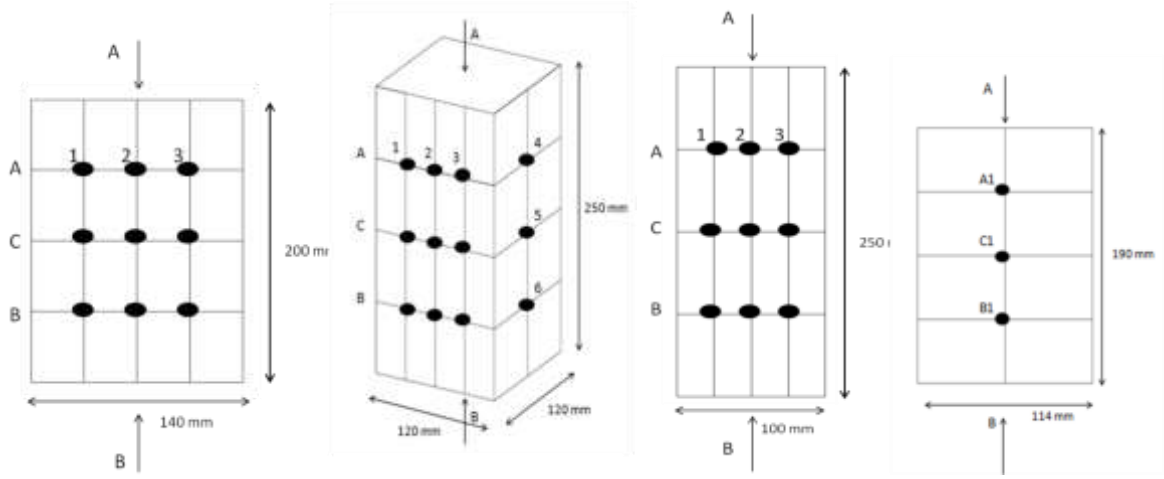

Fig 5.3 - Schematic grid for ultrasonic direct test : Sandstone from Varignana and sandtone from Stuttgart (left); Limestone from Lecce and limestone from Palestine (right) - approximate measurements

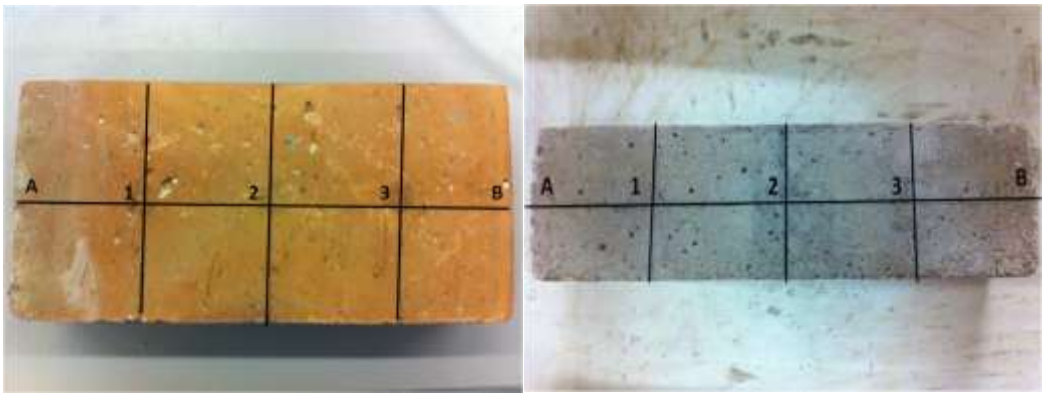

Fig 5.4 - Grid used for ultrasonic test in bricks (left) and mortar prisms (right)

The equipment used was provided by LISG and consists of:

- Device Olympus Epoch 1000;
- Two Olympus Transducers-V603 RB (1MHz), with a latex sheet, 0,5mm;
- One clamp.

The transducers used have 1MHz of frequency and contained a latex sheet to ensure a better dry coupling between the transducer and the surface of the material. To assist the test it was used a clamp that is positioned pressing the transducers in order to apply that same constant pressure in both sides of the samples.

The procedure to perform the ultrasonic test is not difficult. After assembling the material the transmitter and the receiver should be positioned according to the grid in the opposite surfaces and using the clamp to hold the transducers.

The test procedure consists of acquiring images of the waveform in the Olympus Epoch 1000. Time of flight and the attenuation can be obtained by a direct reading on the display of the device, as showed in fig 5.5.

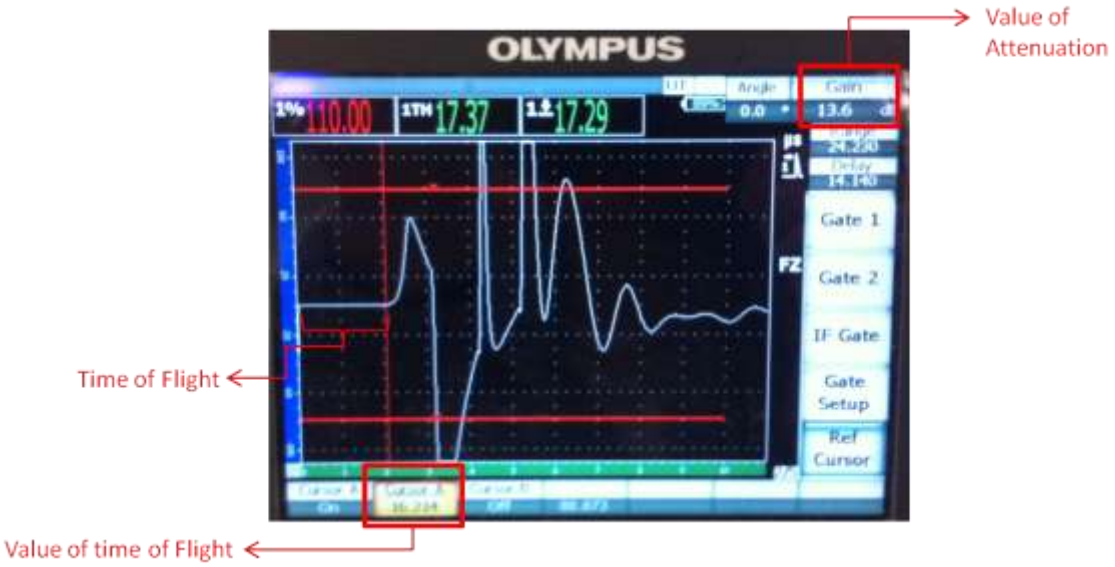

Fig 5.5 - Data acquisition of the ultrasonic test

5.2.1. ULTRASONIC TESTS IN MORTAR PRISMS

Ultrasound test was performed by direct transmission in mortar specimens properly marked with the grid in order to perform the test with the greatest accuracy possible. From the direct reading of the device it was possible to obtain the values of the time of flight and attenuation, subsequently the value of the wave velocity was calculated as: *Vp* = tof / thickness of specimen. The analysis was performed for the four types of specimens: dry, NaCl, Na_2SO_4 and with water. Two paths were considered, longitudinal (A-B) and transversal past in three tests per sample: 1-1', 2-2', 3-3'.

Fig 5.6 - Mortar prisms - US longitudinal path (left) ; US transversal path (right)

Regarding the samples of dry mortar, those that were in contact only with the rain water, and with respect to the longitudinal path, the values obtained for the time of flight, attenuation, and wave velocity are those which constitute the graphs presented in fig 5.7.

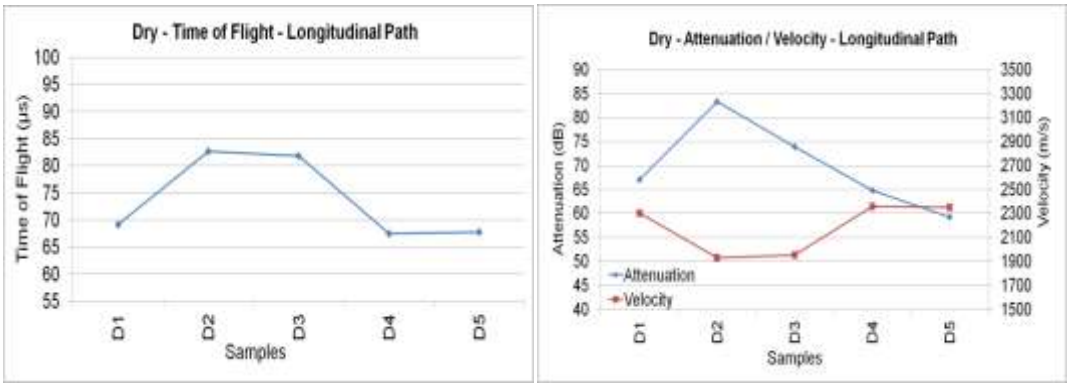

Fig 5.7 - Dry mortar prisms - Time of flight for longitudinal path (left) ; Dry mortar prisms - Attenuation/Velocity for longitudinal path (right)

Looking at the transversal path, the results obtained for the velocity and attenuation values are those presented in fig 5.8 and fig 5.9.

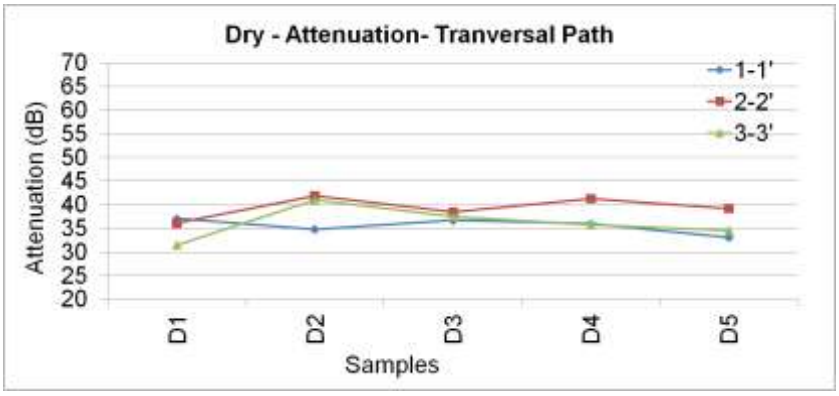

Fig 5.8 - Dry mortar prisms - Attenuation for transversal path

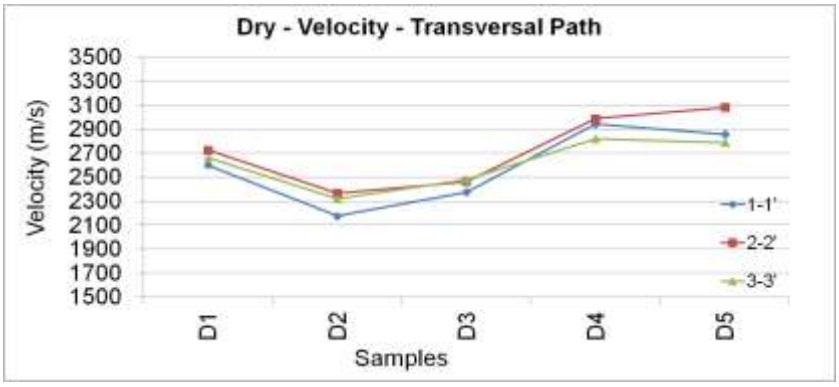

Fig 5.9 - Dry mortar prisms - Velocity for transversal path

In transversal path, attenuation show homogeneous values in all samples, while in transversal path, there are some dispersion of results. Higher attenuation values, are referred to the path 2-2', all values in this way are superior to the others, excluding the sample D1, presenting an attenuation value very close to value of the path 1-1'. It is possible to see in fig 5.9, that values of velocity in boarder paths 1-1' and 3-3' has the same behaviour, resulting in lower values of velocities.

From collected the data for samples with immersion in NaCl, graphics of time of flight , attenuation and velocity are shown in fig 5.10 to 5.12.

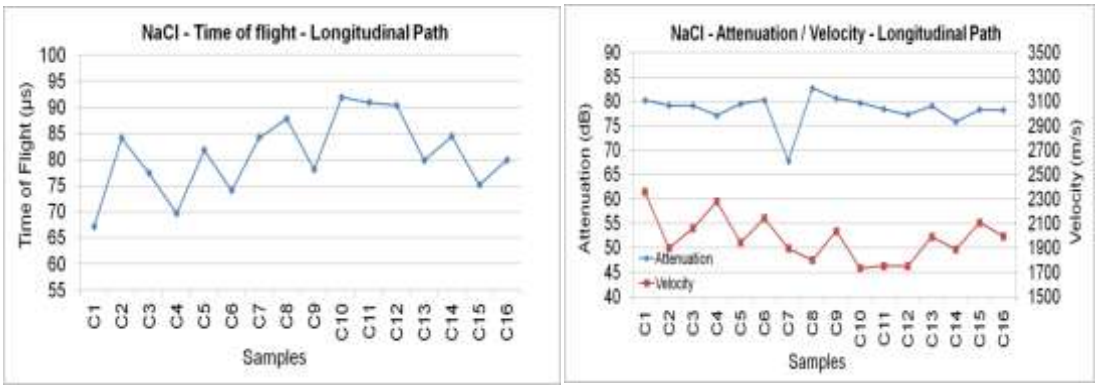

Fig 5.10 - Chloride mortar prisms - Time of flight for longitudinal path (left) ; Chloride mortar prisms - Attenuation/Velocity for longitudinal path (right)

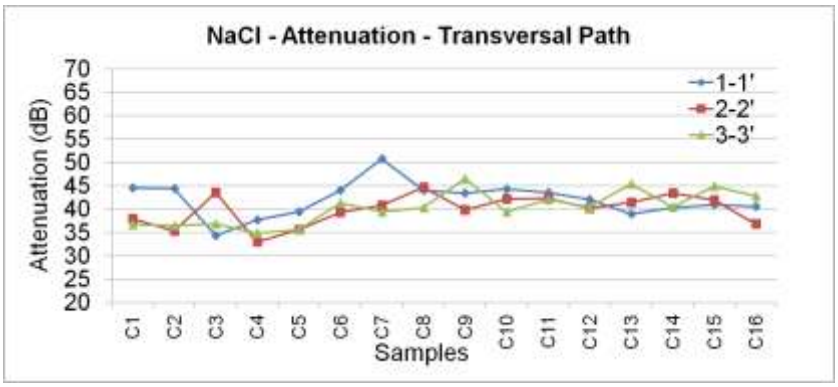

Fig 5.11 - Chloride mortar prisms - Attenuation for transversal path

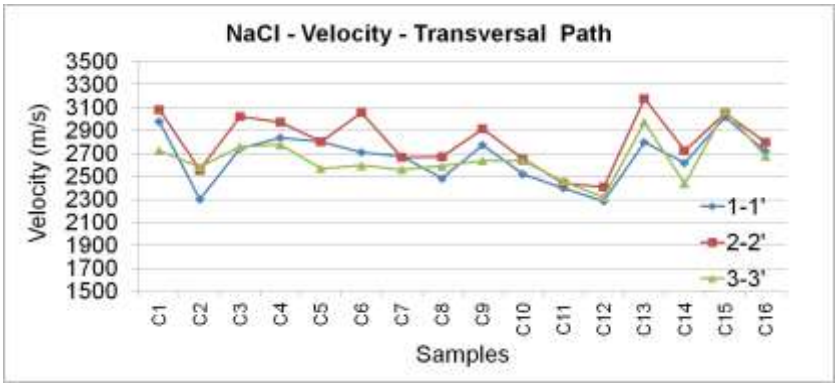

Fig 5.12 - Chloride mortar prisms - Velocity for transversal path

Both longitudinal and transversal paths show constant values for attenuation. As regards transverse path 1-1', it presents the highest average value for attenuation while the path 3-3´, the lowest. Also in the 1-1' longitudinal path, the C7 sample present an attenuation value higher than the average of values thus, it can excluded that may have been a measurement error. The highest average value for velocity correspond path 2-2'. Comparing both longitudinal and transversal paths, the last presents higher values for velocity and lower values for attenuation.

Analyzing the results obtained with ultrasound test specimens immersed in solution of Na_2SO_4, graphs of time of flight, attenuation and velocity are presented in fig 5.13 to 5.15.

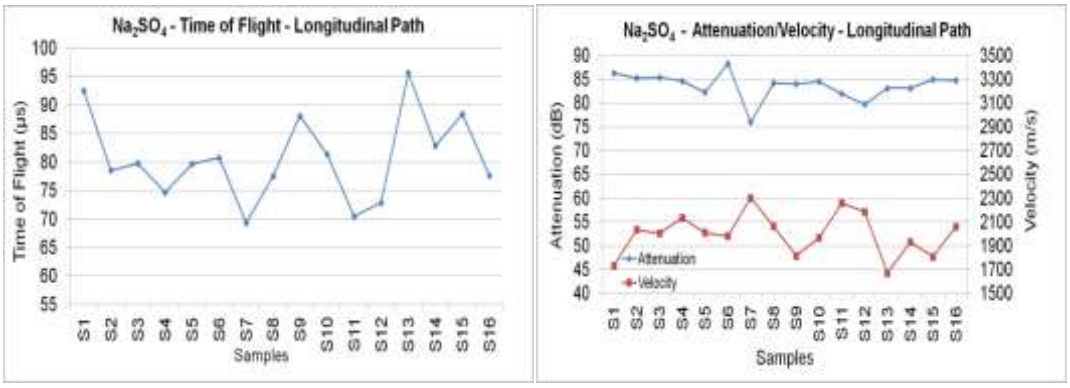

Fig 5.13 - Sulphate mortar prisms - Time of flight for longitudinal path (left) ; Sulphate mortar prisms - Attenuation/Velocity for longitudinal path (right)

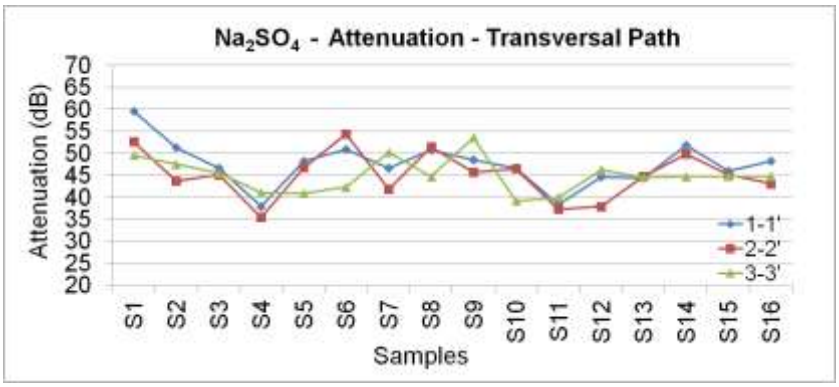

Fig 5.14 - Sulphate mortar prisms - Attenuation for transversal path

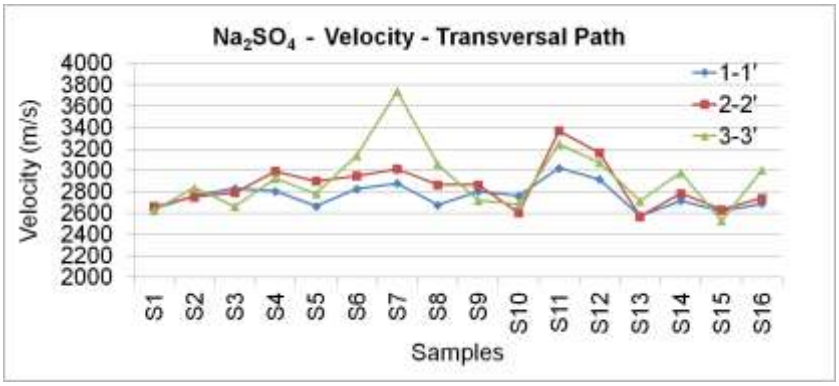

Fig 5.15 - Sulphate mortar prisms - Velocity for transversal path

Concerning the attenuation, the lowest average value was found for path 2-2' and 3-3'. In transversal path, sample S7 also shows a disparity in the velocity value, in this case on path 3-3'. The highest average value for velocity corresponds to path 3-3' while the path 1-1' has lower average velocity. Thus, in this case is not a similarity in behaviour of two boarder paths. Also in this case longitudinal path present higher values for attenuation and lower for the velocity.

Results of tests performed on specimens immersed in water, so without the action of the salts, are presented in fig 5.16 to 5.18.

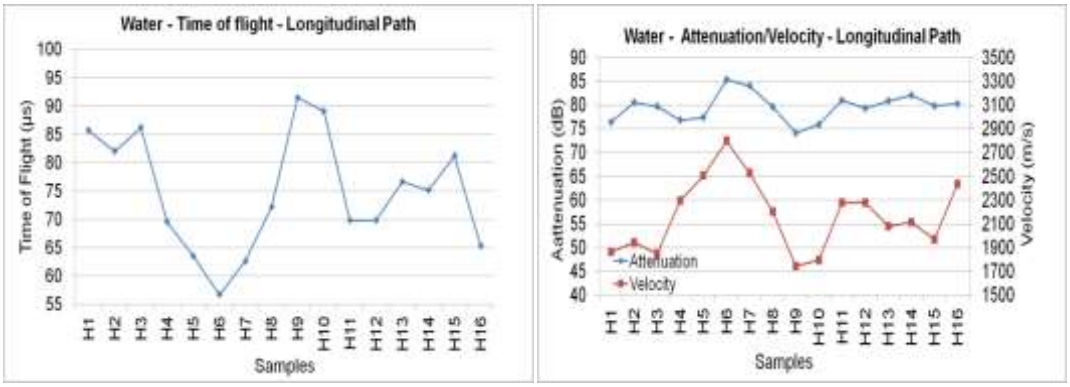

Fig 5.16 - Sulphate mortar prisms - Time of flight for longitudinal path (left) ; Water mortar prisms - Attenuation/Velocity for longitudinal path (right)

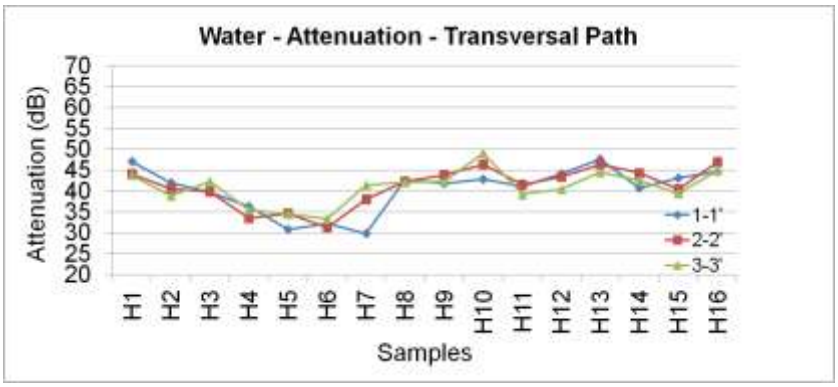

Fig 5.17 - Water mortar prisms - Attenuation for transversal path

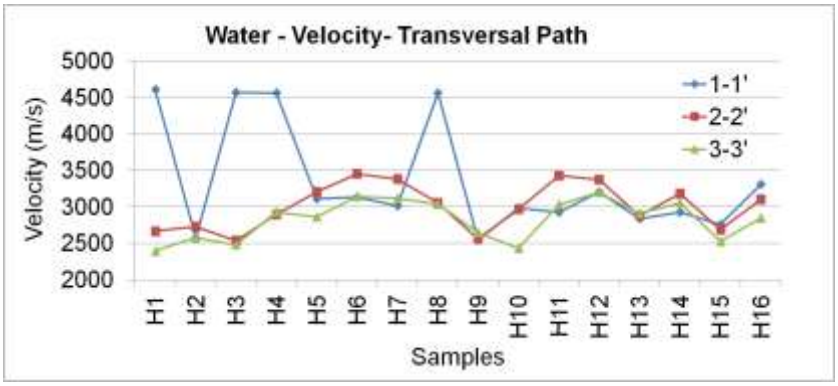

Fig 5.18 - Water mortar prisms - Velocity for transversal path

Water mortar samples show great variability of time of flight values in longitudinal path. Towards the attenuation in transversal path, values presented are quite similar for every paths. In transversal path, particularly in samples H1, H3, H4 and H8, the velocity value is much higher than in other samples. Is important to notice that these are abnormal values for this type of material. The highest velocity average value is found for paths 1-1' and 2-2'.

Table 7 - Mortar Prisms - Average velocity values (longitudinal and transversal path) and coefficient of variation

Series	Nº of Samples	V_m. LP	Nº of measures	C.o.V (%)	V_m. TP	Nº of measures	C.o.V(%)
Dry	5	2179.01	5	10.0	2642.71	15	10.3
NaCl	16	1976.51	16	9.3	2708.87	48	8.3
Na_2SO_4	16	1996.93	16	8.9	2844.29	48	8.0
H_2O	16	2166.13	16	13.9	3062.13	48	17.3

Table 8 - Mortar Prisms - Average attenuation values (longitudinal and transversal path) and coefficient of variation

Series	Nº of Samples	Att_m. LP	Nº of measures	C.o.V (%)	Att_m. TP	Nº of measures	C.o.V(%)
Dry	5	69.64	5	13.3	37.01	15	8.1
NaCl	16	78.31	16	4.1	40.73	48	8.8
Na_2SO_4	16	83.63	16	3.4	45.87	48	10.7
H_2O	16	79.55	16	3.7	40.77	48	11.5

From tables 7 and 8, regarding average values, transversal path presents highest values for velocity and lowest values for attenuation. Values of attenuation on longitudinal path are approximately twice the values for transversal path. Salt samples show low dispersion of velocity and attenuation results.

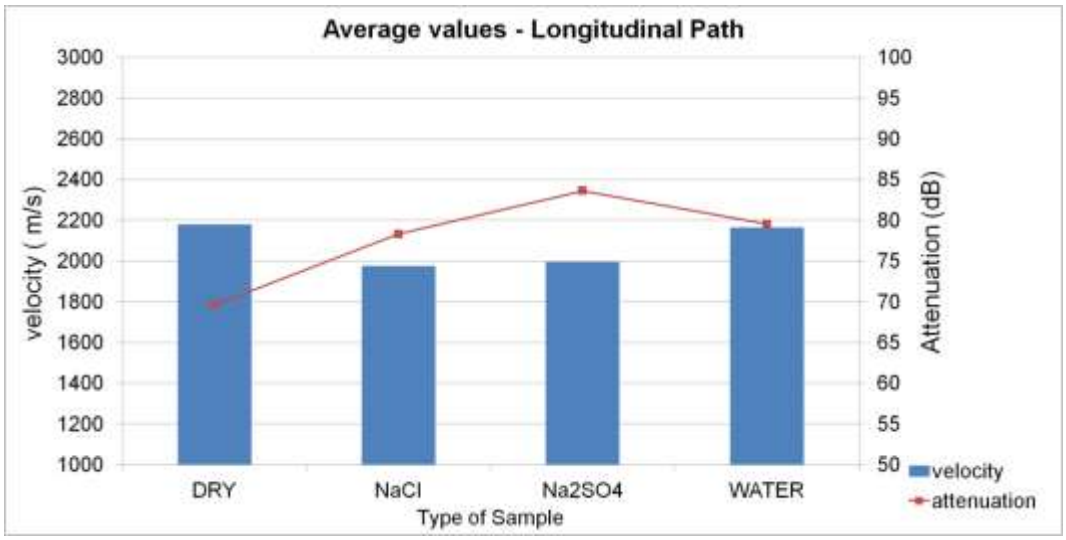

Fig 5.19 - Mortar Prisms - Velocity/Attenuation for longitudinal path, average values

Respecting the longitudinal path, it is noted that the average values of the velocity of the waves is higher when it comes to dry samples or in contact with water, as very similar values were obtained in these two situations. In the presence of salts, the velocity of the waves is lower. Attenuation varies inversely with the speed of the waves, since it has superior values for the samples saturated with salt the value of attenuation is lower for samples with water following the dried samples.

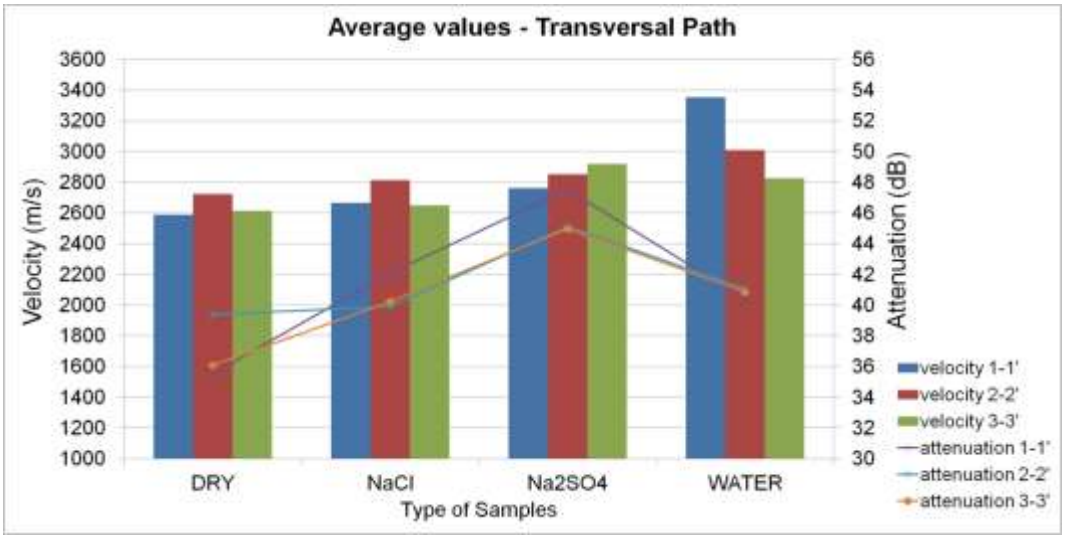

Fig 5.20 - Mortar Prisms - Velocity/Attenuation for transversal path, average values

In transversal path, there is a similar behaviour on dry samples and chloride samples with respect to velocity values, path 2-2' is the one with the highest average speed of the waves whereas the paths 1-1' and 3-3' have lower and very similar values. Samples with Na_2SO_4 and water has an inverse behaviour, with respect to Na_2SO_4, these samples have higher velocity of the waves on path 3-3' and lower value for 1-1' path, reverse situation in the samples with water. Attenuation is quite superior when it comes to the samples with Na_2SO_4 while dry samples present the lowest values for the attenuation.

5.2.2. ULTRASONIC TEST IN BRICKS

The same procedure was applied to samples of brick, as already described in this chapter. Thus, ultrasound tests were also performed via direct transmission in accordance with the grid shown in figure 5.4. The values of time of flight and attenuation at the desired points were also registered. The analysis was performed on three different samples types, immersion in NaCl, Na_2SO_4 and with water.

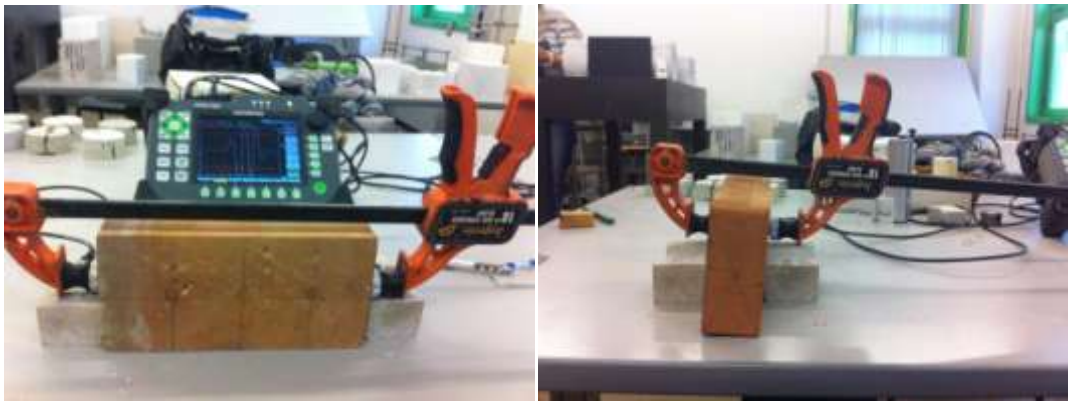

Fig 5.21 - Bricks - US longitudinal path (left) ; US transversal path (right)

With regard to the samples of brick in contact with NaCl solution, values obtained for the time of flight, attenuation, and wave velocity constitute the fig 5.22, 5.23 and 5.24.

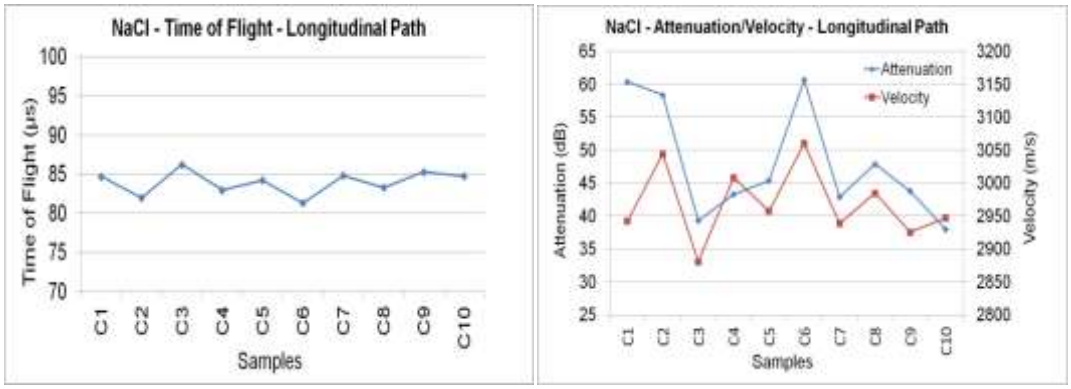

Fig 5.22 - Chloride brick samples - Time of flight for longitudinal path (left) ; Chloride brick samples - Attenuation/Velocity for longitudinal path (right)

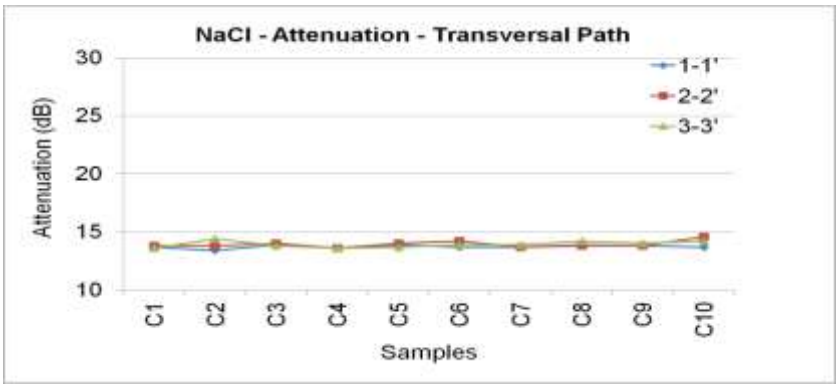

Fig 5.23 - Chloride brick samples - Attenuation for transversal path

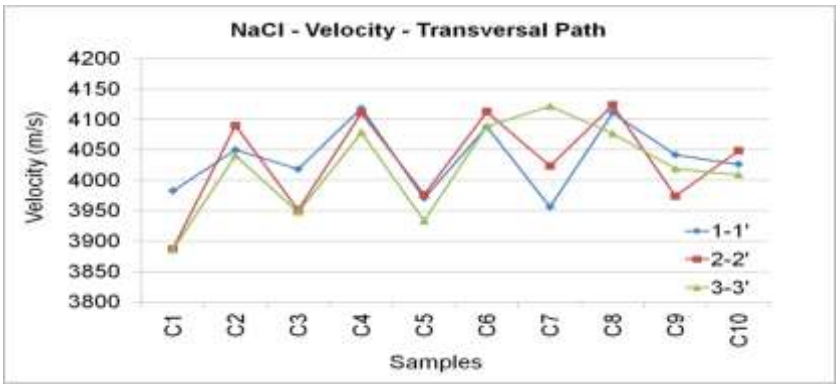

Fig 5.24 - Chloride brick samples - Velocity for transversal path

Time of flight in longitudinal path and attenuation in transversal path do not present dispersion of values otherwise attenuation and velocity in both paths show a great variability of values. The highest average values for the velocity correspond to paths 1-1' and 3-3'.

Analyzing now the results of the samples in immersion over Na_2 SO_4, representative graphs of the results for the longitudinal path are presented in fig 5.25.

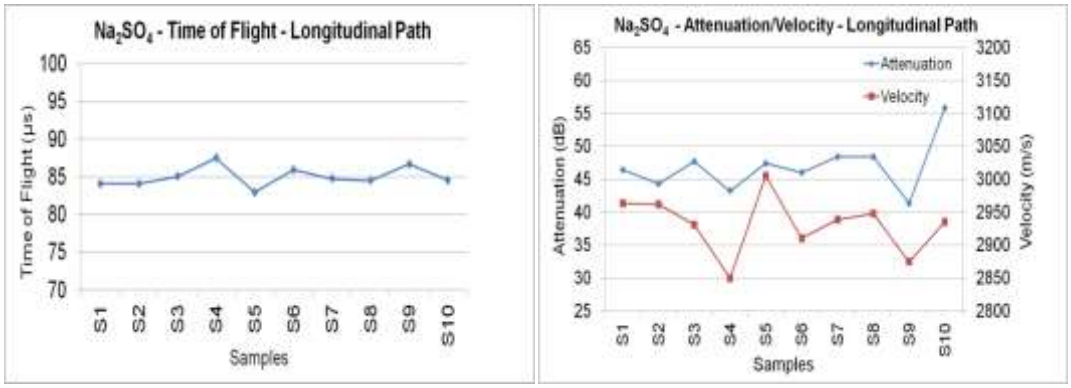

Fig 5.25 - Sulphate brick samples - Time of flight for longitudinal path (left) ; Sulphate brick samples - Attenuation/Velocity for longitudinal path (right)

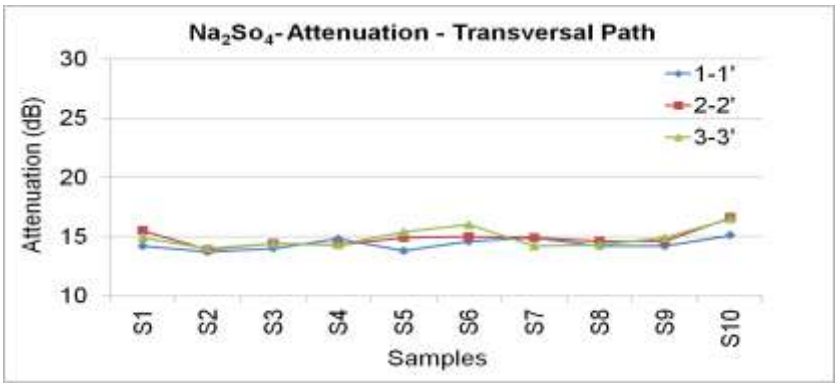

Fig 5.26 - Sulphate brick samples - Attenuation for transversal path

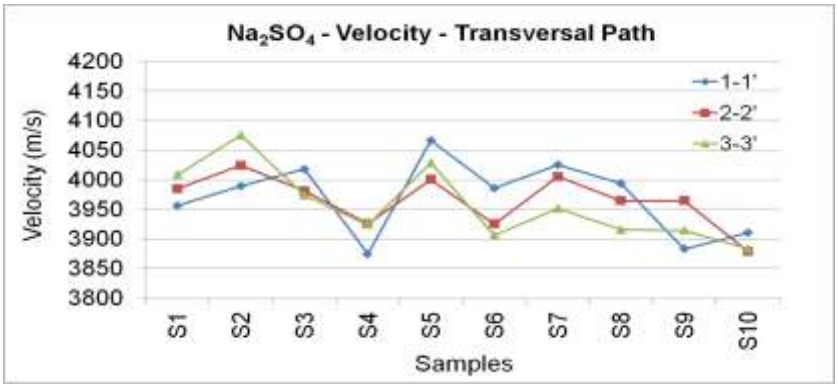

Fig 5.27 - Sulphate brick samples - Velocity for transversal path

As happened with chloride samples values of time of flight for longitudinal path and attenuation for transversal path present very constant values. In this case, the highest mean values for velocity, correspond to paths 1-1' and 2-2'.

Analysing the results obtained for samples in contact with water, the graphics of the time of flight, speed and attenuation of waves are those presented in fig 5.28 to 5.30.

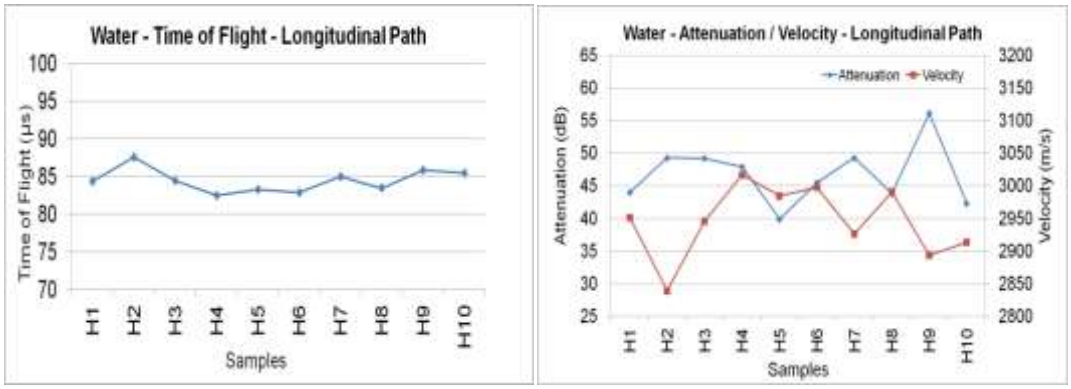

Fig 5.28 - Water brick samples - Time of flight for longitudinal path (left) ; Water brick samples - Attenuation/Velocity for longitudinal path (right)

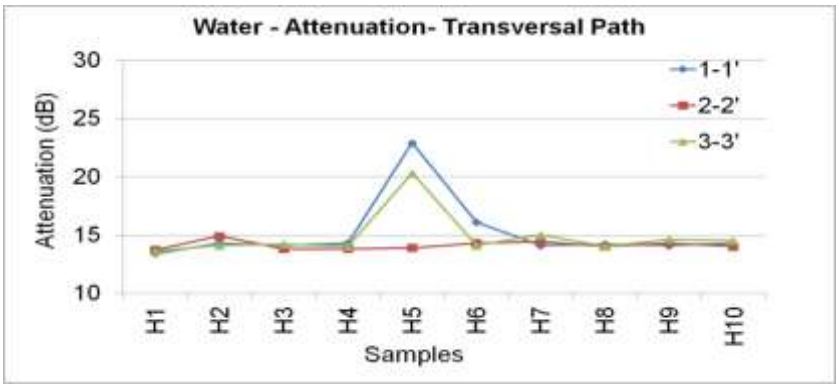

Fig 5.29 - Water brick samples - Attenuation for transversal path

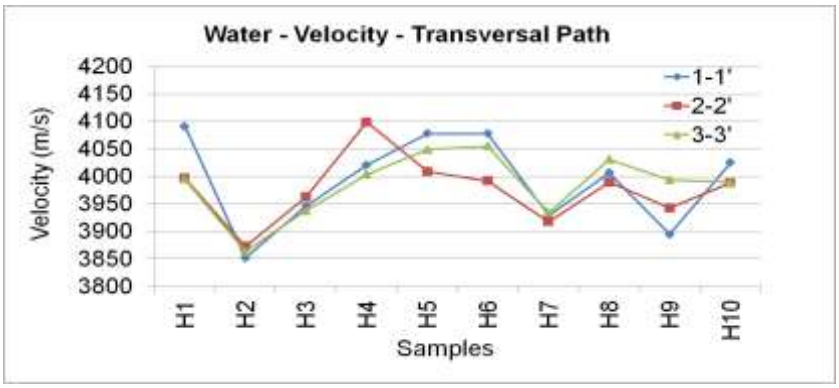

Fig 5.30 - Water brick samples - Velocity for transversal path

Also in this case time of flight in longitudinal path and attenuation values in transversal path present very close values to each other. H5 specimen having a value excessively high for attenuation in the path 1-1' and 2-2', was not recorded in the average value of the attenuation since its value may have been due to an error in testing. The highest average values for the velocity correspond to paths 1-1' and 3-3', having these boarder paths similar behaviours.

Table 9 - Bricks - Average velocity values (longitudinal and transversal path) and coefficient of variation

Series	Nº of Samples	V_m. LP	Nº of measures	C.o.V (%)	V_m. TP	Nº of measures	C.o.V(%)
NaCl	10	2969.06	10	1.9	4028.72	30	1.7
Na_2SO_4	10	2931.46	10	1.5	3964.58	30	1.0
H_2O	10	2946.03	10	1.9	3984.44	30	2.0

Table 10 - Bricks - Average attenuation values (longitudinal and transversal path) and coefficient of variation

Series	Nº of Samples	Att_m. LP	Nº of measures	C.o.V (%)	Att_m. TP	Nº of measures	C.o.V(%)
NaCl	10	48.01	10	17.9	13.86	30	1.9
Na_2SO_4	10	46.89	10	8.3	14.70	27	4.9
H_2O	10	46.73	10	9.9	14.71	30	13.4

From the tables 9 and 10, comparing average values of velocity, transversal path present highest values for velocity and lowest values for attenuation as happened with mortar samples. Values of attenuation on longitudinal path are much lower than values for longitudinal path and velocity values quite superior. Velocity show low dispersion in their values both in longitudinal and transversal paths. However attenuation present a quite high C.o.V for chloride samples in longitudinal path and water samples in transversal path..

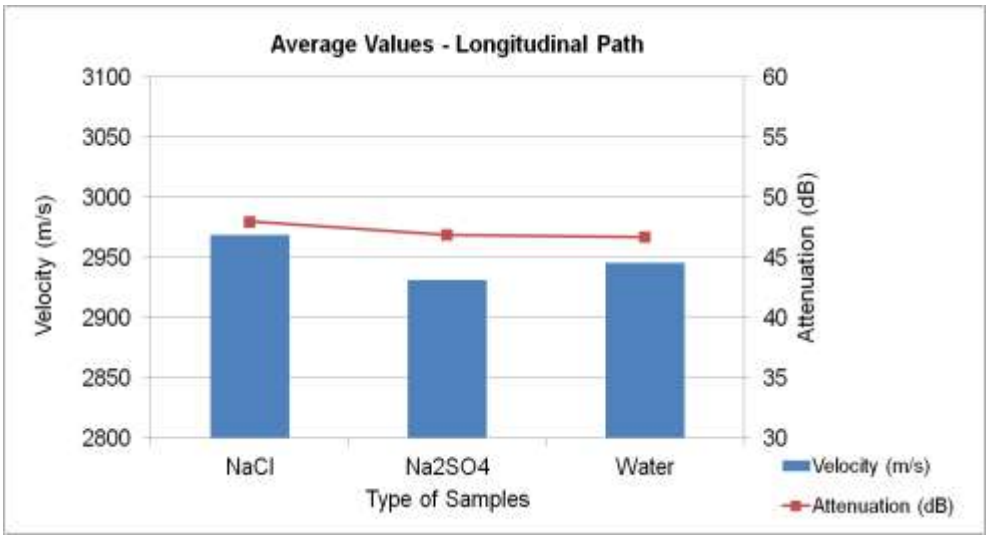

Fig 5.31 - Brick samples - Average values of Velocity/Attenuation for longitudinal path

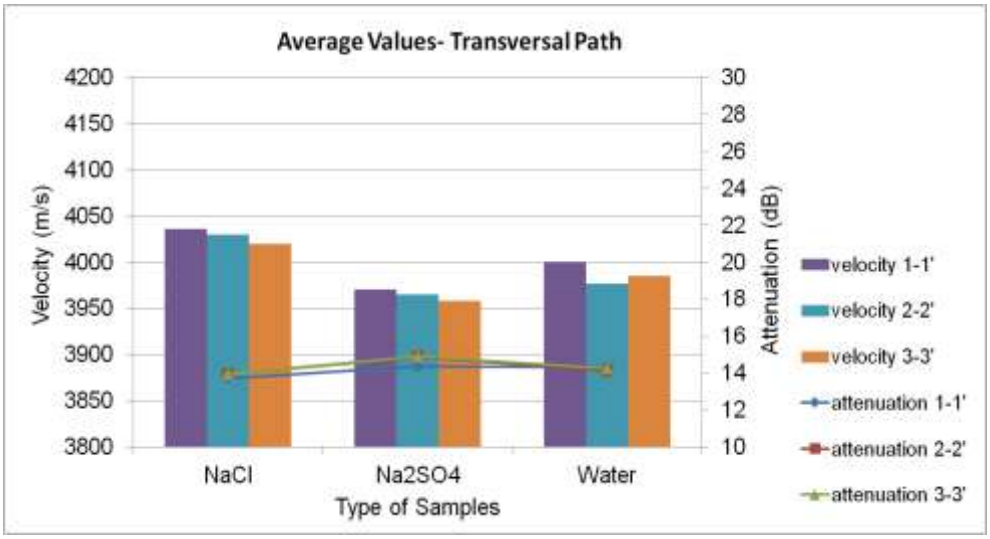

Fig 5.32 - Brick samples - Average values of Velocity/Attenuation for transversal path

Regarding to the longitudinal path it appears that the average values of the velocity of the waves are higher in the samples in contact with NaCl and water. In the presence of Na_2SO_4, the speed of the waves is minor. Attenuation do not present significant changes for each type of sample.

In transverse path exists similarity in samples with NaCl and in samples with Na_2SO_4 with respect to the velocity values. For salt sample, path 1-1' is the one with the highest average velocity of the waves while path 3-3' show lower values. The samples in contact with water have a higher speed in the path 1-1'and 3-3'. Regarding to attenuation values, these are higher in samples with Na_2SO_4. and present very similar values for chloride and water samples.

5.2.3. ULTRASONIC TEST IN STONES

As described in this chapter, the ultrasonic test was also performed on samples of different types of stones. In this case, the direct test was made in accordance with the grid presented in fig.5.3. Two different transversal paths were considered (A, B and C), (4-4', 5-5' and 6-6'). The analysis was performed on four different samples types of stone, sandstone from the "Varignana", sandstone from "Stuttgart", a Limestone from "Leccese", and a Limestone from Palestine.

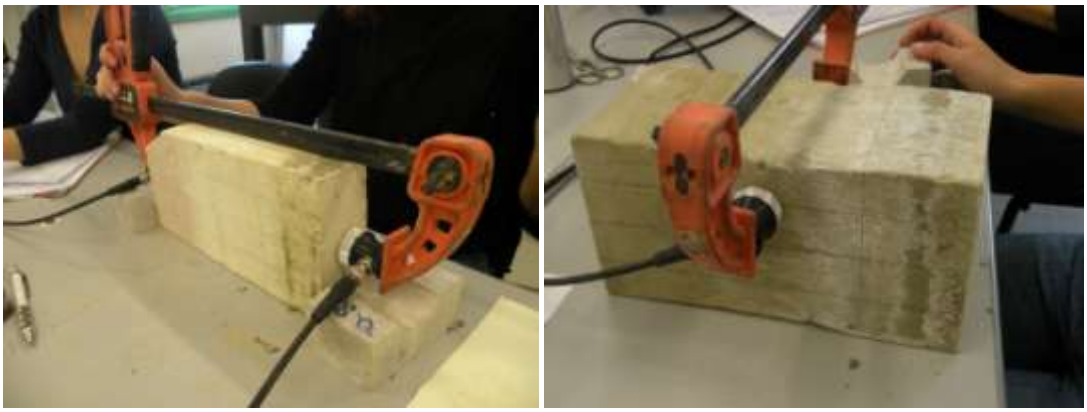

Fig 5.33 - Stones - US Longitudinal Path (left) ; US Transversal Path (right)

Regarding the limestone samples from Lecce, and with respect to the longitudinal path, the values obtained for the time of flight, attenuation, and wave velocity are those which constitute the figures 5.34, 5.35 and 5.36.

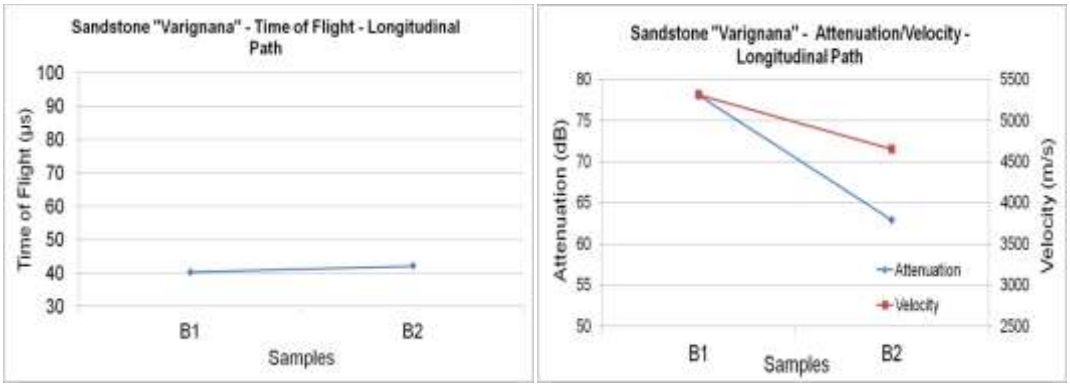

Fig 5.34 - "Varignana" stone samples - Time of flight for longitudinal path (left) ; "Varignana" stone samples - Attenuation/Velocity for longitudinal path (right)

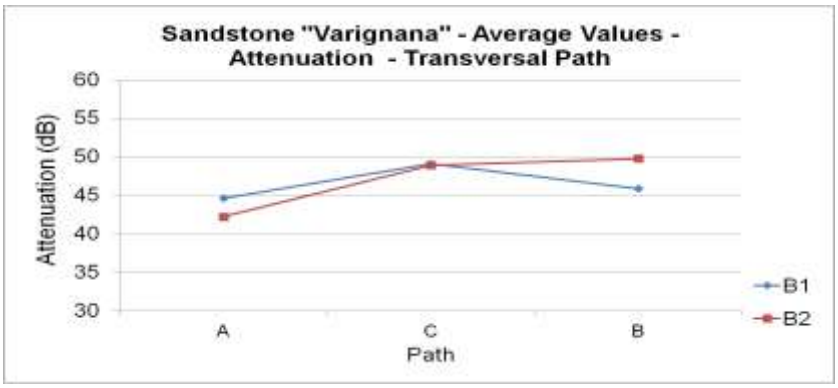

Fig 5.35 - "Varignana" stone samples - Attenuation for transversal path

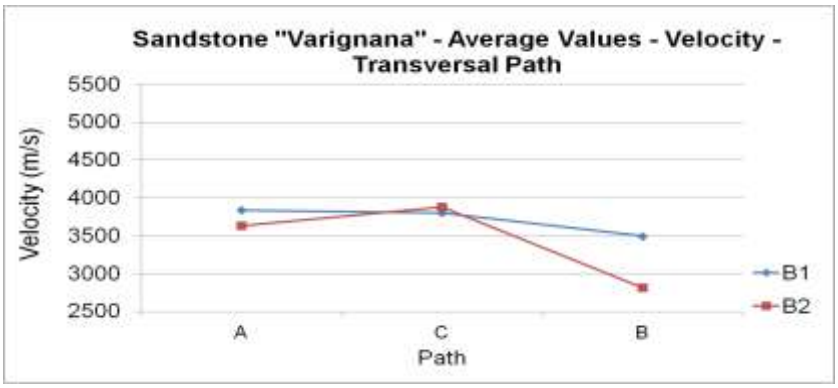

Fig 5.36 - "Varignana" stone samples - Attenuation for transversal path

For "Varignana" stone B1, the highest value for attenuation in middle path C while in the stone B2 is in path B. The values of velocity do not exhibit great variation, excluding the samples B2, in the path B.

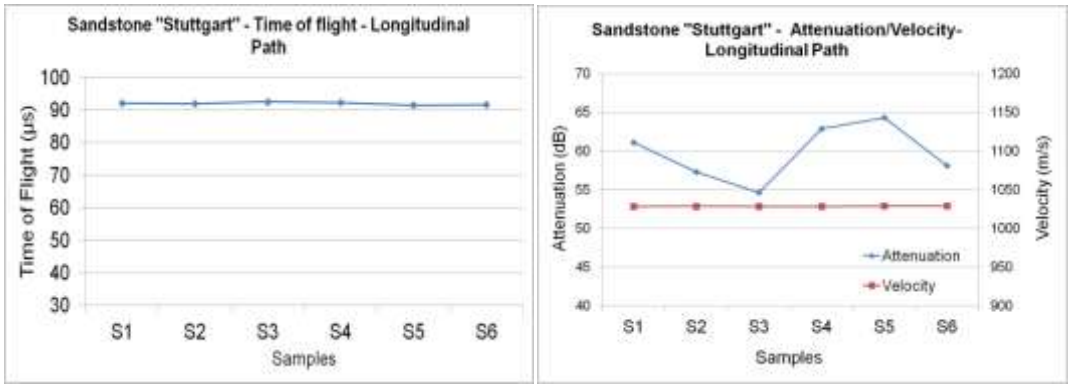

Fig 5.37 - "Stuttgart" stone samples - Time of flight for longitudinal path (Left) ; "Stuttgart" stone samples - Attenuation/Velocity for longitudinal path (right)

From the analysis of the graphs in fig 5.37, it is observed that the values for the time of flight and velocity are very similar, presenting almost no changes between them. The behaviour of the attenuation is quite different showing some dispersion of values.

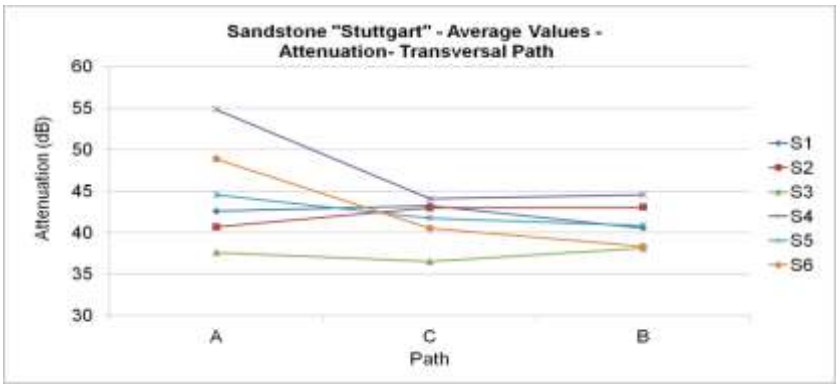

Fig 5.38 - "Stuttgart" stone samples - Attenuation for transversal path (A,B,C)

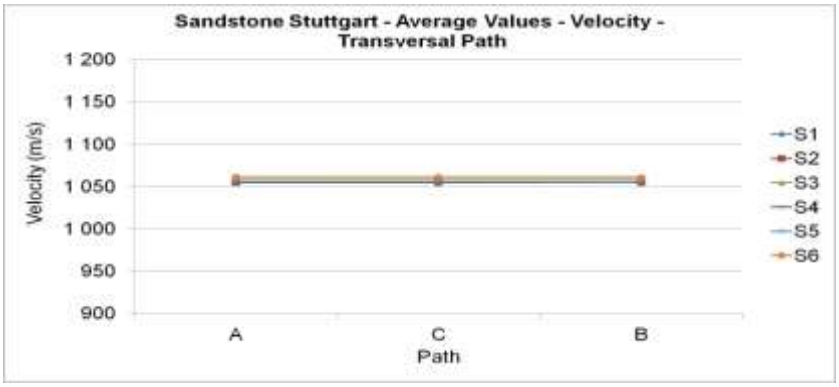

Fig 5.39 - "Stuttgart" stone samples - Velocity for transversal path (A,B,C)

Attenuation graph shows in general, for each sample, lower values for C path, with regard to velocity, there is almost no changes is their values.

Through the figure 5.40, is possible to observe that both the attenuation and velocity of "Stuttgart" samples show no homogeneity in the distribution of its values in this transversal path.

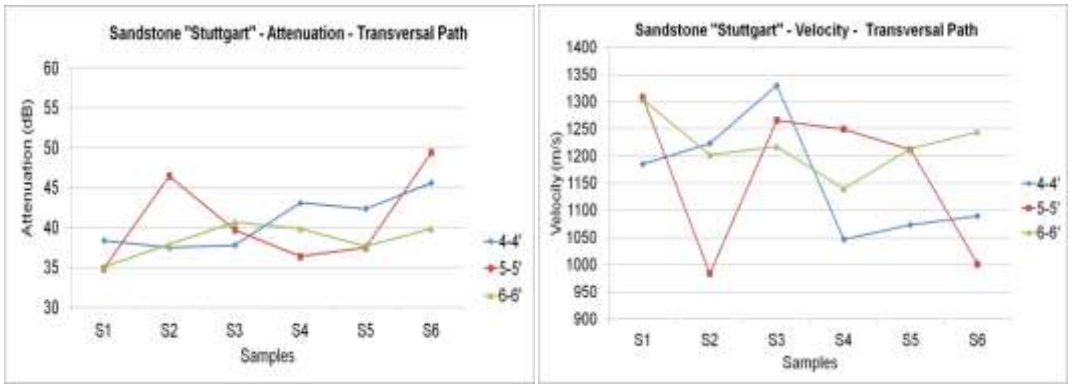

Fig 5.40 - "Stuttgart" stone samples - Attenuation for transversal path (4,5,6) (left) ; "Stuttgart" stone samples - Velocity for transversal path (4,5,6) (right)

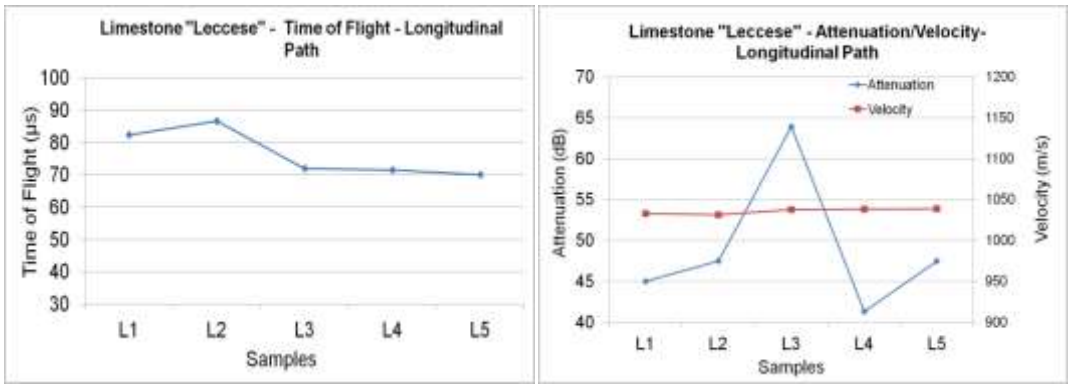

Fig 5.41 - "Leccese" stone samples - Time of flight for longitudinal path (Left) ; "Leccese" stone samples - Attenuation/Velocity for longitudinal path (right**)**

The values obtained for the time of flight attenuation and velocity in longitudinal path on specimens of limestone from Lecce are shown in figure 5.41.Values of time of flight and velocity are quite constant, otherwise velocity for this type of stone presents great dispersion of results. The highest and the lowest values for velocity are found for sulphate (0.05%) impregnated samples L3 and L4. The results obtained for the attenuation in the transversal path present values with no significant dispersion in the results.

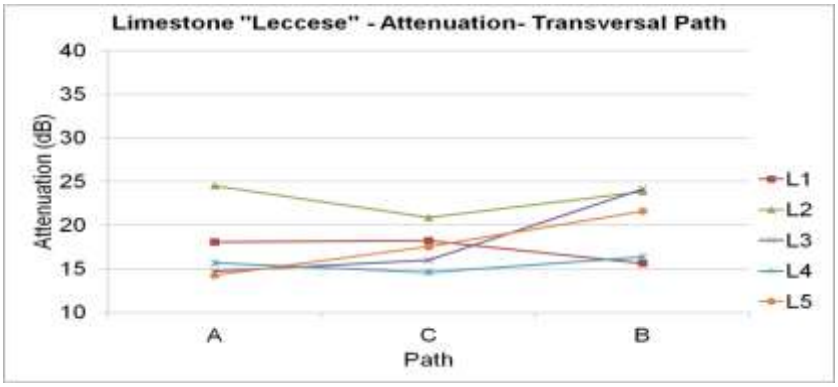

Fig 5.42 - "Leccese" stone samples - Attenuation for transversal path (A,B,C)

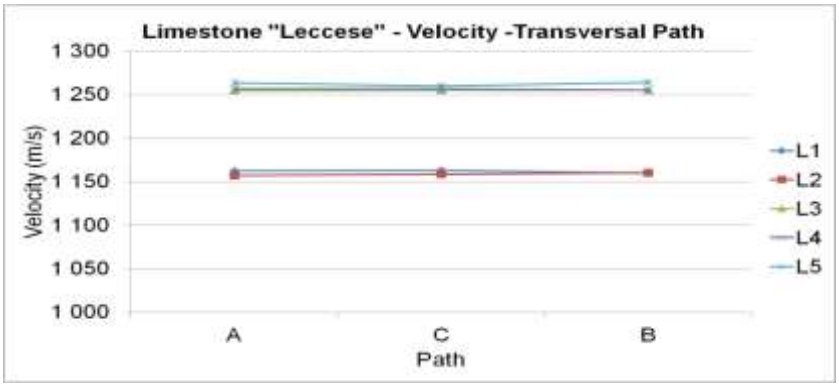

Fig 5.43 - "Leccese" stone samples - Velocity for transversal path (A,B,C)

From chart of attenuation in fig 5.43 it is observed homogeneity of values for the six samples regarding the three different paths. There are two groups having different values for the velocity. The chloride samples L1 and L2 have lower values, while sulphate samples L3, L4 and L5 have the highest values for velocity. However, for each sample the recorded speeds are very homogenous in the three paths, A, C and B.

Is was recorded, for the Palestine Stone, 54.9 (μs) for the time of flight, 48.8 (dB) for the attenuation and velocity 1050.07 m/s. The values for the transversal path are shown in the fig 5.44.

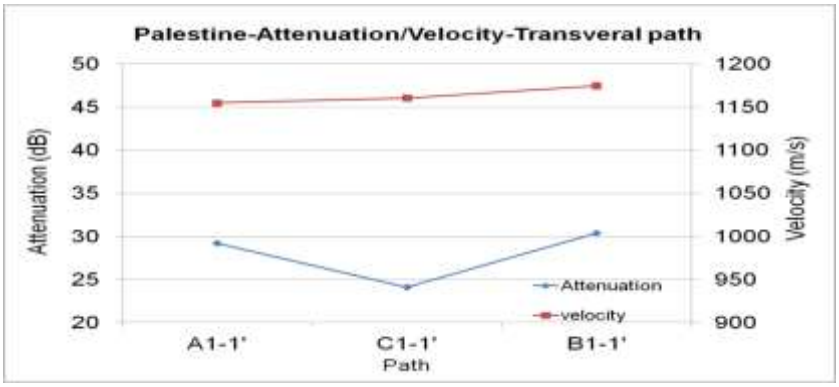

Fig 5.44 - Palestine samples - Attenuation/velocity for transversal path

Table 11 - Stone Samples - Average velocity values (longitudinal and transversal path)

Series	Samples	Average Vel. LP	Nº of measures	Average Vel. TP (A;B;C)	Nº of measures	Average Vel. TP (4;5;6)	Nº of measures
Varignana	B1;B2	4981.37	2	3575.25	18	-	-
Sttutgart	S1	1028.46	1	1056.13	9	1265.28	3
	S2;S3	1028.43	2	1057.80	18	1203.54	6
	S4	1028.42	1	1055.93	9	1144.88	3
	S5	1028.66	1	1056.34	9	1166.12	3
	S6	1028.60	1	1061.14	9	1111.53	3
Lecce	L1	1032.83	1	1161.32	9	-	-
	L2	1031.19	1	1158.48	9	-	-
	L3;L4	1037.90	2	1255.36	18	-	-
	L5	1038.87	1	1262.21	9	-	-
Palestine	RWQ	1050.07	1	1163.43	3	-	-

Table 12 - Stone Samples - Average attenuation values (longitudinal and transversal path)

Series	Samples	Average Att. LP	Nº of measures	Average Att. TP (A;B;C)	Nº of measures	Average Att. TP (4;5;6)	Nº of measures
Varignana	B1;B2	70.45	2	46.73	18	-	-
Sttutgart	S1	61.10	1	42.14	9	36.13	3
	S2;S3	55.95	2	39.84	18	40.02	6
	S4	62.90	1	47.83	9	39.80	3
	S5	64.30	1	42.39	9	39.20	3
	S6	58.10	1	42.58	9	44.97	3
Lecce	L1	45.00	1	17.32	9	-	-
	L2	47.50	1	23.09	9	-	-
	L3;L4	52.60	2	16.93	18	-	-
	L5	47.50	1	17.80	9	-	-
Palestine	RWQ	48.80	1	27.90	3	-	-

From the tables 11 and 12, it is shown that velocity are quite similar between longitudinal and transversal paths in every type of stones. Regarding attenuation values, these are lower for transversal path comparing with longitudinal path.

5.3. DETERMINATION OF DYNAMIC MODULUS OF ELASTICITY FROM ULTRASOUND VELOCITIES

According to the European Norm (IN12504-4, 2004) it is possible to calculate the dynamic modulus of elasticity of an isotropic, elastic and infinite dimensions medium through the relationship between elastic properties and the velocity of ultrasonic waves.

The following equation represents the relationship between the elastic characteristics of the material and the velocity of the waves determined through the ultrasonic test where V_P (m/s) is the velocity of the sound waves; E_d (Pa) is the dynamic modulus of Elasticity; $\boldsymbol{\upsilon}$ is the Poisson ratio and ρ (Kg/m^3) is the density of the material.

$$Vp = \sqrt{\frac{Ed}{\rho}\frac{(1-\upsilon)}{(1+\upsilon)(1-2\upsilon)}} \quad (1.6)$$

Being this equation applied to isotropic materials, when applied to mortar, brick and stone, it is necessary to note the lack of accuracy of the results obtained. In order to compare the values of the static and dynamic modulus of elasticity obtained, it is a common practice to consider 70 % of the dynamic modulus of elasticity, this assumption has been previously used in the context of research this thesis is inserted in, so this was the criterion adopted.

The calculation of the dynamic modulus of elasticity for each specimen was carried out using the results of the P-wave velocity in the longitudinal path acquired with the direct ultrasonic test, in each point. From the P-wave velocity, these values were subsequently used to calculate the value of the dynamic modulus of elasticity through the equation (1.6). The average values of Poisson ratio, shown in chapter 7, obtained from the compressing test were used to determine the dynamic modulus of elasticity of bricks. For mortars and stones as mineral construction material is adopted for the Poisson ration the value 0.2. The charts above show the results of the dynamic Modulus of Elasticity (E_d), calculated for the mortar, bricks and stone samples.

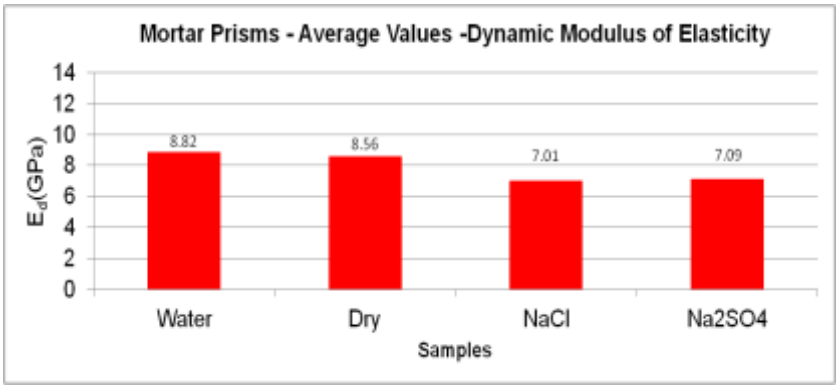

Fig 5.45 - Mortar prisms - Dynamic modulus of elasticity, average values

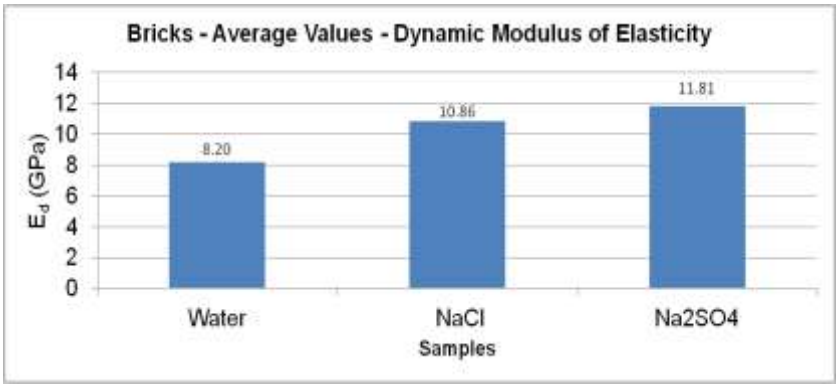

Fig 5.46 - Bricks - Dynamic modulus of elasticity, average values

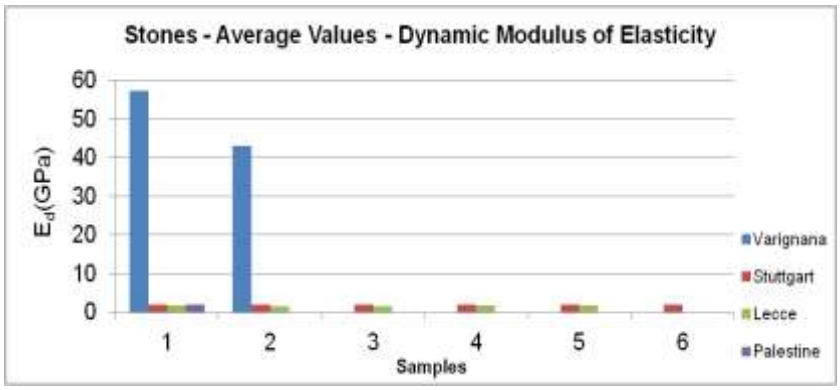

Fig 5.47 - Stones - Dynamic modulus of elasticity, average values

Regarding mortar samples, the average values for the dry and water samples are very similar and present the higher values. On the other hand, the values of samples in contact with salts have also similar but lower values. The brick cubes with sulphate present the higher values for E_d while the water the lowest values, this behaviour is similar comparing with average values of static modulus of elasticity of bricks, shown in chapter 7.

The values of modulus of elasticity in the stones are not presented in terms of their average value because within the same stone set there are different types of samples. By analyzing the graph, the value of the modulus of elasticity of sandstone from "Varignana", have a much higher values in comparison with the other stones. Sandstones from Sttutgart" and Limestone from "Lecce" present very similar values.

Table 13 - Mortars, bricks and stones, Dynamic modulus of elasticity - Values and coefficient of variation

Specimens		E_d (GPa) - Average Values	E_d - Coefficient of variation (%)	Number of Specimens
Mortar Prisms	**Water**	8.82	29	16
	Dry	8.56	21	5
	NaCl	7.01	21	16
	Na_2SO_4	7.09	18	16
Bricks	**Water**	8.20	4	10
	NaCl	10.86	4	10
	Na_2SO_4	11.81	3	10
Stones	**Varignana**	50.19	20	2
	Stuttgart	2.05	0.5	6
	Lecce	1.69	3	5
	Palestine	2.04	-	1

Thus, through table 13, it can be observed that mortar samples have a higher dispersion of results than samples of brick, as they present a value of dynamic modulus of elasticity very homogeneous among themselves. With respect to the stones , "Varignana" samples present the higher values for the modulus of elasticity, in contrast "Stuttgart" and "Lecce" stones have very low values for the dynamic modulus of elasticity. It is important to notice that these are not accurate values.

5.4. DIMENSIONAL ASSESSMENT

5.4.1. MORTAR PRISMS

After the exposure to environmental agents, the mortar samples were weighed. It was collected the powder resulting from the degradation and the samples were also measured in order to calculate their volume.

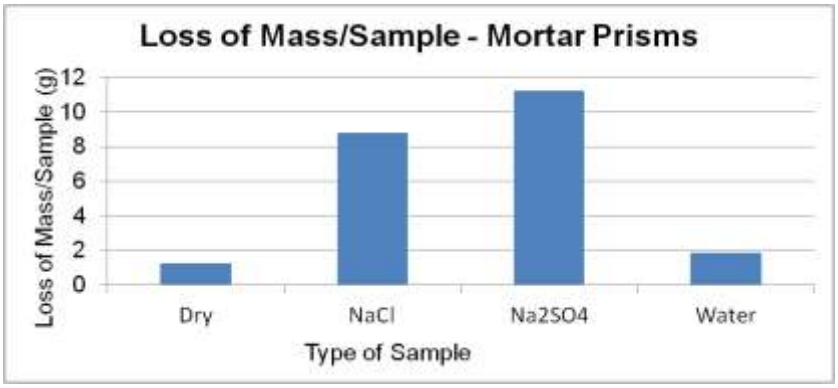

Fig 5.48 - Mortar Prisms - Loss of Mass/Sample

The research showed that the weight loss of salt mortar samples has the highest value. Lost of mass is lower for dry samples and for those in contact only with the water, higher rates of mass loss for samples in contact with NaCl and Na_2SO_4 salts, were obtained.

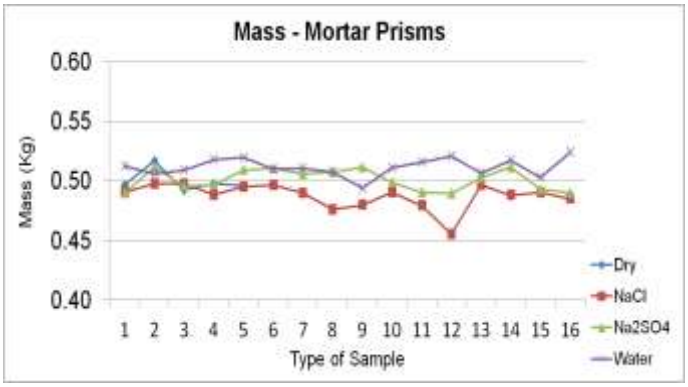

Fig 5.49 - Mortar prisms - Mass

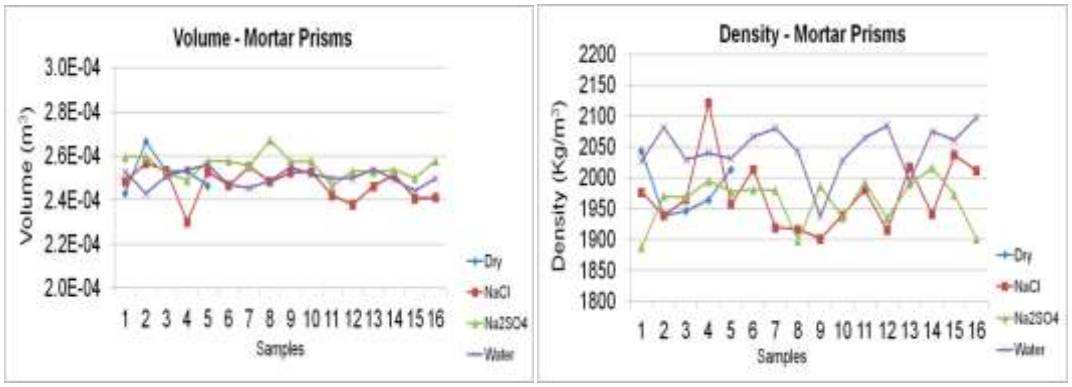

Fig 5.50 - Mortar prisms - Volume (left) ; Mortar prisms - Density (right)

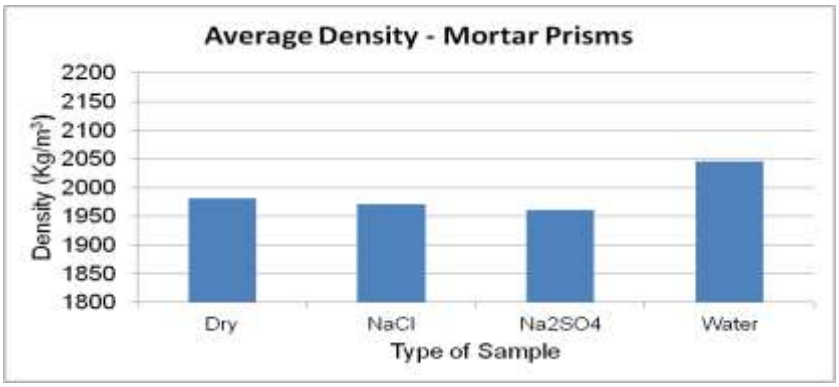

Fig 5.51 - Mortar prisms - Average density

Graph in fig 5.51, presents the average density for each type of samples, thus, the presence of salt decreases the value of density of mortar samples, mainly Na_2SO_4. Samples in contact only with the water and dry samples present the highest average density values.

5.4.2. BRICKS

For samples of brick, the analysis of the mass lost due to degradation of the material after the period of exposure to weathering and immersion in different solutions, was not taken because there was no significant weight loss. Only an evaluation of the mass, volume and density was made.

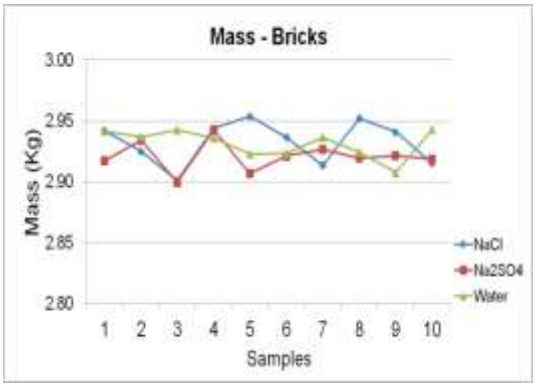

Fig 5.52 - Bricks - Mass

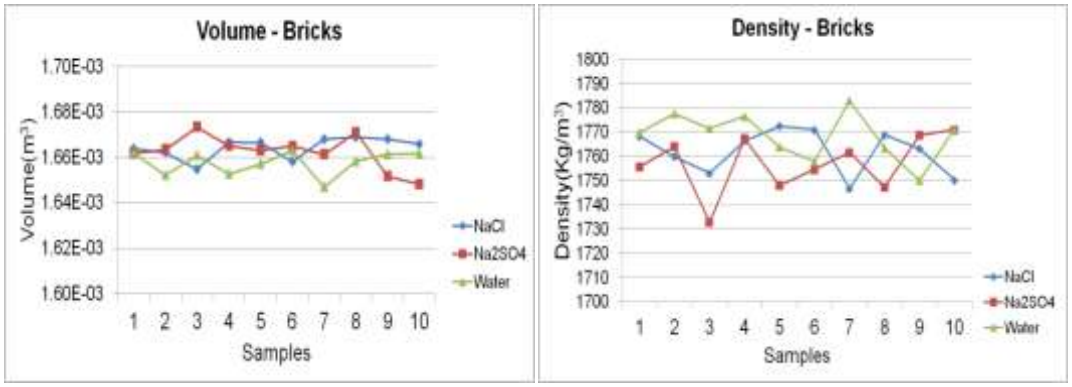

Fig 5.53 - Bricks - Volume (left) ; Bricks - Density (right)

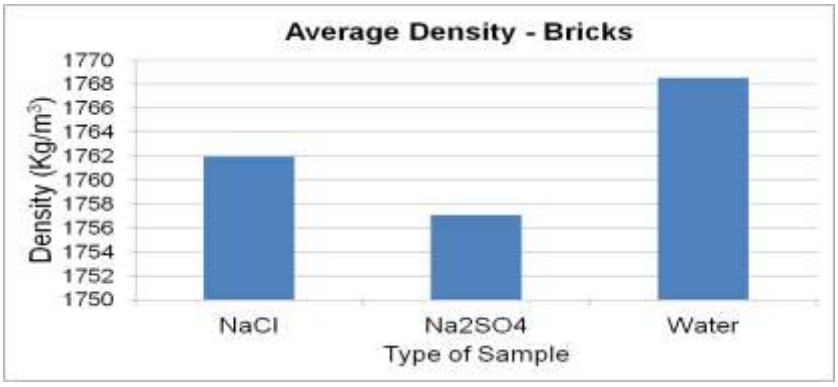

Fig 5.54 - Brick samples - Average Density

Figure 5.51 show the average values of density for brick samples. As happened for mortar prisms, the presence of salt causes a decrease in density of material, particularly sodium sulphate. Thus, the lowest value of density is found for sulphate brick samples, and the highest value for water brick samples.

5.4.3. STONES

After the exposure to environmental agents, stone samples were also weighed and powder resulting from degradation of material was collected. Samples that show greater amount of mass loss are from "Lecce" set, L3/L4 (Na_2SO_4 0.05%), and L5 (Na_2SO_4 0.1%), from Stuttgart set S4 (NaCl 0.1%) and S6 (Na_2SO_4 0.1%), fig 5.52. So, it is possible to observe that also in case of stone samples higher values of mass lost correspond to samples in contact with sodium sulphate.

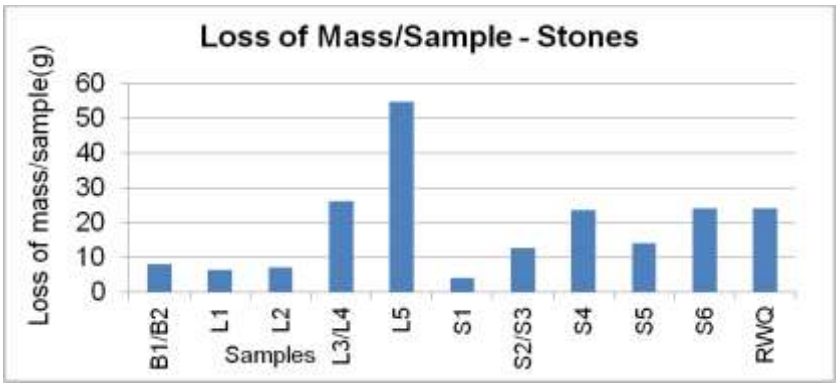

Fig 5.55 - Stones - Loss of Mass/Sample

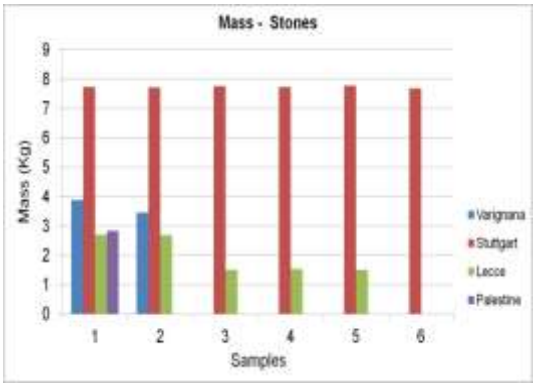

Fig 5.56 - Stones samples - Mass

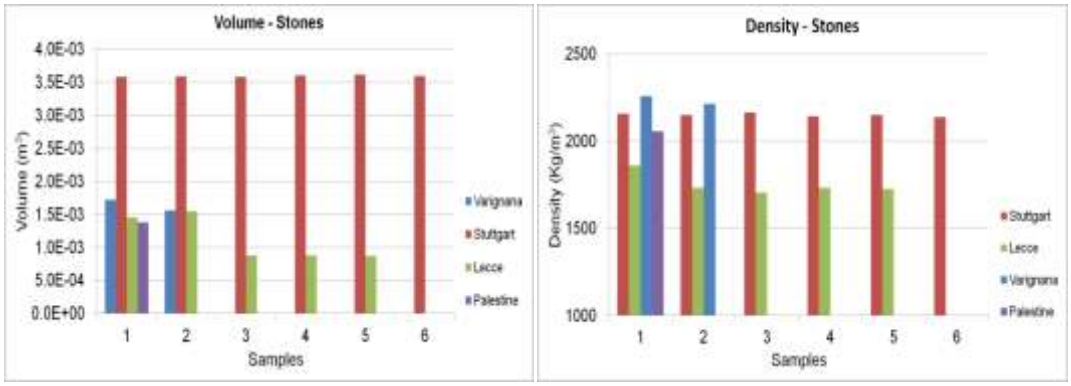

Fig 5.57 - Stones samples - Volume (left) ; Stones samples - Density (right)

From density chart presented in fig 5.57 (right), "Varignana" samples B1, B2, all "Stuttgart" samples and Palestine stone present the highest average density, however, between each type of stones, density present very constant values.

Fig 5.58 - Powder collected from mortar prisms (left) ; Powder collected from stones (right)

6
EXPERIMENTAL WORK OUTDOORS

6.1. VISUAL INSPECTION

By visual inspection of the masonry wall (PNDE), outside the laboratory, it appears that this is very damaged in its lower part, with erosion and delamination of bricks. It is possible also to observe the existence of efflorescences in lower part, coinciding with the most damaged part of the wall. Visually defined is also the moist part of the wall that presents a colour change (darker) of the material. Moreover, by visual analysis of the others walls, it possible to observe that the high concentration of salts in solution in contact with the wall encourages the development and dissemination of efflorescence. Sulphate impregnated walls are those that present more efflorescence and damaged material.

Fig 6.1 - Efflorescence in the Wall PNDE (left) ; Detail of damaged part of the wall PNDE (right)

6.2. SONIC TESTS ON LARGE-SCALE WALLS

6.2.1. MATERIAL AND PROCEDURE

In this chapter are described the sonic tests conducted in the outside wall PNDE, subjected to capillarity rise with a solution of sodium sulphate (0.05% by weight) at its base and weathering decay due to four seasons of exposure of the climate agents. As for the other non-destructive tests, the sonic device was available at the University of Bologna and all the test was carried out in LISG (Laboratory of Structural and Geotechnical Engineering).

The procedure to perform the sonic test is not very easy since it is necessary more than one person (mainly in direct test) to hold the instrument and another to read and save the data. The process is

based on applying a small bump at the desired point while holding the accelerometer in contact with the surface of the material. The equipment used for the sonic test consists of:

- Computer, fig 6.2 (left)
- Amplifier, fig 6.2 (right)
- Hammer PCB 086-berillium tip, fig 6.3 (left)
- Microaccelerometer, fig 6.3 (right)
- Display

Fig 6.2 - Computer (left) ; Amplifier (right)

Fig 6.3 - Hammer PCB 086 (left) ; Microaccelerometer (right)

Data is acquired on the computer using software Labview and shown in the display through the wave-form of emitted and received waves generated by the impact of the hammer. Data processing is done, acquiring the value for the time of flight and attenuation of the waves through the software Elasonic, fig 6.4. Data was acquired with an amplification of 10x, so the reduction to the real values of the data was made in order to obtain the attenuation. Blue line, showed in fig 6.4, corresponds to the wave caused by impact of the hammer, while the red line corresponds to the wave received in the acceler-ometer.

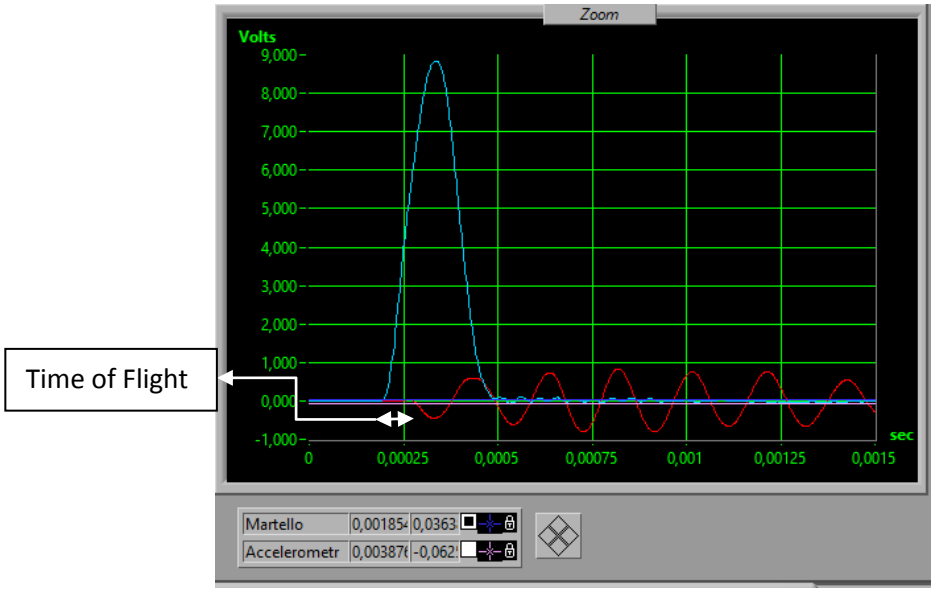

Fig 6.4 - Example of sonic waveforms acquired with the software Elasonic

Different geometric configurations can be used to perform the indirect tests, by columns, in which the emitter remains at the same point and the accelerometer runs the various points contained in the same vertical or horizontal line, the test can be also made crossing points in a diagonal to capture the signal from the emitter at varying distances.

In this case, in order to accomplish the ultrasonic superficial tests, the wall was previously marked with a grid shown in the fig 6.5, to help performing the tests with precision and the same points previously carried out. The grid consists of 6 circumferences with radius from 10cm to 60 cm, the stations are numbered from 1 to a 190. Shown in the grid are the vertical and horizontal stations.

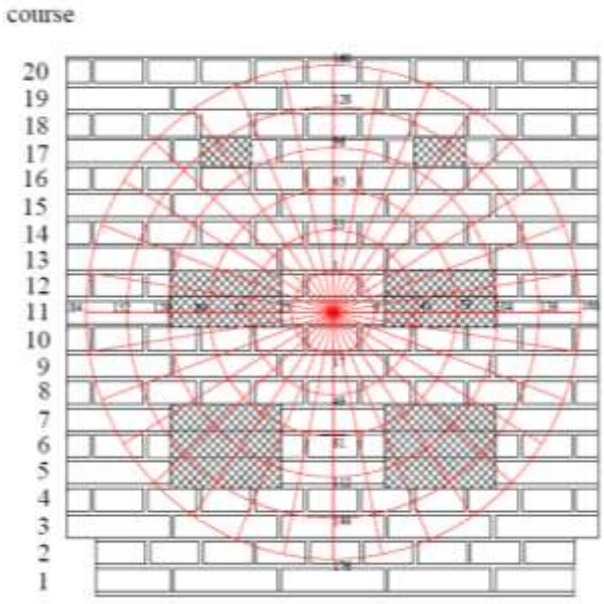

Fig 6.5 - Grid for the superficial sonic test - Stations at intersection between 6 circumferences (radius: 10 cm to 60 cm) and 16 diameters

Also direct sonic tests were performed in this wall, according to the grid shown in fig 6.6. In this case hammer and accelerometer are placed in line on opposite sides of the masonry element. 18 courses were analysed from 3 to 20, for a total of 171measurements.

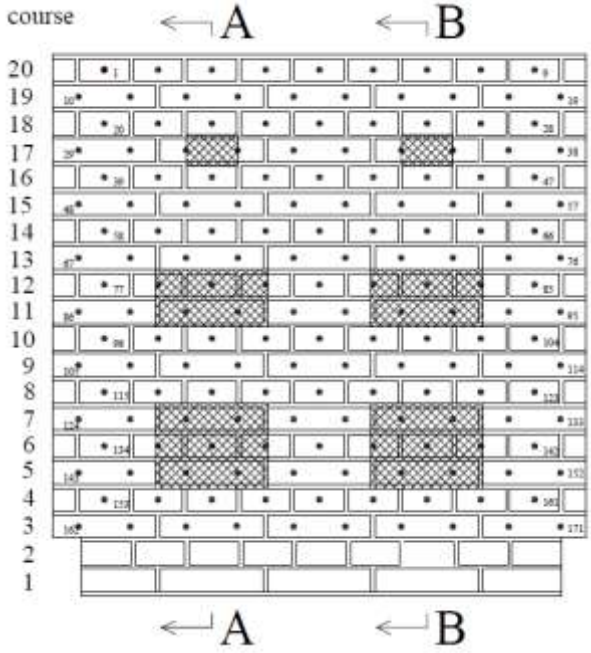

Fig 6.6 - Grid for direct sonic test on the wall PNDE: stations and courses

6.2.2. ANALYSIS AND INTERPRETATION OF RESULTS

Both direct and superficial sonic tests were performed in order to analyse the behaviour of the time of flight, attenuation and velocity in masonry walls. The results obtained for superficial tests are presented in the graphs in fig 6.7 to 6.15. Simultaneously with the test, a visual analysis was also made in order to compare the influence of parameters such as the existence of efflorescence, damaged material or mortar.

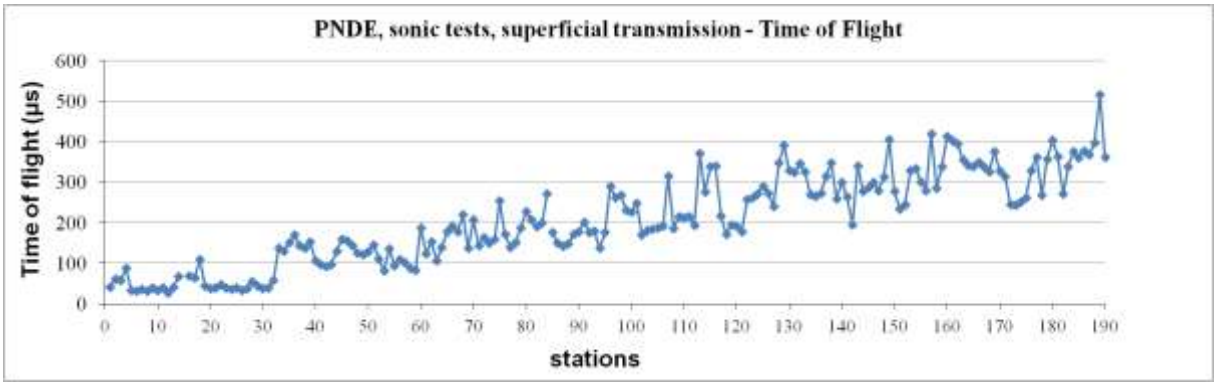

Fig 6.7 - PNDE, superficial sonic test- Time of flight

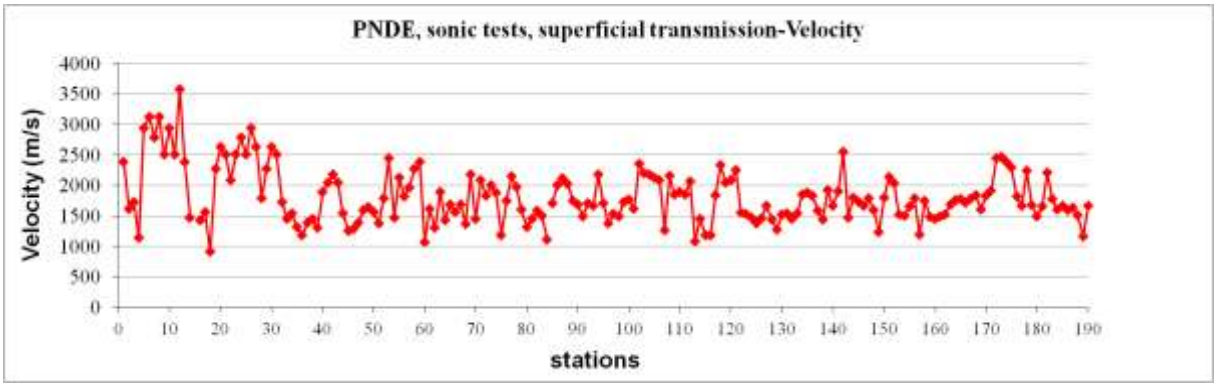

Fig 6.8 - PNDE, superficial sonic test - Velocity

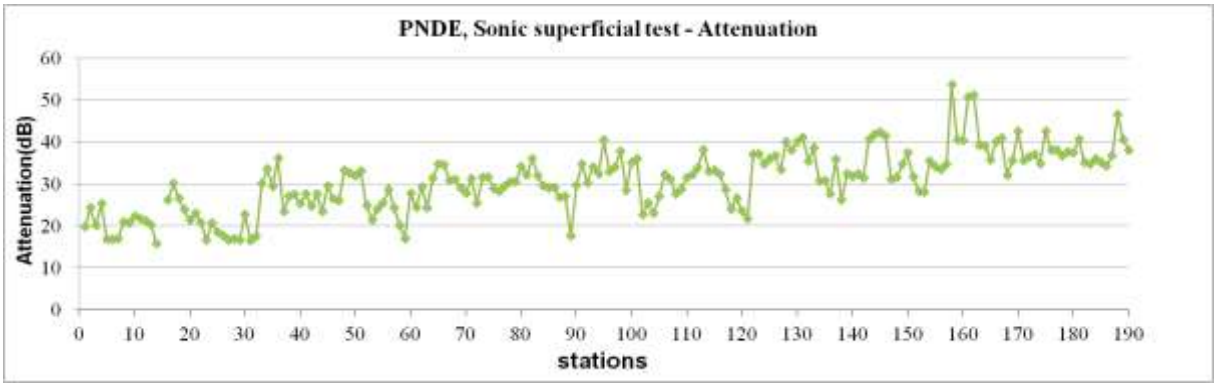

Fig 6.9 - PNDE, superficial sonic test - Attenuation

From the fig 6.7, 6.8, and 6.9 it is found that in the first part of the graph, corresponding to the 1st circumference, time of flight has constant and lower values, while velocity show the highest values. Attenuation values tend to increase slightly as we go through the circles, ie, we move away from the centre of the wall. It also appears that the maximum attenuation of the waves correspond to the points where the test was performed with the hammer in contact with the mortar. The presence of mortar cause a decrease of velocity and an increase of attenuation while the existence of efflorescence cause a decrease of attenuation value and an increase of velocity.

For each circumference the values for the velocity of the waves are shown in the graphs 6.10 to 6.15. From the velocity distribution, it is possible to analyse values in each circumference individually. By visual inspection the points with mortar, delaminations and damaged material, present lower values for the velocity of wave velocity.

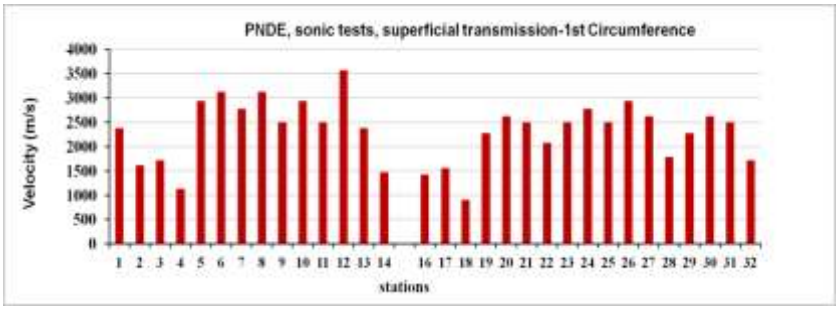

Fig 6.10 - PNDE, sonic test, superficial transmission - 1st circumference

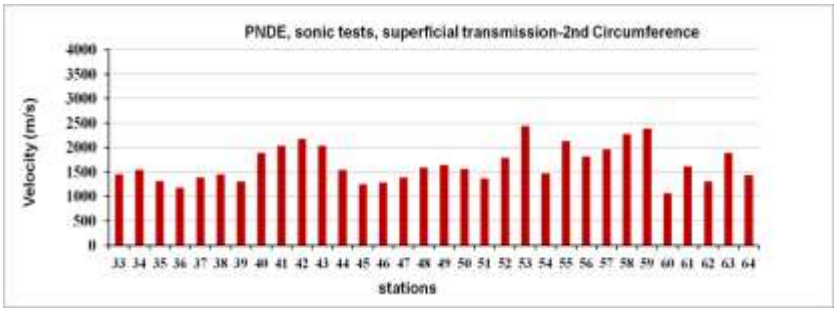

Fig 6.11 - PNDE, sonic test, superficial transmission - 2nd circumference

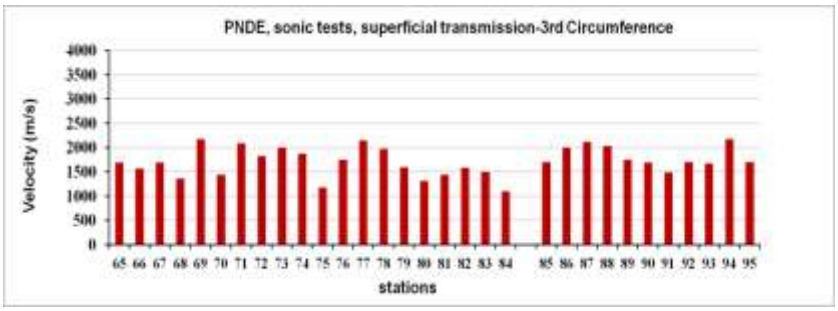

Fig 6.12 - PNDE, sonic test, superficial transmission - 3rd circumference

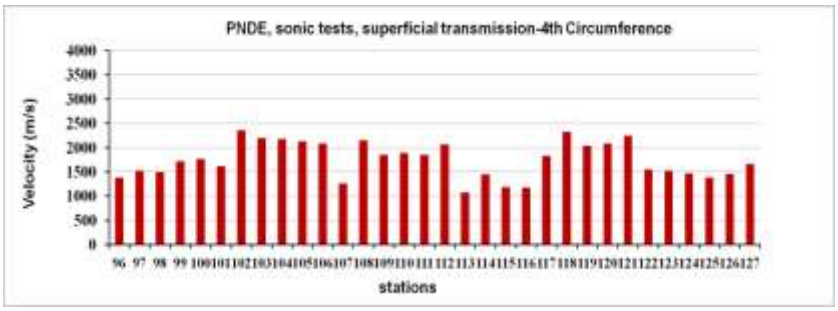

Fig 6.13 - PNDE, sonic test, superficial transmission - 4th circumference

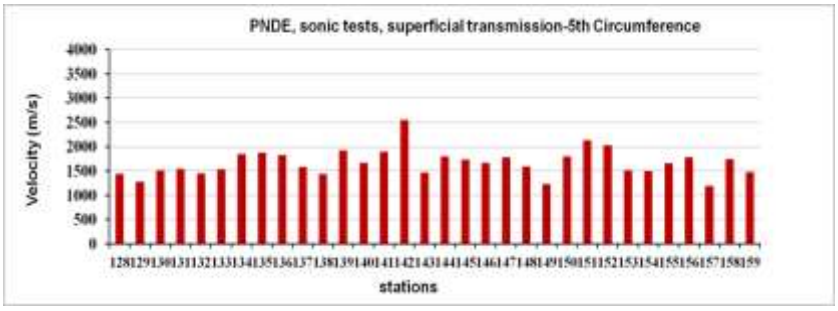

Fig 6.14 - PNDE, sonic test, superficial transmission - 5th circumference

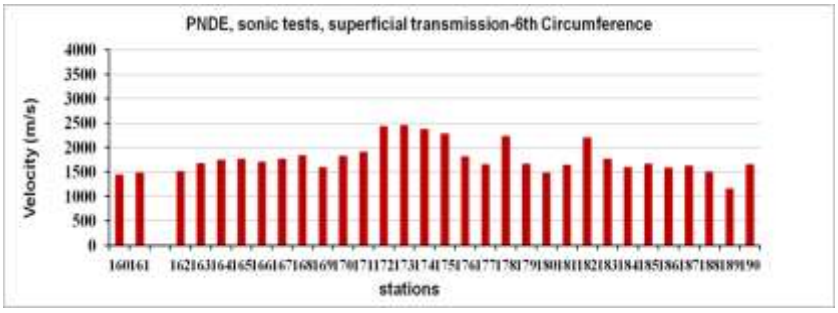

Fig 6.15 - PNDE, sonic test, superficial transmission - 6th circumference

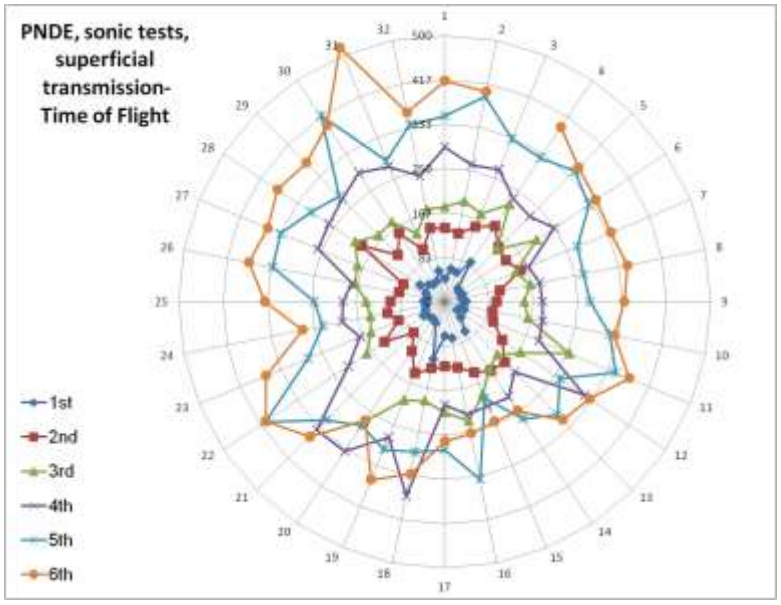

Fig 6.16 - PNDE, superficial sonic test - Time of flight distribution

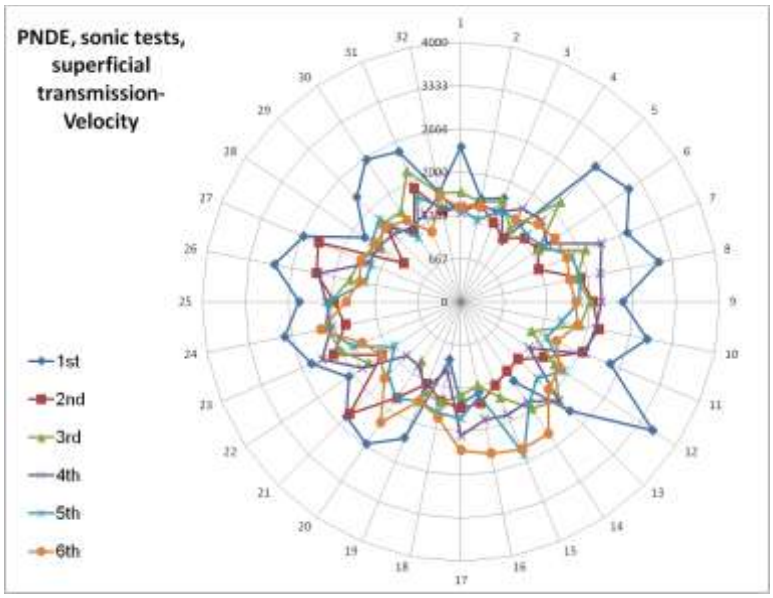

Fig 6.17 - PNDE, superficial sonic test - Velocity distribution

The graphs of time of flight and wave velocity presented in Fig. 6.16 and 6.17 are in accordance with the grid shown in fig 6.5. Both time of flight and the velocity depends on the distance of the hammer

to centre of the circle where the accelerometer is placed, thus, it is intended to analyze, for each circumference, the varying results. With regard to time of flight and velocity, the values are more dispersed in the lower half of the circumferences where the material is more degraded and with visual presence of moisture and efflorescence.

Table 14 - Average Velocity - Circumferences

Average Velocity (m/s)	
Circ1	2317
Circ2	1653
Circ3	1718
Circ4	1749
Circ5	1671
Circ6	1781

Table 15 - Average Velocity - Above and below horizontal diameter

Average Velocity (m/s)		
	Above horizontal diameter	Below horizontal diameter
Circ1	2371	2552
Circ2	1614	1698
Circ3	1749	1686
Circ4	1742	1757
Circ5	1600	1751
Circ6	1613	1960

Average velocity values, table 14, present for the first circumference higher velocity than the others, this is due to a minor number of mortar joints tested in this circumference. Also, below the horizontal diameter, are found higher values for the velocity, since the wall present some moisture content in this area and also the presence of efflorescences.

With regard to direct sonic test, the values of the time of flight, velocity and attenuation are presented in the fig 6.18, 6.19 and 6.20.

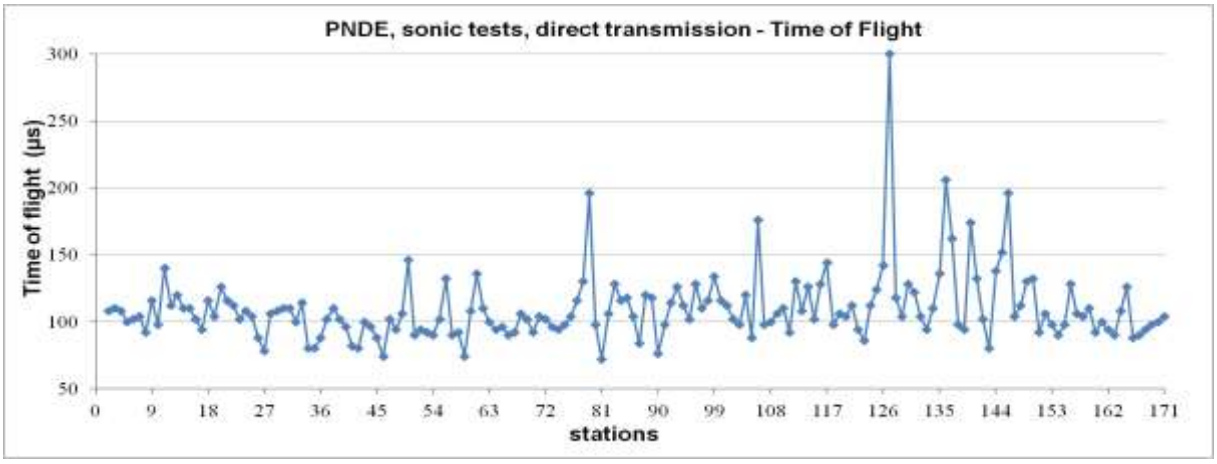

Fig 6.18 - PNDE, direct sonic test - Time of flight

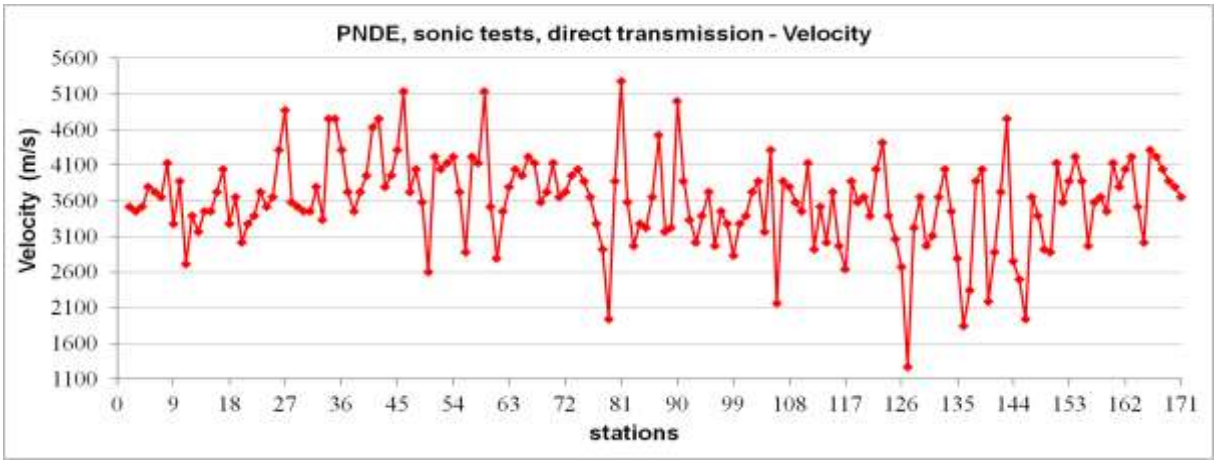

Fig 6.19 - PNDE, direct sonic test - Velocity

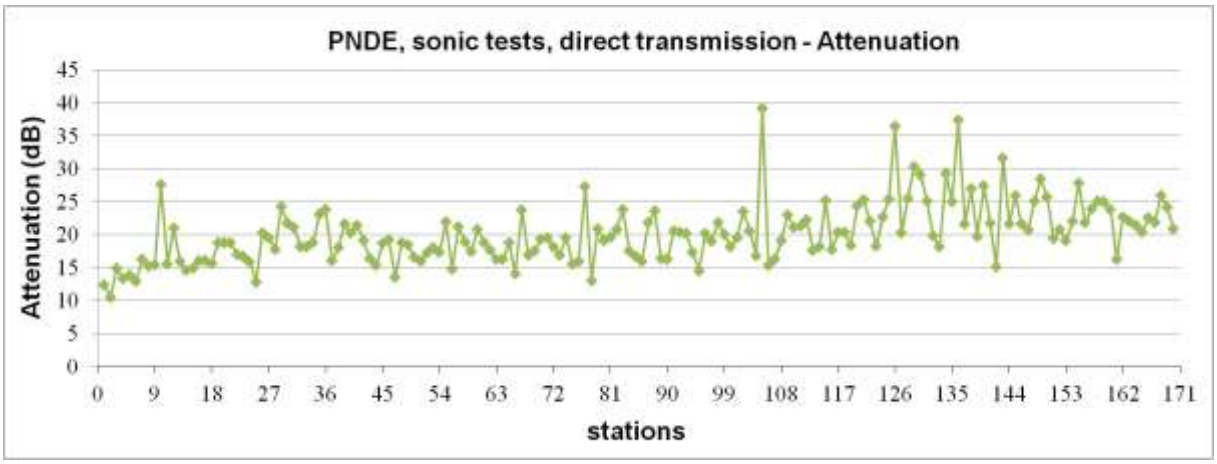

Fig 6.20 - PNDE, direct sonic test - Attenuation

It is clearly visible in the graphs 6.19 and 6.20, in their final part, and especially between stations 124 and 153, ie between courses 8 and 5, a great dispersion of results with a decrease in velocity values and an increase in attenuation. By visual inspection it can be seen that in this zone the material's surface is damaged, presenting delaminations and salt efflorescence. Furthermore, the sonic direst test is very sensitive to the presence of holes inside the wall, that correspond to the lowest picks observed in the graph of velocity and the highest picks in the attenuation chart.

From the average values of velocity and attenuation for each course, vertical profiles in wall PNDE were created (Figure 6.19). As expected, also through these charts, the location of the damaged area in the wall is perfectly identified, with a decrease of velocity and an increase of attenuation, corresponding to the courses 5 to 8.

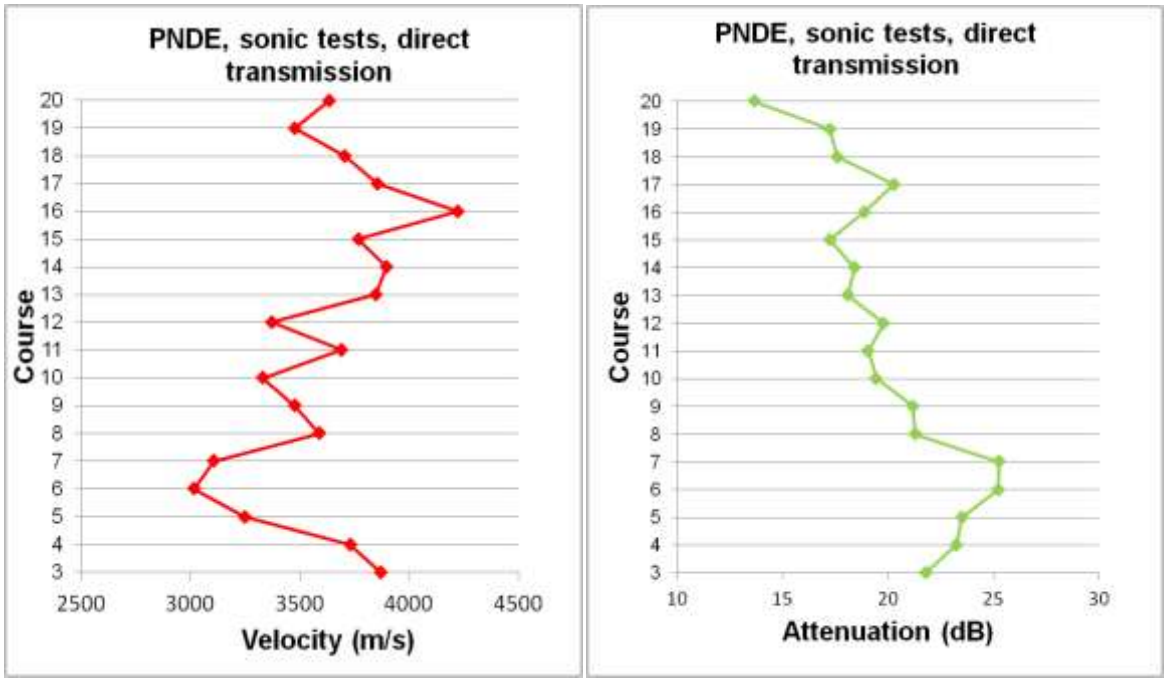

Fig 6.21 - PNDE, vertical profile - Velocity (left) ; PNDE, vertical profile - Attenuation (right)

Some voids at different depths constitute the internal features of the wall PNDE, in order to verify the effectiveness of sonic test in detecting this internal characteristics, vertical profiles of velocity and attenuation corresponding to the sections A and B, fig 6.6, were designed. In odd courses, direct sonic test do not analyse points corresponding to these vertical profiles , so, an average values of two near-est point were taken. By the fig 6.22 and 6.23, variation of velocity and attenuation can be compared with the right position of the holes inside the wall. It is clearly visible a great reduction of velocity in points where test coincides with voids (course 6 and 12). Also the behaviour of attenuation is quite evident showing an increase in its values when a void is detected.

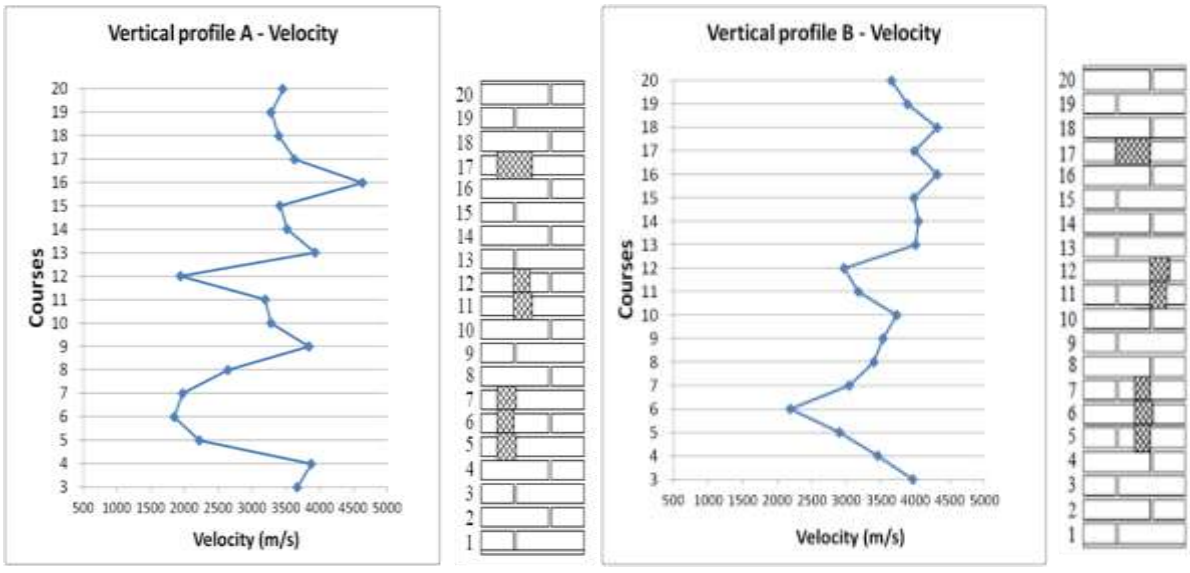

Fig 6.22 - PNDE, vertical profile A - Velocity (left) ; PNDE, vertical profile B - Velocity (right)

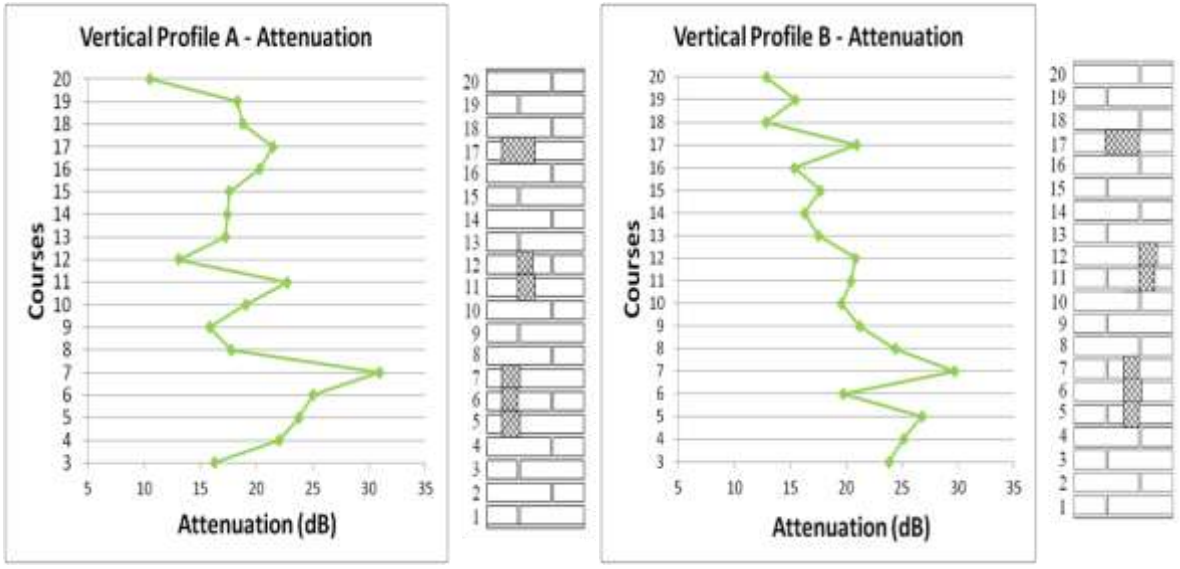

Fig 6.23 - PNDE, vertical profile A - Attenuation (left) ; PNDE, vertical profile B - Attenuation (right)

6.3. THERMOGRAPHY

6.3.1. SPECIMENS TESTING

IR Thermography tests have been performed in order to evaluate the effectiveness of this technique to qualitatively detect defects and inhomogeneities in masonry walls. The investigations were carried out at LISG, considering three walls: PNDA, PNDC, PNDD and PNDE.

Since the goal is only to show anomalies, only passive thermography measurements were accomplished to make a qualitative data analysis. Relative temperature variations and not absolute have been taken into account, as the real material emissivity has not been measured. Material emissivity was set to the value 1. The analysis of thermograms allows the identification of the most degraded areas or the ways that moisture follows and therefore to correlate the visible effects with those showed in the thermograms.

The temperatures scale visualized in each thermogram has been used to compare temperatures between areas in the same frame or between the same points in the thermograms acquired. The thermograms obtained during the day (26 ºC and RH=52%), were post-processed by identifying the appropriate thermal scale colour for the display, that allows identifying areas where there are salt efflorencence and moisture. The input data in the software is the emissivity, temperature, relative humidity and the distance between the wall and thermocamera.

For investigation in large-scale walls in laboratory, a FLIR 620 thermaCAM has been employed. This camera has a thermal sensitivity of 40mK and an accuracy of ±2ºC. This equipment has 640x480 pixels and digital photos were simultaneously stored with thermograms for subsequent analysis. Data analysis and reporting has been performed by FLIR QuickReporter2.1 software.

6.3.2. ANALYSIS AND INTERPRETATION OF RESULTS

Fig 6.24 - Wall PNDE front (left) ; thermogram (IR_21932)

Thermographic test in wall PNDE was performed on 5th of June 2014 and with a distance from the wall of 4.70m. The presented thermogram (IR_21932) was post-processed in order to better identify the characteristics of the wall From the picture taken to PNDE wall front (Fig 6.24, left), immersed in a solution of Na_2SO_4 (0.05% by weight), different colours can be observed in surface material. This wall also presents a white line corresponding to the formation of salt efflorescence; below this line, the darker material is due presence of moisture by the action of rising damp. The dark coloration at the top

is due to the rain precipitation to which the wall has been subjected and that somehow caused a colour change of material.

From the thermogram (IR_21932) obtained, the contrast of colours, thus the temperatures, between the top and bottom of the wall is very evident. The darkest part at the top of the wall does not present a lower temperature than the contiguous part, so it can be said that there is only a colour variation of the material surface which is not visible in thermogram. A very dark colour is shown at the base of the wall, due to the existence of an high concentration of moisture in the area.

Fig 6.25 - Wall PNDE front, thermogram (IR_21932) of wall PNDE, areas and temperatures

The same thermogram for the wall PNDE (IR_21932) is presented in figure 6.25, showing maximum and minimum temperature values for different areas in the wall. The upper part, marked as (Ar3) above the efflorescence, has a maximum temperature of 41.3 °C, while the lower part (Ar2) containing moisture has a slightly lower maximum temperature, 39.5 °C. The darkest part of the thermogram (Ar1) has a maximum temperature value much lower: 36.7 °C, this correspond to the moist area of the wall.

Table 16 - Wall PNDE, temperatures from the 3 areas in fig. 6.25

	Tmax (ºC)	Tmin (ºC)	Tmax-Tmin (ºC)
Ar3	41.3	37.1	4.2
Ar2	39.5	36.4	3.1
Ar1	36.7	35.5	1.2

Observing differences between the maximum and the minimum temperature in table 16, higher is the level of moisture, lower is the difference between maximum and minimum values for the temperature.

The graphs obtained from the temperature distribution along the vertical lines (L1, L2 and L3) shown in Fig 6.26, 6.27 and 6.28 identify clearly the position of mortar joints, with a lower temperature and the height position of capillary moisture in the base of the wall, through a sudden decrease in temperature, identified by the vertical lines in the graphs. Through the lower peak temperatures at the bottom of the wall, it is possible to get an idea of the humidity level reaches (above the second joint).

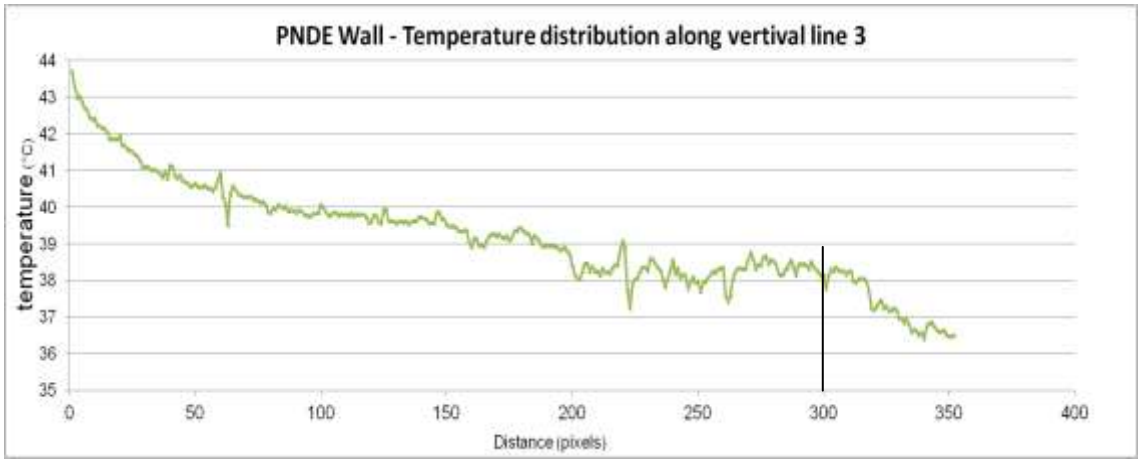

Fig 6.26 - Wall PNDE front: Temperature vs. Height profile (line3)

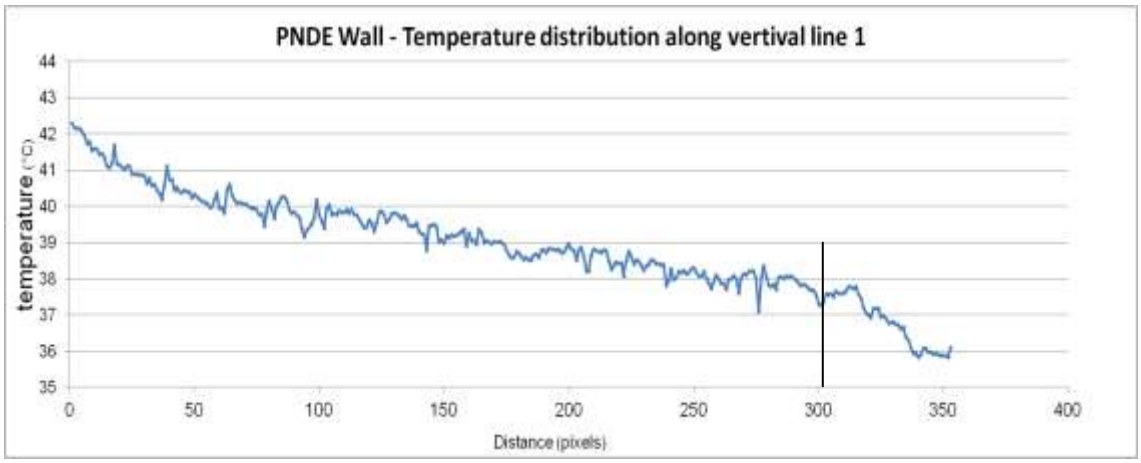

Fig 6.27 - Wall PNDE front: Temperature vs. Height profile (line1)

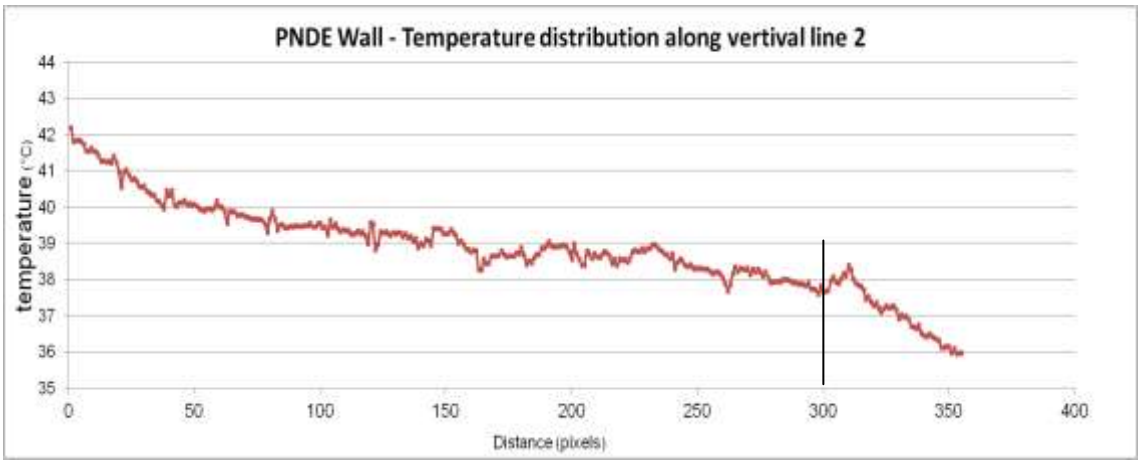

:

Fig 6.28 - Wall PNDE front: Temperature vs. Height profile (line2)

From the figures above it is possible to observe some differences between the three lines. The first part of the line 1 and 3 is more horizontal, presenting more constant values for the temperature, while the line 3 present a decrease of temperature.

Thermograms corresponding to the walls PNDA, PNDC and PNDd were post-processed choosing same range temperatures (32.2ºC; 43.9ºC) in order to make a comparison between walls.

Fig 6.29 - Wall PNDA rear (left) ; thermogram (IR_22008) of wall PNDA (right)

The wall PNDA, fig 6.29, immersion on NaCl (0.1% by weight), has plaster on the rear, the presence of efflorescence is visible by a dark stripe in the thermagram with a very lower temperature. Infrared thermography technique is also able to accurately detect the phenomena of rising damp in plastered brick masonry walls.

Fig 6.30 - Wall PNDD, front (left) ; thermogram (IR_22004) of wall PNDD (right)

In thermogram of wall PNDD (Na_2SO_4, 0.1% by weight), fig 6.30, it is visible formation of salt efflorescence and also the moisture path identified by a symmetric shape in both sides of the wall as a cold spots..

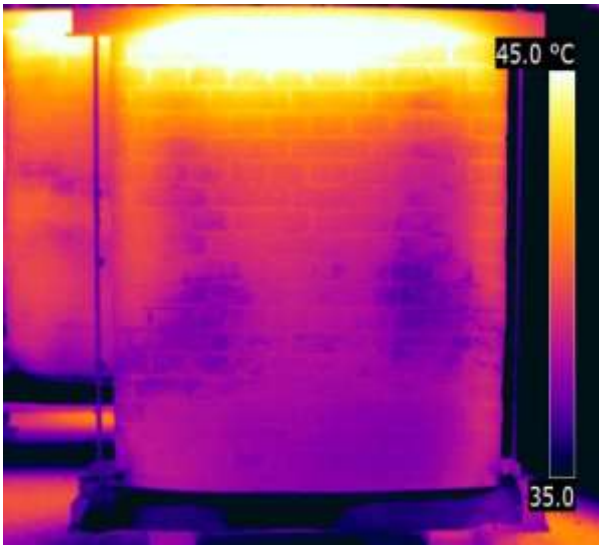

Fig 6.31 - Wall PNDD, front (left) ; thermogram (IR_22004) of wall PNDD - different range of temperatures (right)

In order to better identify temperature variation in the wall PNDD, a different range in temperatures is shown in fig 6.31. From this thermogam, the moisture level is clearly identified, reaching half the height of the wall as well as the presence of salt efflorescence as coldest areas in the thermogram.

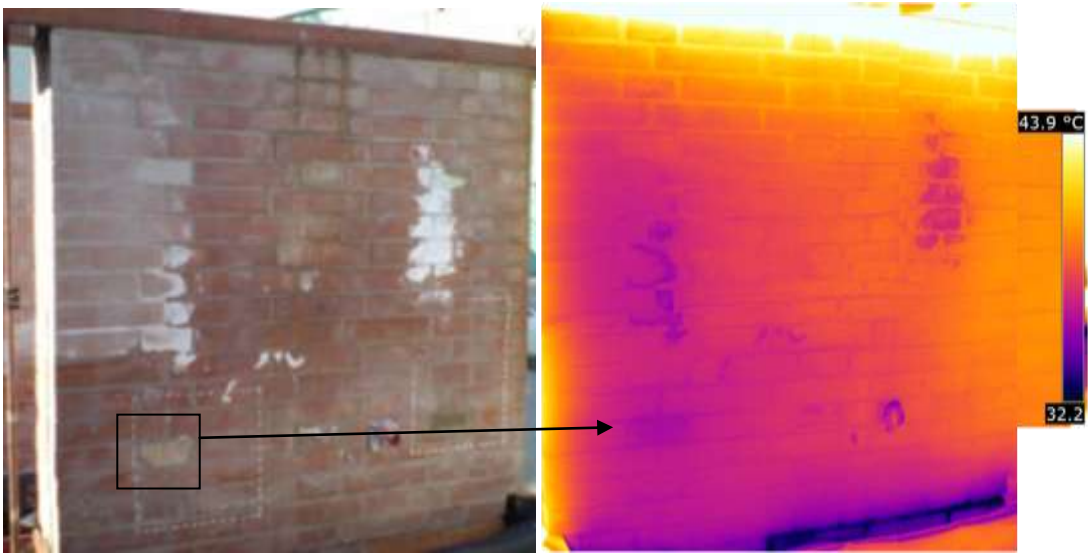

Fig 6.32 - Wall PNDC, front (left) ; mosaic thermogram of wall PNDC (right)

Wall PNDC thermogram, is a mosaic construction constituted by small thermograms, this wall was subjected only to the action of rain water, however, salt efflorescence are also visible with cold spots within moist area. Some details are easily detectable by the analysis of the thermogram. The presence of moisture and its path is clearly defined in this wall, it reaches an high level mainly in left side of the wall. At the base, a big decrease of the temperature suggest a saturation of the wall material in that local. Also some constituent materials can be identified, such as the stone inclusion indicated in the figure 6.32 and presence of a hole.

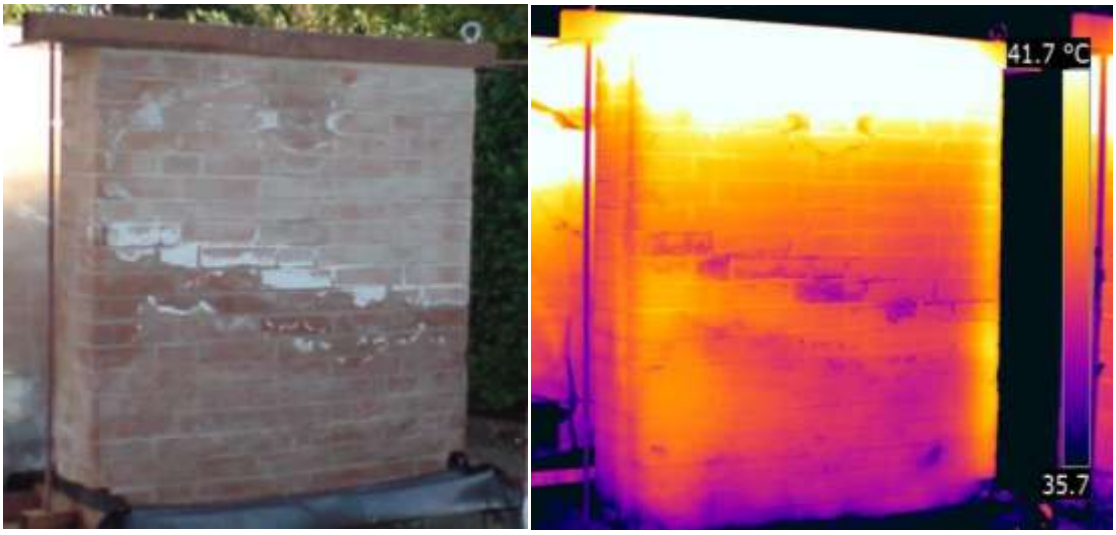

Fig 6.33 - Wall PNDC, rear ; thermogram (IR_22006) of wall PNDC

For the opposite side of the wall PNDC, corresponding themogram is shown in fig.6.33. In this case a change in range temperature was made to evidence the temperature differences. From the thermogram (IR_22006) it is possible to identify, a different level of moisture (lower) in this side of the wall as well as a different salt efflorescence configurations as a "horizontal" stripe with a decrease in temperature. Also the moist area appears different with a lower height.

6.4. GPR RADAR

6.4.1. MATERIAL AL PROCEDURE

Radar tests were performed on front side of brick wall PNDE in order to obtain information about the inner geometry (some intentional voids of various size are present at different depths and levels), and about the moist state of the material. As for the other non-destructive tests, also the GPR RADAR test was conducted at LISG, University of Bologna. Due to complexity of the post-processing only a qualitative assessment of acquired data and interpretation of obtained radargrams were made.

Radar test were carried out using a GSSI SIR-3000 system in reflection mode and a Palm antenna of 2.0 GHz frequency, equipped with a survey wheel for precise recording of antenna position along the survey lines. Both vertical (F001 to F0023) and horizontal lines (F0024 to F0046) were performed according to a grid with dense mesh (5*5 cm), fig 6.35. Vertical lines were recorded in the downwards direction and the horizontal lines in the from-left-to-right direction. 3-D post-processing was made using the software RADAN 6.6.

Radar has been operated in reflection mode with 1024 samples/scan at 16 bits. By use of RADAN 6.6. fig 6.36 to 6.41, it is possible to visualize post-processed data files obtained from vertical or horizontal radar survey lines, as well as time-slices (these are plan view parallel to the tested surface, at various depths). Data post-processing included time-zero position correction and gain increase.

At the time of testing, the wall had already undergone 4 seasons of natural ageing and capillary rise by 0.05%-wt sulphate brine. The moisture content of the wall should have been fairly poor, as no capillary rise was underway at the time of radar testing, nor in the months before.

The cross-section of the wall is a 3-header, it means that the thickness of 38 cm is made of 3 brick heads (3 x 12 cm in width) with 2 mortar joints (1 cm each) in between. The wall is about 1.3 m wide and about 1.3 m high, or 20 brick courses.

Fig 6.34 - Data acquisition on brick masonry wall PNDE by Palm 2 GHz antenna, using a 5x5 cm grid (left) ; Radar GSSI SIR-3000 (right)

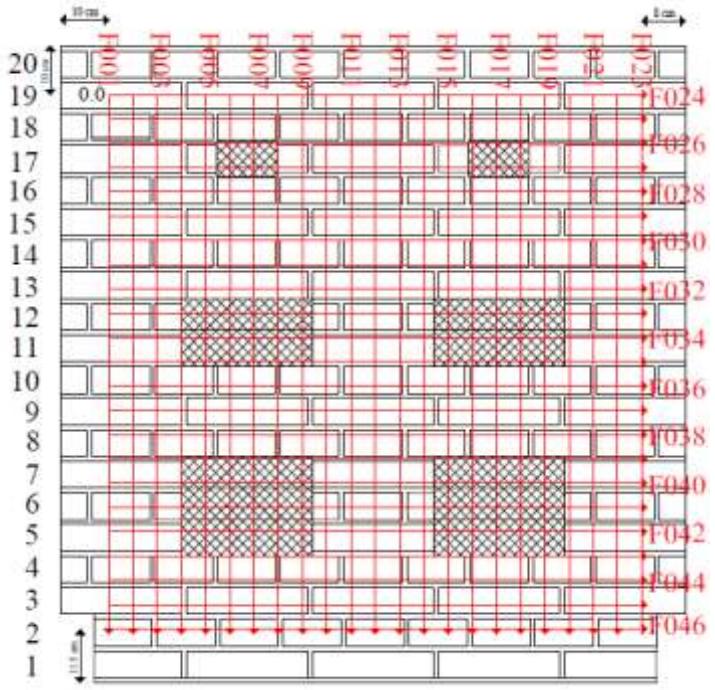

Fig 6.35 - Vertical and horizontal survey lines along the 5x5 cm grid, during GPR radar acquisition.

6.4.2. ANALYSIS AND INTERPRETATION OF RESULTS

Radargram presented in fig 6.36 corresponds to the vertical line (F012) in the middle section of the wall, at 65 cm from the lateral borders. It shows along the vertical direction the height of the wall, from the top (course 20) to the bottom at (course 3), for a length of about 1,1 m. On the horizontal direction in the radargram, depth through the wall is shown in meters. The tones of grey indicate the signal reflection intensity, with white and black being the strongest reflections.

During the test, a convenient value of dielectric constant was used of ε=6.25, however the real dielectric constant of the masonry material was calculated during the data analysis (ε= 5.4) from the thickness of the wall (0.38 m) and the wave velocity 0.129 m/ns.

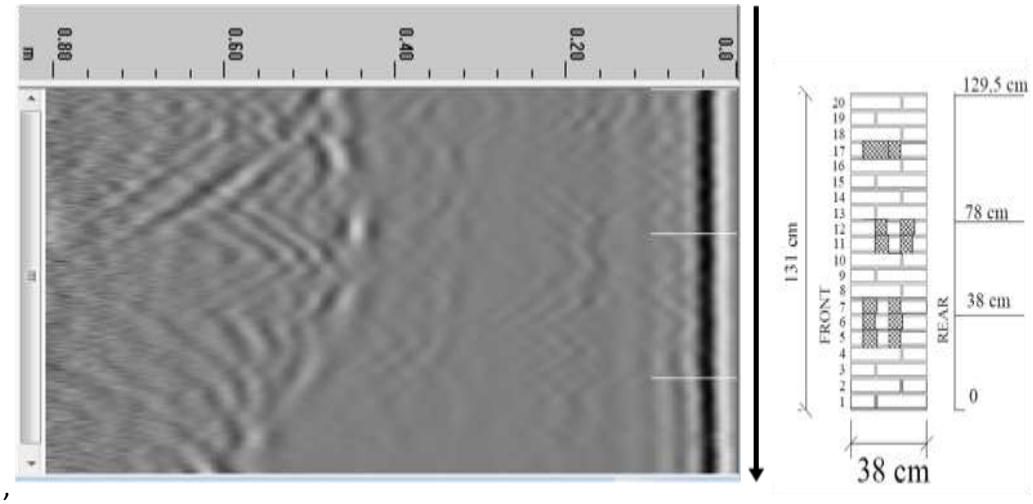

Fig 6.36 - Post-Processed radargram (F012) (left) ; Vertical section wall PNDE (right)

The vertical axis represents the distance travelled by the antenna, in m (the white segments are marks automatically placed at 40 cm, 40cm and 30cm from the top to the bottom) while the horizontal axis indicates the depth of reflection (in ns) of the radar signal within the material. These depths can be converted in meters by having the value of dielectric constant or signal speed .

Reflection from the surface is visible at the right side of the radargram as a black straight line. The vertical section considered corresponds to three bricks with two 1-cm mortar joints between the front and the rear side of the wall. The brick and mortar layout is visible by a band of reflection hyperbolas at about 0.14 m and 0.28 correspond to the mortar joint, configuration, fig 6.36.

The reflection from the opposite side of the wall is also clearly defined. An increase in the moisture content is visible in the lower part of the wall as a delay in the rear side reflection since, in presence of water, the wave velocity decreases, appearing as an increase in thickness, thus, capillary rise level can be estimated with a quite good accuracy. Also in the top part of the radargram, from the increase of the thickness it is possible to observe a little increase in humidity at the top of the wall.

From the vertical line F012 four different sets of cores were taken, dried in oven and weighted until a constant weight were achieved. Thus, the percentage of weight loss correspond to the percentage of humidity contained in wall when the GPR RADAR test was performed. Microcores with different lengths were taken from courses 6,9,12 and 15. Fig 6.37 presents the percentage of moisture lost in each course, it is possible to observe that deeper in the wall, higher is the moisture content for each course.

Course 6, present the highest percentage of moisture lost, this course has about 33 cm from the bottom of the wall, this height in radargram correspond to the increase of the thickness in radargram then, an increase of moisture value, fig 6.38. Above course 6 the level of humidity is lower as it can be seen through the radargram, fig 6.36 and the graph in fig 6.37.

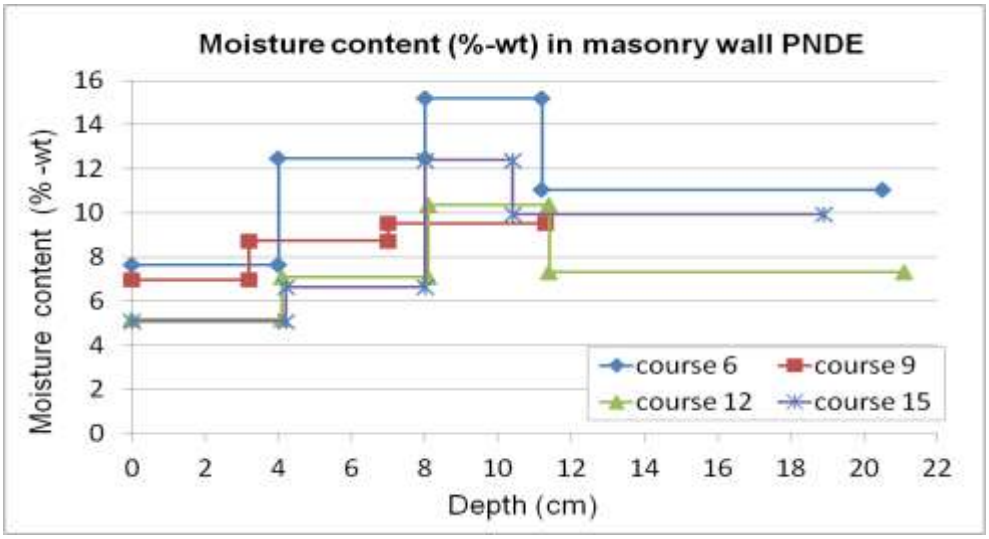

Fig 6.37 - Percentage of moisture lost in courses 6, 9, 12 and 15

In fig 6.38 (left), it is presented the radargram of vertical survey line (F007). In this section there are three different internal voids, as shown in vertical section, figure 6.38 (right). Please note that the radargram and the sketch on the right of fig. 6.37 are mirrored. The same dielectric constant was adopted (ε= 5.4).

The vertical position and depth of the voids are clearly identified as hyperbolas in the right side of the radargram. First hyperbole, in the top, at about 0.06m correspond to the first void, the second hyper-

bole at 0.12m show the position of the second void and finally, the third hyperbole in the bottom, represent the last void. Also the dimensions of voids are identifiable by the vertical length of hyperbolas and their intensity. So it is possible to accurately detect the internal features of the wall.

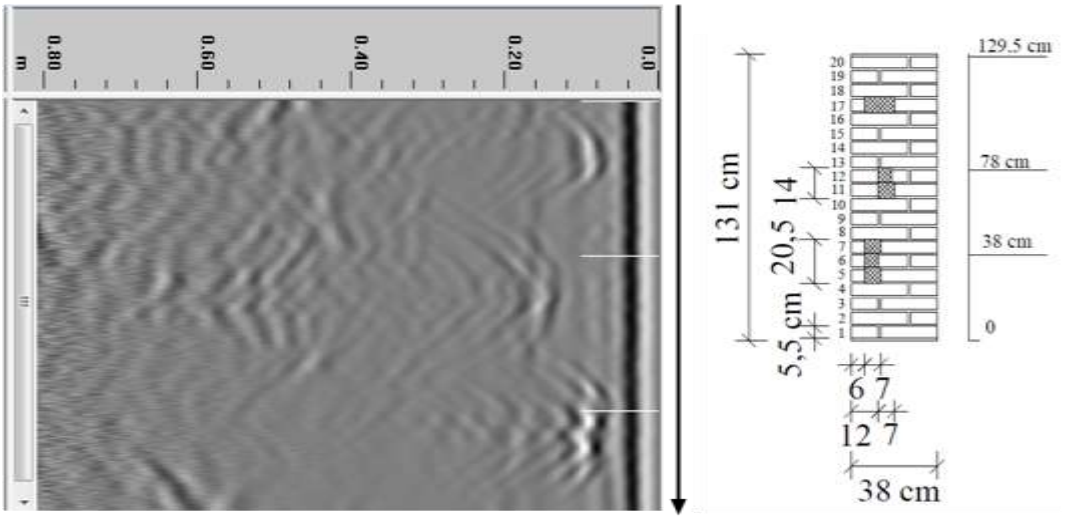

Fig 6.38 - Post-Processed radargram on vertical line (F007) (left) ; Vertical section wall PNDE (F007) (right)

The radargram corresponding to horizontal line (F027) is placed close to the top of wall, on the 2 defects at course 17. It is shown after time-zero correction (4.43 ns) and gain amplification (gain: 1.9-1), fig. 6.38. Also in this case the two small voids are clearly located at 2 different depths as a small hyperbolas

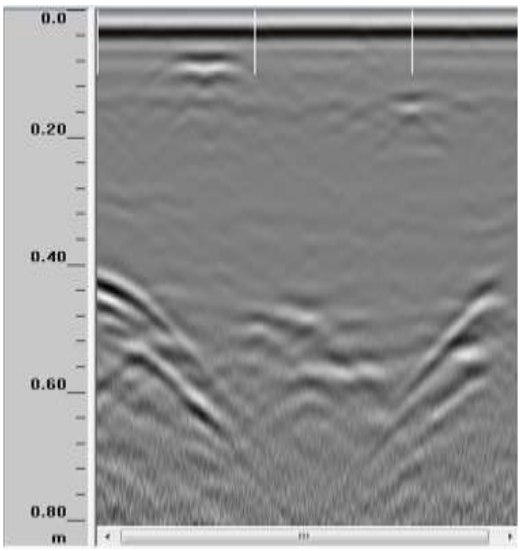

Fig 6.39 - Post-Processed radargram on horizontal line (F027)

In Fig. 6.39, a time slice is shown from the 3D volume of all the data. The post processing has included time zero correction (4.43 ns), gain amplification (gain: 2-0.7) and background removal (319, gain: 1.5-1). This is a sub-superficial image of a plan at 0.13 m of depth below the tested surface of the wall. It shows 4 of the 6 voids, as white areas. The intensity and the extension of these white areas correspond to the size of the real voids in the wall.

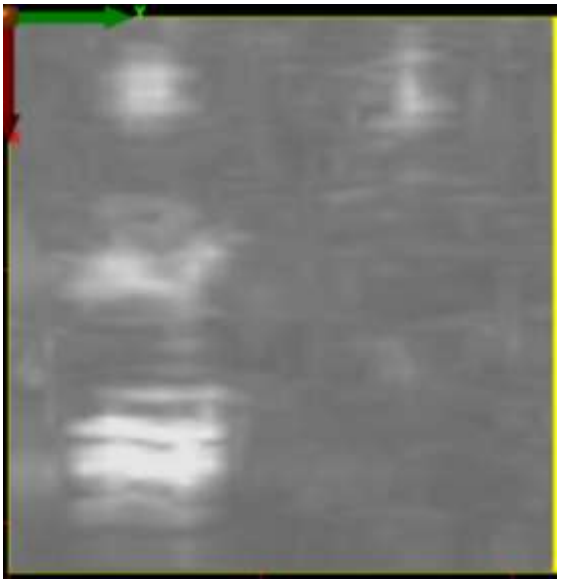

Fig 6.40 - Time slice - 3D volume of all data

The position of the four voids can be measured in the software, corresponding to the coordinates on the radar grid used:

- First void at (x=0.15,y=0.3);
- Second void at (x=0.3,y=0.3);
- Third void at (x=0.85, y=0.3);
- Fourth void at (x=0.15,y=0.8) at depth of z=0.13 m.

Finally, thanks to a transparency function in the software, a new image was produced, showing only the high-intensity reflections, which mainly correspond to the positions of the 6 voids in the specimen. These are shown as pale grey volumes in the image, fig. 6.41.

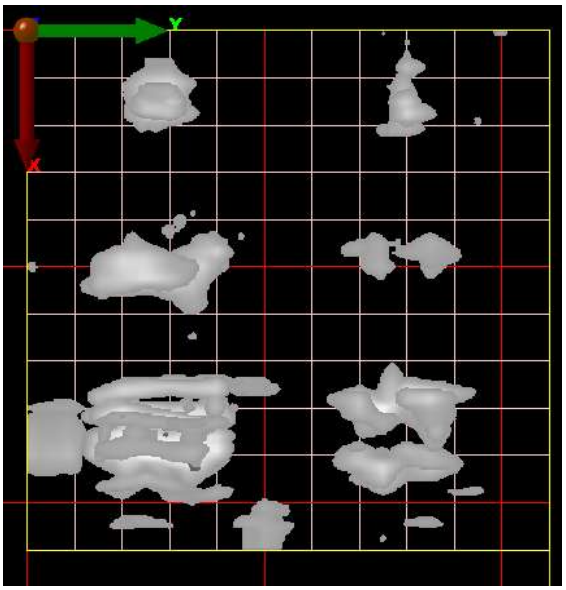

Fig 6.41 - High-intensity reflections

7

MECHANICAL ASSESSMENT OF MORTAR AND BRICK SAMPLES

7.1. INTRODUCTION

In this chapter, the experimental procedure for an quantitative assessment of materials degradation is described, together with an evaluation of the mechanical performance of water saturated mortar and bricks samples after capillary rise and affected by weathering cycles by sodium sulphate, sodium chloride and tap water. The test aims were getting the value for the modulus of elasticity of the materials and their compression strength. All tests were carried out in LISG (Laboratory of Structural and Geotechnical Engineering), in the University of Bologna.

The elastic properties of the material are characterized by the static modulus of Elasticity E_s, which represents the relationship between the applied force and the deformation occurred following the Hooke's Law (1.7); where σ (N/mm^2) is the stress, E, the modulus of elasticity (N/mm^2) and ε, the deformation of the material (dimensionless).

$$\sigma = E * \varepsilon \tag{1.7}$$

Modulus of elasticity, or Young's modulus, is a mechanical characteristic of solids that gives a sense of stiffness to the material. Two different types of modulus can be obtained, the static and the dynamic modulus of elasticity. The relation between the static and dynamic modulus of elasticity cannot be directly compared because their values are influenced by the conditions in which the test is performed. First of all, time of application of the force is different in the two tests: in static testing, it lasts several minutes while in the dynamic tests it only lasts a few microseconds. The values of the pressure applied in the static tests is in the order of MPa, while in dynamic tests, the impact pressure does not exceed the value of 100Pa. Uniaxial loading can cause the closure of microcracks, which leads to an increased deformation and consequently to a decrease in static modulus of elasticity, $E_{s.}$ Non-destructive dynamic tests have a great advantage, since they do not alter the structure of the material.

.

7.2. SPECIMENS PREPARATION

These mechanical experiments were undertaken in order to determine the Young's Modulus, static Modulus of Elasticity and the compression strength of masonry units. In this laboratory test, the same type of samples analysed with ultrasound test were used in order to assess their mechanical character-

istics after four seasons of exposure to atmospheric agents and contamination by different types of solutions. Four different positions of the same sample were considered for the bricks

Three mortar samples were used without any change, however, each brick was cut and numbered according to the examples in fig 7.2. After cutting and smoothing of the surfaces the small samples of bricks were dried in the oven for at least one day. Special care was taken to obtain representative specimens which are straight and uniform in cross section. It was necessary to verify their planarity, (faces planar and parallel), in order to apply an uniform load in the sample. After this procedure the samples were dried again at 70ºC for 16 hours.

Fig 7.1 - Set of mortar samples, three used in compression test

Fig 7.2 - Example of the brick C6 and its notation, cut into 4 small bricks (left) ; Sets of different bricks (right)

From the set of 72 small cubes (6 bricks of each series NaCl, Na_2SO_4 and Water were cut into four small bricks), 12 samples were taken (4 with NaCl; 4 with Na_2SO_4; and 4 with water) to perform the mechanical test with the electric extensimeter. The remaining 60 samples were used to perform compression tests without extensometers. The 12 cubes were first measured and weighted, and then instrumented with two strain gauge or with two rosettes on opposite vertical faces, according table 17.

Table 17 - Instrumented samples with strain gauges and rosettes.

Specimens		**2 Single Strain Gauges**	**2 Rosette**
Mortar Prisms	**NaCl**	(C7)	-
	Na_2SO_4	(S7)	-
	Water	(H14)	-
Brick Cubes	**NaCl**	(C2 1.0; C4 2.3)	(C1 2.1; C3 3.0)
	Na_2SO_4	(S1 2.3; S5 1.0)	(S5 2.1; S3 3.0)
	Water	(H4 1.0; H3 2.3)	(H4 2.1; H2 3.0)

7.3. COMPRESSION TESTS

7.3.1. UNIAXIAL COMPRESSION TEST USING ELECTRIC EXTENSIMETERS

Compression test to obtain the static Modulus of Elasticity was performed using an electric extensimeter. It is a method for the experimental analysis of the deformations using a device which measures mechanical deformation (strain). The strain gauge is a device able to measure the deformation of the object on which it is positioned due to a measurement of electrical resistance. Normally, the strain gauge is attached to a structural element, and uses the change of electrical resistance of a semiconductor under tension.

The strain gauge converts a small mechanical motion into a electrical signal because when a semiconductor is stretched, its resistance increases. The change in resistance is a measure of the mechanical motion following the equation (1.8), where ε is the deformation ($\mu\varepsilon$), k is the gauge factor, $\Delta R(\Omega) = (Rf - Rg)$ is the variation of resistance of the extensometer and R_g (Ω) is the initial resistance extensometer and R_f (Ω) the final resistance of extensimeter.

$$\varepsilon = \frac{1}{k} * \frac{\Delta R}{Rg} \tag{1.8}$$

According to the European Standard (EN772-1, 2002), the compression tests were performed through the use of a strain gauge to determine the deformation of the material. The utilization of the extensometer was made according the European Norms (EN10478-1; EN10478-2; EN10478-3; EN10478-4 and EN10478-5, 1998).

Two types of strain gauges were applied (table 17): With the single strain gauge it is possible to determine only the deformation in the load direction while rosette allows us to obtain the deformation of both vertical direction and perpendicular direction to the applied load and thus allows us to determine the Poisson's ratio. Figure 7.3 show the instrumented samples used to carry out the compression test.

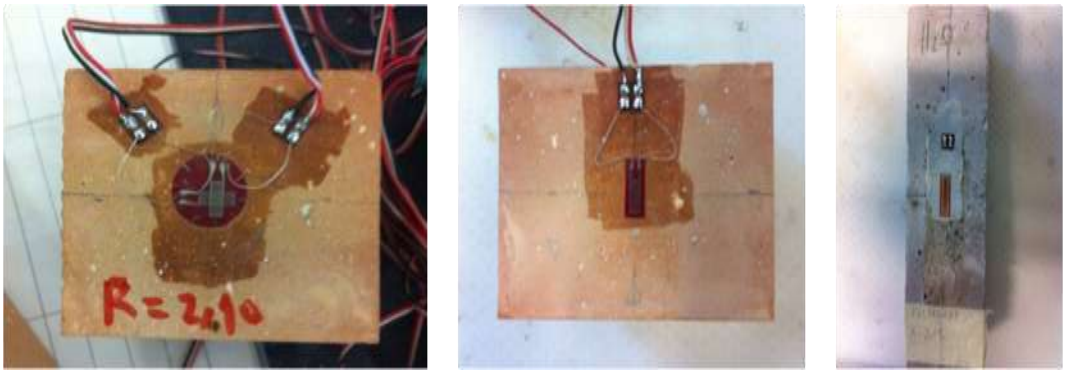

Fig 7.3 - Brick cube instrumented with rosette (left) ; Mortar Prism instrumented with strain gauge (middle);

Brick cube instrumented with strain gauge (right)

7.3.2. ANALYSIS AND INTERPRETATION OF THE RESULTS

Uniaxial compression tests were carried out by means of a load control testing machine by increasing the load until the failure of the masonry specimen.

To measure the global movements of the samples under compression, 2 different strain gauges were employed in two main faces of each sample. The measuring instruments were connected to a data acquisition control unit using Labview software.

The axial and transversal (applying rosettes) displacements measured via the stain gauges were used to recover the stress-strain diagram and thus to determine some parameters characterizing the behaviour of the samples under compression, the static Modulus of Elasticity, Poisson ratio and compressive strength. According to the European Standard (EN1015-11, 2007), the tests to determine the compressive strength were performed in 3 different types of mortar samples (NaCl, Na_aSO_4 and Water). For each mortar sample, the test consists in applying three load cycles. The first of 100 N, the second of 150 N and the third cycle in order to achieve rupture, fig 7.4. With regard to the bricks samples, just one load was applied until the rupture, fig 7.5, each compressive test was performed with a velocity of 1MPa/s. Data is directly acquired from the computer, that gives a chart of load /displacement.

Fig 7.4 - Compression test in mortar sample S7(Left) ; Compression test in mortar sample S7 - Rupture (middle); Data acquired in the computer (right)

Fig 7.5 - Compression test in mortar sample C1_2.1 (left) ; Compression test in mortar sample C1_2.1 - Rupture (right)

From the compressive testes carried out were obtained the graphics of stress-strain for the three mortar prisms tests presented in the fig 7.6, 7.7 and 7.8. Figures 7.9 and 7.10 are two examples of stress strain graphs for the bricks cubes, C2_10 (strain gauges) and C1_21 (rosette). The deformation correspond to the average deformation for the two strain gauges instrumented in samples.

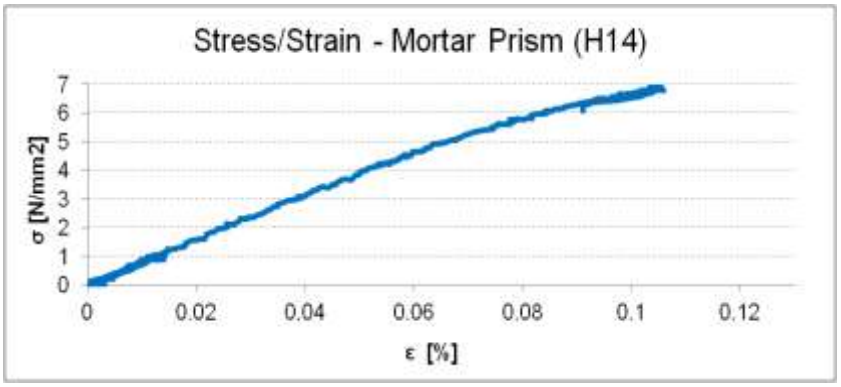

Fig 7.6 - Mortar sample H14, water contaminated, stress-strain curve

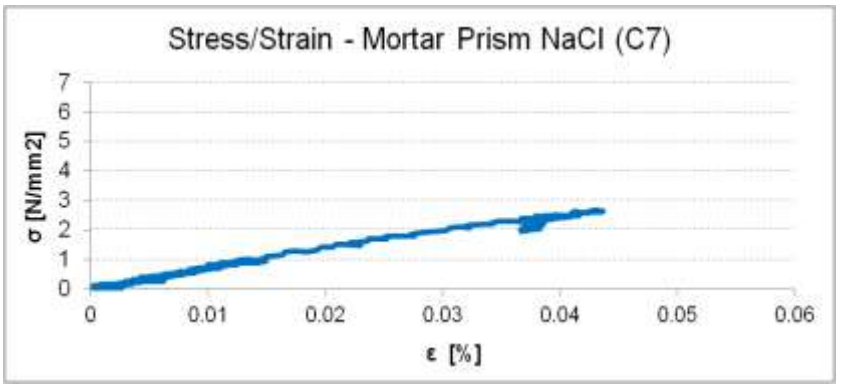

Fig 7.7 - Mortar Prism C7, chloride contaminated, stress-strain curve

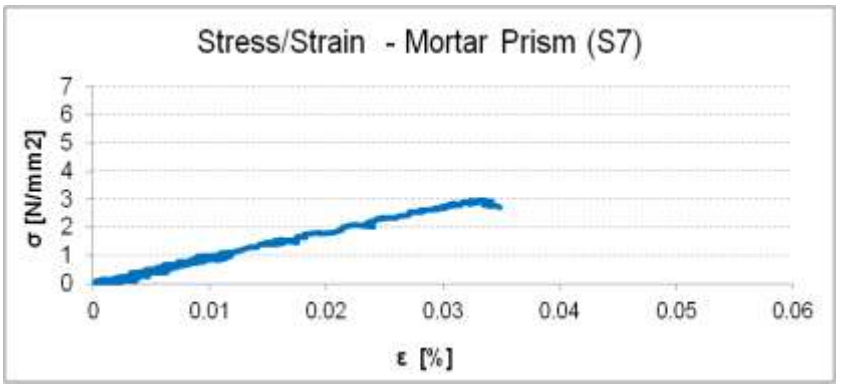

Fig 7.8 - Mortar Prism S7, sulphate contaminated, stress-strain curve

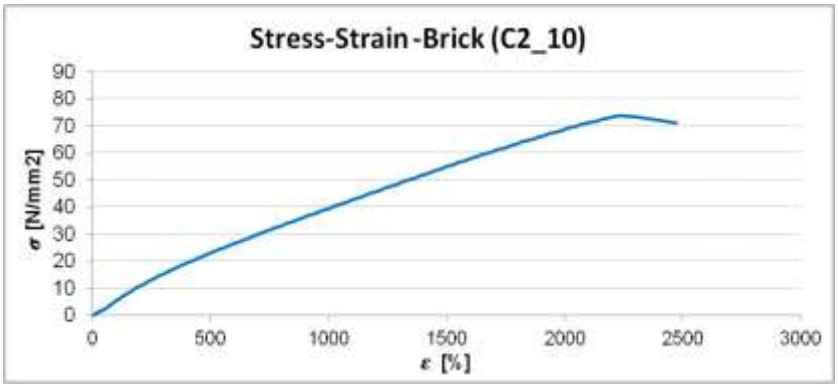

Fig 7.9 - Brick cube C2_10, stress-Strain curve (strain gauge)

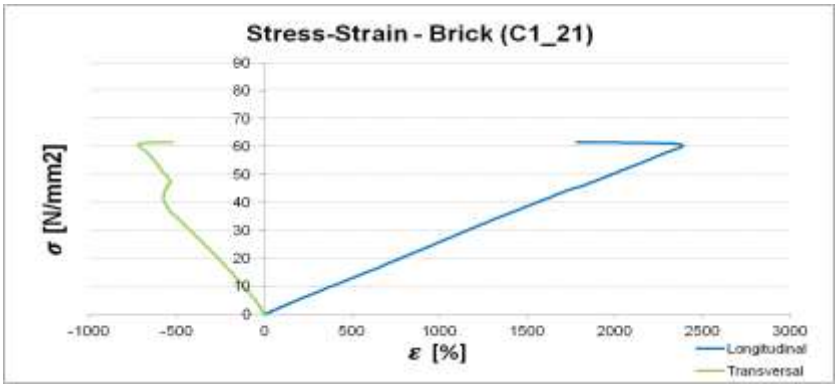

Fig 7.10 - Brick cube C1_21, stress-strain curve (rosette)

Table 18 - Mortar samples, compressive strength

Sample Code	Compressive Strength (MPa)
H14	6.9
C7	2.7
S7	3.0

Table 19 - Instrumented brick cubes, compressive strength

Sample Code	Compressive Strength (MPa)	Average Compressive Strength (MPa)
H4_10	82	77
H4_21	69	
H3_23	77	
H2_30	79	
C2_10	74	72
C1_21	61	
C4_23	73	
C3_30	82	
S5_10	78	69
S5_21	55	
S1_23	68	
S3_30	76	

From the peak value in stress-strain graphs is possible to obtain the compressive strength of material. Mortar and bricks present a similar behaviour for the compression strength. Regarding the mortar sample (table 18), the highest value is founded for the water mortar prism, both chloride and sulphate samples present lower and very similar values. Also for the bricks (table 19) the presence of salts decreases the value of the compressive strength, in this case also the highest value correspond to water bricks, while chloride and sulphate present similar and lower values for compressive strength.

Results of compression tests in brick cubes without electric extensimeter are presented in table 20. In this case, deformation of material is measured by two sensors (LVDT) coupled in machine test, the use of this mechanism instead of strain gauges may be not to accurate because not only the deformation of material is recorded.

Table 20 - Brick cubes, compressive strength and coefficient of variation

Sample Code	Compressive Strength (MPa)	Average Compressive Strength (MPa)	C.o.V (%)
H1_10	75	79	9
H1_21	77		
H1_23	84		
H1_30	73		
H2_10	76		
H2_21	74		
H2_23	88		
H3_10	93		
H3_21	86		
H3_30	84		
H4_23	83		
H4_30	73		
H5_10	73		
H5_21	78		
H5_23	76		
H5_30	86		
H6_10	85		
H6_21	69		
H6_23	71		
H6_30	81		
C1_10	70	76	8
C1_23	84		
C1_30	76		
C2_21	79		
C2_23	66		
C2_30	75		
C3_10	74		
C3_21	68		
C3_23	77		
C3_30	77		
C4_10	65		
C4_21	72		
C4_30	71		
C5_10	74		
C5_21	82		
C5_23	76		

C6_10	79		
C6_21	81		
C6_23	81		
C6_30	86		
S1_10	68		
S1_21	69		
S1_30	74		
S2_10	76		
S2_21	68		
S2_23	80		
S2_30	64		
S3_10	81		
S3_21	73		
S3_23	71	73	8
S4_10	78		
S4_21	66		
S4_23	77		
S4_30	70		
S5_23	66		
S5_30	71		
S6_10	76		
S6_21	75		
S6_23	66		
S6_30	85		

By the values of compressive strength shown in table 20, also in this case salt brick cubes present lower values of compression strength, while water bricks show the highest values. Very similar coefficient of variation is presented for each type of brick cube.

7.3.3. DETERMINATION OF THE STATIC MODULUS OF ELASTICITY FROM MECHANICAL TESTS

Static modulus of elasticity for mortar and brick were calculated by stress/strain graph. For mortar prisms, the value was obtained by the tangent corresponding to the values between 30% and 60% of the maximum stress value while for the brick samples, between 10% and 30%. The values for static modulus of elasticity are presented in tables 20 and 21 and figures 7.11 to 7.15. From the specimens instrumented with rosette, the Poisson ration was also calculated since it gives the displacement in both longitudinal and transversal directions.

Table 21 - Mortar samples, static Modulus of Elasticity

Sample Code	**E_s (GPa)**
H14	7.6
C7	6.0
S7	9.2

Table 22 - Brick cubes, static Modulus of Elasticity

Sample Code	Static Modulus of Elasticity - E_s (GPa)	Average Static Modulus of Elasticity - E_s (GPa)
H4_10	36	35
H4_21	30	
H3_23	39	
H2_30	35	
C2_10	43	38
C1_21	24	
C4_23	45	
C3_30	42	
S5_10	31	44
S5_21	36	
S1_23	52	
S3_30	55	

Table 23 - Brick cubes, Poisson Ratio

Sample Code	Poisson Ratio (υ)	Average Poisson Ratio (υ)
H2_30	0.38	0.38
H1_21	0.38	
C1_21	0.36	0.32
C3_30	0.28	
S5_21	0.30	0.28
S3_30	0.26	

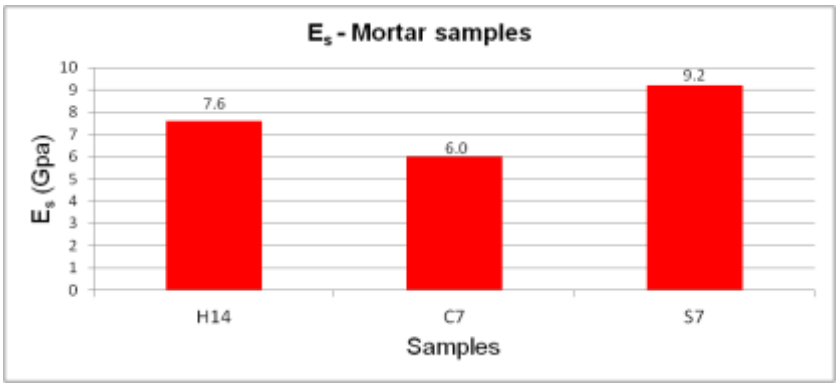

Fig 7.11 - Mortar Prisms, static Modulus of Elasticity

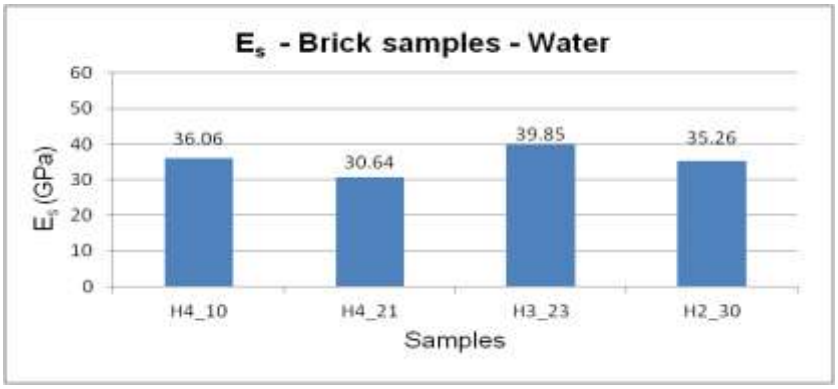

Fig 7.12 - Brick cubes, water contaminated, static Modulus of Elasticity

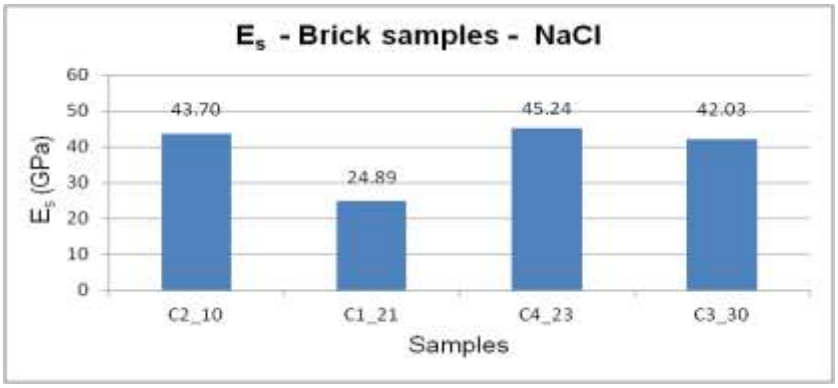

Fig 7.13 - Brick cubes chloride contaminated, static Modulus of Elasticity

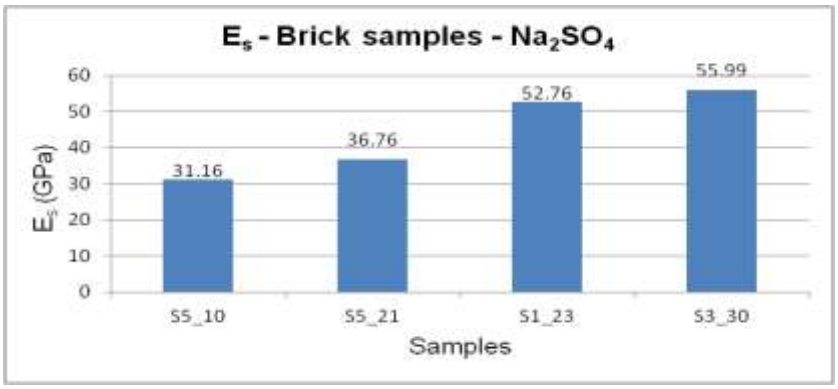

Fig 7.14 - Brick cubes sulphate contaminated, static Modulus of Elasticity

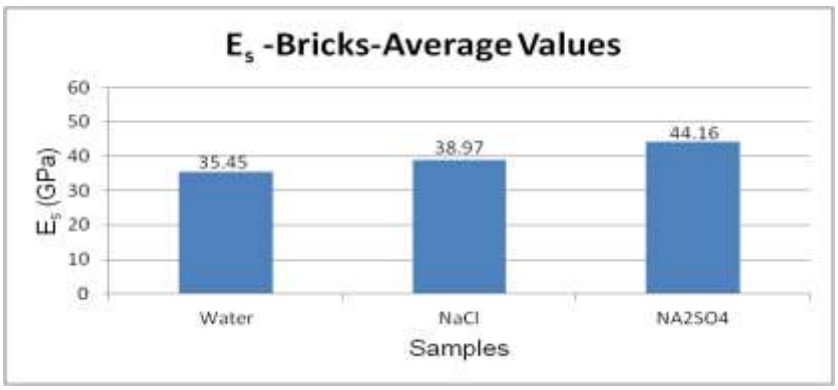

Fig 7.15 - Brick cubes, static Modulus of Elasticity - Average Values

Regarding the mortar samples, just three specimens were analysed due to a small number of specimens to continue the research in the next years. Between the static modulus of elasticity values, the higher one is for the sample with Na_2SO_4, while the chloride prism present the lower value for the modulus.

The analysis of bricks samples was made dividing the samples by type of solution and its position in the original brick. For water and chloride samples higher values are for positions "10" and "23" while sulphate samples present the highest values for positions "23" and "30" corresponding to the those were in contact with solution in the last season. Average values show the highest modulus of elasticity for salt bricks: Na_2SO_4 and the lowest for water bricks.

Both mortar prisms and brick cubes present the highest value of static modulus of elasticity for samples impregnated with sodium sulphate.

Table 24 - Mortar samples, static and dynamic modulus of elasticity

Sample Code	E_d (GPa)	0.7*E_d (GPa)*	E_s (GPa)
C7	6.20	4.3	6.0
S7	8.34	5.8	9.2
H14	9.44	6.6	7.6

*30% of reduction to the value for the static modulus of elasticity obtained by mechanical test.

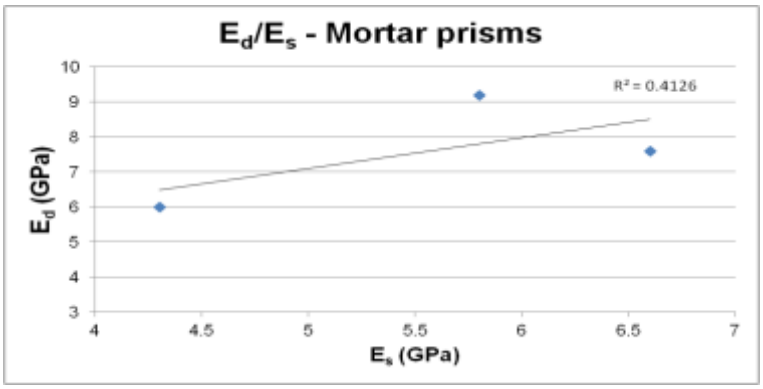

Fig 7.16 - Mortar prisms, comparison between E_d and E_s

Comparing the static and the dynamic modulus of elasticity from the ultrasonic tests, for the mortar samples there is not a very good relation between them. For brick specimens the comparison between E_s and E_d could not be made because the original bricks were cut.

Diagram showed below in fig 7.17 is a synthesis of the experimental work presented in chapter 5, 6 and 7.

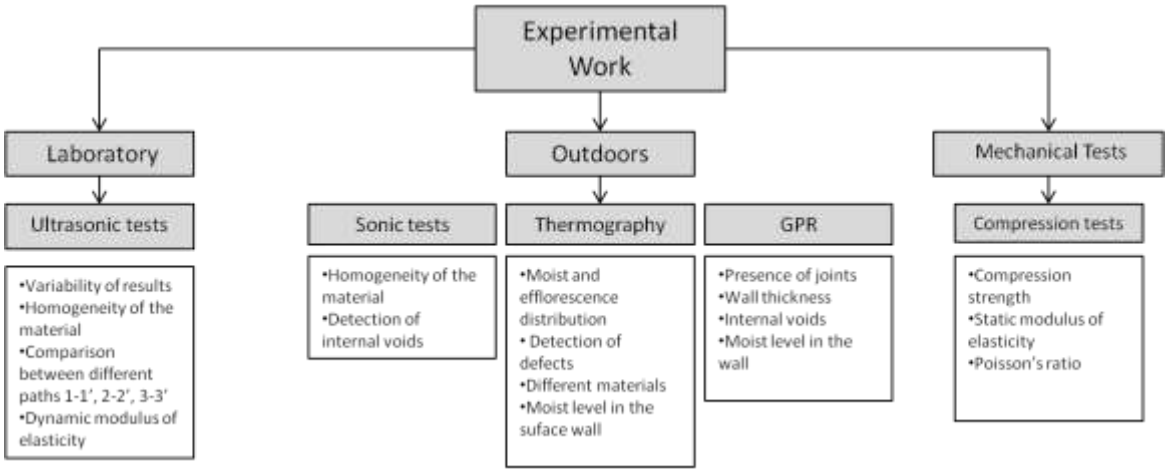

Fig 7.17 - Synthesis of experimental work presented in chapters 5, 6 and 7

8

CONCLUSIONS

8.1. CONCLUSIONS

The final conclusions of this study relate to a critical analysis of testing but also some personal thoughts about the experience was the preparation of this thesis.

The present work is part of a enlarged research work developed and complements the studies that have been done since 2010. An experimental procedure aimed at testing the damaging effects of natural weathering in masonry specimens subjected to the phenomenon of capillary rise with different types of solutions using non-destructive tests was performed. The mechanical behaviour of masonry samples has been presented.

Two different types of material were used, samples of masonry of bricks, mortar prisms and stones and large scale walls. The masonry samples were tested by ultrasound and their mechanical behaviour were analysed. Three different non-destructive tests were applied on wall, sonic tests, infrared thermography and gpr radar.

In this work all non-destructive tests performed have provided valuable information on the detection of moisture, salt transport and inhomogeneities and reveal to be easily applicable on-site, in an assessment of a real structure, since its portability and easy execution. However the knowledge of how to handle the material and especially some deep knowledge of how to make the analysis of data and their correct interpretation, imposes some restriction on these tests. Mainly, the gpr radar, presents a very high difficulty in possessing of data which was not the subject of this thesis, but only the qualitative analysis of the acquired data.

It was found that the degradation of the individual materials is quite different from that which takes place in complete masonry structure, particularly in brick. Constituent bricks in walls presents a very advanced state of decay, with delamination of the material, whereas the samples of brick under the same conditions of natural aging, do not exhibit the same characteristics.

The effect of sodium chloride and sodium sulphate cycles in the assemblies show different efflorescence distribution, the presence of sodium sulphate increase the efflorescence and damaging of material. The high concentration of salts in solution in contact with the wall encourages the development and dissemination of efflorescence.

Moisture is an important factor of damage in the test samples due to the rising damp. Because of being porous materials, all mortar and stone samples suffered weight loss to some degree, mainly the Na_sSO_4 samples and it was, also, found that these samples present lowest values for density. Otherwise, brick samples do not present apparent loss of mass, also for the brick samples the effect of Na_sSO_4, causes decrease of density.

Ultrasonic testing due to its high frequency wave and high attenuation, has limitation on the width of the object, while sonic tests allow greater propagation of waves in the medium, then analyze the elements of greater thickness. Ultrasound test can detect the influence of the salts in samples. There is some similarity in the results of the propagation velocity of the waves in the paths of the edges, especially with a decrease of speed in path 3-3 ', the latter being in contact with the salt solution.

The sequence of the wetting/drying cycles in water influences the structural behaviour of the masonry specimens, so modulus of elasticity and compressive strength are sensitive to the presence of different salts. For mortar prisms and bricks samples subjected to sulphate crystallisation cycles appear stiffer than samples aged in solutions of NaCl and water, even if the peak loads are reached at smaller displacements by the reduction of porosity due to salts accumulation inside the pores and the opening of new micro cracks due to the disruptive effect of crystallisation.

Was not obtained a good quantitative correlation between the mechanical results and the same values determined from the data recorded with ultrasonic test. It is important to point that just three mortar samples were analysed and a principle for homogeneous material was applied to masonry. The values for the Poisson ratio are quite good for this type of material.

The procedure to perform the sonic test is not easy since it is necessary more than one person (mainly in direct test) to hold the instrument and another to read and save the data sonic tests. With vertical profiles of velocity and attenuation, clear indications of variations of internal features and also surface characteristics of the wall can be observed which correspond with the visual inspection of the material.

IR Thermography tests carried out have shown the possible useful applications in masonry walls detecting the presence of moisture and surface characteristics in the walls. The work has been conducted with a passive methodology and, still, valuable information could be extracted from the data acquired.

All the procedures to obtain the thermograms is easy and fast execution, but interpretation of thermograms is a delicate task, as there are several parameters that can influence the results obtained and may lead to erroneous conclusions in the interpretation of thermograms. This test could be easily apply on site, in particular for being a non contact test and due to the portability of the equipment.

GPR have shown to be suitable for the assessment of brick masonry as it can provide reliable and accurate information on construction details as (wall thickness, position and number of mortar joints, inclusions) and internal structure (voids). With regard to the transport of moisture and salt, radar is very sensitive even with low brine content; the estimated rise levels compared satisfactorily with those extracted from the visual inspection on the surface of the wall.

8.2. FUTURE DEVELOPMENTS

Presently, the research is in progress, so it is important to continue with this analysis for a reliable monitoring the evolution of salt transport decay and to detect the beginning of the damages in the masonry specimens.

Non-destructive tests are known and used in civil engineering, the development of studies that may increase the confidence of users of these tests is important, particularly to improve the application of this tests in on-site investigations.

Particularly for the masonry there is no standards for the assessment of decay, so the progress of this study should be helpful to determine some procedures.

REFERENCES

http://store.flir.com/. 9/05/2014

http://www.olympus-ims.com/pt/ut-flaw/epoch1000/.3/5/2014

BALARAS, C.; ARGIRIOU, A. - Infrared thermography for building diagnostics. Energy and buildings. vol. 34 (2002), p. 171-183.

BINDA, L.; SAISI, A. - State of the Art of Research on Historic Structures in Italy, 2001.

BINDA, L.; SAISI, A.; TIRABOSCHI, C. - Investigation procedures for the diagnosis of historic masonries. Construction and Building Materials. vol. 14 (2000), p. 199-233.

BINDA, L.; SAISI, A.; ZANZI, L. - "Radar investigation and diagnosos of historic masonry ". Presented in Structural Falts & Repair in Edinburgh, 2008.

BOSILJKOV, V.; URANJEK, M.; ŽARNIĆ, R.; BOKAN-BOSILJKOV, V. - An integrated diagnostic approach for the assessment of historic masonry structures. Journal of Cultural Heritage. vol. 11 (2010), p. 239-249.

CARINO, N.J. - "The impact-echo method: an overview". Presented in Proceedings of the 2001 Structures Congress & Exposition, 2001.

CASCANTE, G.; NAJJARAN, H.; CRESPI, P. - Novel methodology for nondestructive evaluation of brick walls: fuzzy logic analysis of MASW tests. Journal of infrastructure systems. vol. 14 (2008), p. 117-128.

CLARK, M.R.; MCCANN, D.M.; FORDE, M.C. - Application of infrared thermography to the non-destructive testing of concrete and masonry bridges. NDT & E International. vol. 36 (2003), p. 265-275.

COLLA, C. - "Non-Destructive evaluation of brick masonry via scanning impact-echo testing ". Presented in 9th North American Masonry Conference in Clemson, South Carolina, USA, 2003.

COLLA, C.; LAUSCH, R. - Influence of source frequency on impact-echo data quality for testing concrete structures. NDT & E International. vol. 36 (2003), p. 203-213.

COLLA, C.; GABRIELLI . - Smart Monitoring of Historic Structures: D5.2. Smoohs Report, 2010.

CULTURALI, M.P.I.B.E.L.A. - Line Guida pel la valutazione e riduzione del rischio sismico del patrimonio culturale, 2010.

EN772-1 - Methods of test for masonry units: Determination of compressive strength, 2002.

EN1015-11 - Methods of test for mortar for masonry: Determination of flexural and compressive strength of hardened mortar, 2007.

EN12504-4 - Testing Concrete. Determination of ultrasonic pulse velocity, 2004.

FERNANDES, F.M. - Evaluation of two novel NDT techniques : microdrilling of clay bricks and ground penetrating radar in masonry. PhD thesis. Universidade do Minho, 2006

FRANZONI, E. - Rising damp removal from historical masonries: A still open challenge. Construction and Building Materials. vol. 54 (2014), p. 123-136.

FREITAS, V.P.D.; TORRES, M.I.; GUIMARÃES, A.S. - Humidade Ascensional Porto: Faculdade de Engenharia, 2008.

GENTILINI, C.; FRANZONI, E.; BANDINI, S.; NOBILE, L. - Effect of salt crystallisation on the shear behaviour of masonry walls: An experimental study. Construction and Building Materials. vol. 37 (2012), p. 181-189.

GOUVEIA, J.P.; LOURENÇO, P.B.; VASCONCELOS, G. - "Soluções Construtivas em Alvenaria". Presented in Congresso Construção 2007 - 3.º Congresso Nacional, in Universidade de Coimbra. Dec17th-19th, 2007.

HALABE, U.B.; PYAKUREL, S. - "3D GPR Imaging of Wooden Logs". Presented in Review of Progress in Quantitative Nondestructive Evaluation. AIP Conference Proceedings, 2007.

HENDRY, E.A. - Masonry walls: materials and construction. Construction and Building Materials. vol. 15 (2001), p. 323-330.

ISO15686-1 - Buildings and constructed assets - Service life planning: Part 1: General principles and framewor, 2011.

KORDATOS, E.Z.; EXARCHOS, D.A.; STAVRAKOS, C.; MOROPOULOU, A.; MATIKAS, T.E. - Infrared thermographic inspection of murals and characterization of degradation in historic monuments. Construction and Building Materials. vol. 48 (2013), p. 1261-1265.

KROGGEL, O.; WILHELM, T.; MARCHAND, J.; BISSONNETTE, B.; GAGNÉ, R.; JOLIN, M.; PARADIS, F. - "Stress-Memory of Concrete - Ultrasonic Investigations". Presented in 2nd International RILEM Symposium on Advances in Concrete through Science and Engineering, 2006.

MAIERHOFER, C.; KÖPP, C. - On-site investigation techniques for the structural evaluation of historic masonry buildings. Brussels: European Commission, 2006.

MAIERHOFER, C.; LEIPOLD, S. - Radar investigation of masonry structures. NDT & E International. vol. 34 (2001), p. 139-147.

MALDAGUE, X.P. - Introduction to NDT by active infrared thermography. Materials Evaluation. vol. 60 (2002), p. 1060-1073.

MCCANN, D.; FORDE, M. - Review of NDT methods in the assessment of concrete and masonry structures. NDT & E International. vol. 34 (2001), p. 71-84.

MENDITTO, G.; MENDITTO, S. - Indagini semidistruttive e non distruttive nell'ingegneria civile: disciplina tecnica, applicativa e normativa Bologna. PITAGORA, 2008.

MODENA, C.; VIENTZILEOU, E.; TOMAZEVIC, M.; LOURENÇO, P.; CAPOZUCCA, R.; CHIDIAC, S.; JAEGER, W. - Guide for the structural rehabilitation of heritage buildings CIB Commission, 2010.

MOROPOULOU, A.; LABROPOULOS, K.C.; DELEGOU, E.T.; KAROGLOU, M.; BAKOLAS, A. - Non-destructive techniques as a tool for the protection of built cultural heritage. Construction and Building Materials. vol. 48 (2013), p. 1222-1239.

PASCALE, G. - Diagnostica a ultrasuoni per l'edilizia. Flaccovio,D., 2008.

PASCALE, G.; COLLA, C.; CARLI, R.; BONFIGLIOLI, B. - "Wave propagation based methods for investigation of concrete and masonry architectural members ". Presented in Non Destructive Investigations and Microanalysis for the Diagnostics and a Conservation of the Cultural and Environmental Heritage, in Lecce, Italy. May 15th-19th, 2005.

PORTO, F.; VALLUZZI, M.R.; MODENA, C. - "Use of Sonic Tomography for the Diagnosis and the Control of Intervention in Historic Masonry Buildings.". Presented in International Symposium – Non-Destructive Testing in Civil Engineering, 2003.

QIXIAN, L.; BUNGEY, J.H. - Using compression wave ultrasonic transducers to measure the velocity of surface waves and hence determine dynamic modulus of elasticity for concrete. Construction and Building Materials. vol. 10 (1996), p. 237-242.

RIRSCH, E.; ZHANG, Z. - Rising damp in masonry walls and the importance of mortar properties. Construction and Building Materials. vol. 24 (2010), p. 1815-1820.

RODRIGUEZ, C.; DOEHNE, E. - Salt weathering: influence of evaporation rate, supersaturation and crystallization pattern. Earth Surf. Process. Landforms. vol. 24 (1999), p. 191-209.

SADRI, A. - Application of impact-echo technique in diagnoses and repair of stone masonry structures. NDT & E International. vol. 36 (2003), p. 195-202.

SCHULLER, M.P. - Nondestructive testing and damage assessment of masonry structures. Progress in Structural Engineering and Materials. vol. 5 (2003), p. 239-251.

SENSALONE, M.J.; STREETT, W.B. - Impact-Echo -Non Destructive Evaluation of Concrete and Masonry BullBrier Press, 1997.

SHOOKOUHI, P.; GUCUNSKY, N.; WIGGENHAUSER, H. - "Using Impact-Echo for Non-Destructive Detection of Delamination in Concrete Bridges Decks ". Presented in 7th Structural Materials Technology: NDE/NDT for highways and Bridges and 6th Internation Symposium on NDT in Civil Engineering in St.Louis, Missouri. Aug 14th-18th, 2006.

SOUSA, H. - Construções am Alvenaria, Notes. FEUP, 2003.

TEDESCHI, C.; BINDA, L.; GARAVAGLIA, E. - "Probabilistic Evaluation of the Durability of Ready Mix Mortars on the Maintenance of Historic Masonry". Presented in International Conference on Durability of Building materials and Components, 2011.

TEDESCHI, C.; TACCIA, M.; PEREGO, S. - Sea salt weathering on asian south-east historical buildings vol. (1998).

THEOULAKIS, P.; MOROPOULOU, A. - Salt crystal growth as weathering mechanism of porous stone on historic masonry. Journal of Porous Materials. vol. 6 (1999), p. 345-358.

WARKE, P.A. - Weathering in Arid Regions. San Diego: Academic Press, 2013.